# THE TOTAL SYNTHESIS OF (±) 7-HDHA

MINHAO ZHANG

A THESIS SUBMITTED TO
THE FACULTY OF GRADUATE STUDIES
IN PARTIAL FULFILLMENT OF THE REQUIREMENTS
FOR THE DEGREE OF
MASTER OF SCIENCE

GRADUATE PROGRAM IN CHEMISTRY
YORK UNIVERSITY
TORONTO, ONTARIO

September 2019

# Abstract

Fatty acid (±) 7-HDHA was recently identified as an endogenous ligand for PPAR$\alpha/\gamma$ receptors by one of our collaborators Dr. Henry Krause group. While this discovery is promising in understanding PPARs mechanism of effects and related diseases (Alzheimer's disease, cerebral ischemia, retina inflammation, *etc.*), the study of 7-HDHA in relation to PPARs has been hampered by the high cost and limited supply of 7-HDHA.

The total synthesis of 7-HDHA was attempted using four different strategies, and finally achieved in 11 steps in the longest reaction sequence, starting from commercially available (triisopropylsilyl)acetylene and 2-pentyn-1-ol. The overall yield of this synthesis was 12%. This concise route mainly relies on the one-step generation of three Z-double bonds with the semi-hydrogenation catalyst P2-Nickel, and a late-stage semi-hydrogenation with Zn(Cu/Ag) reagent. The completion of this synthesis will now provide large quantities of 7-HDHA quickly, and thus enable extensive studies of PPAR – 7-HDHA interaction.

## Acknowledgment

Foremost, I would like to express my wholehearted appreciation to my parents. Thank you very much for always sparing no efforts in supporting me to study aboard, for always respecting my choices and interests in life, for always taking care of me even from thousands of miles away.

To my supervisor, Dr. Arturo Orellana, thank you for your continuous support of my master's study and research, for your patience, motivation, enthusiasm and tremendous knowledge. You showed me the beauty of organic chemistry, the temple of science. Your guidance helped me in all phases of my study, I could not imagine a better supervisor for my graduate study. Your role in my life has gone beyond a supervisor, the things you teach me, such as integrity, discipline, passion, and attitude, made me a better scientist, and more importantly, a better human being. You will always be my coach.

I have a special "thank you" for my personal hero Dr. Howard Hunter, for always being there for me when I needed technical support and general counseling. I will not forget that you all the time unconditionally and go out of your schedule to help my study and research. Your passion for NMR spectroscopy deeply influenced me, and I have learned so much from you. I think York is extremely lucky for having you. It is always a delight when I talk to you, and I will certainly miss that.

I would also like to thank my committee members, Dr. Pierre Potvin, Dr. Christopher, and my former committee member Dr. Edward Lee-Ruff. It is an honor to have you on my committee, your constructive criticism and encouragement throughout the years guided me in the right direction.

To my all colleagues, you are the first family I had since I came to Canada 9 years ago. Everyone says research is hard, but it is really not bad with you guys around. Nour, Andrei, Anmol, Ashik, Liam, Faizan, and Izzy, working with you side-by-side has given me so much gold memory. We share, teach, encourage and comfort each other, looking back, I remember all of you when I first saw you, and I am happy that we all have grown so much. To my friends outside of York, Craig, Jee, Murtaza, Xiepeng and Li Shaohong, I

am grateful to have you in my life, I learned so much from every one of you. Life is like a powerful current, it sometimes will push us away from each other, but these friendships, I vow to protect forever.

Last but not least, to my girlfriend Irina Oganesyan. This chapter of my life was much more vivid and brighter because of you. You have always been understanding and encouraging, I am truly blessed to be part of your life.

# Table of Contents

# List of Schemes

# List of Figures

# List of Symbols and Abbreviations

| | |
|---|---|
| β | 1,3 relative position |
| η | hapticity |
| Δ | reflux |
| 1D | one-dimensional |
| 2D | two-dimensional |
| Å | angstrom |
| Ac | acetyl |
| ACS | American Chemical Society |
| ADMET | acyclic diene metathesis |
| ALOX5 | arachidonate 5-lipoxygenase |
| bpy | 2,2'-bipyridine |
| cAMP | cyclic adenosine monophosphate |
| Cat. | Catalytic |
| CDI | carbonyldiimidazole |
| Cdk-5 | cyclin-dependent kinase 5 |
| CNS | central nervous system |
| COSY | ($^1$H-$^1$H)-homonuclear correlation spectroscopy |
| Cp | cyclopentadienyl |
| CREB | cAMP response element binding |

| | |
|---|---|
| Cy | cyclohexyl |
| d | doublet |
| DBU | 1,8-Diazabicyclo[5.4.0]undec-7-ene |
| DCC | N,N'-Dicyclohexylcarbodiimide |
| DCM | dichloromethane |
| dd | doublet of doublets |
| DEPT | distortionless enhancement by polarization transfer |
| DHA | docosahexaenoic acid |
| DIBAL-H | diisobutylaluminium hydride |
| DMAP | 4-dimethylaminopyridine |
| DMF | dimethylformamide |
| DNA | deoxyribonucleic acid |
| e.u. | entropy unit |
| equiv. | equivalent |
| Et | ethyl |
| HCl | hydrochloric acid |
| HDHA | hydroxydocosahexaenoic acid |
| HEPA | hydroxyeicosapentaenoic acid |
| HETE | hydroxyeicosatetraenoic acid |
| HMBC | heteronuclear multiple bond correlation |

| | |
|---|---|
| HODE | hydroxyoctadecadienoic acid |
| HPLC | High Performance Liquid Chromatography |
| HSQC | heteronuclear single quantum correlation |
| *J* | coupling constant |
| KHMDS | potassium bis(trimethylsilyl)amide |
| LDA | lithium diisopropylamide |
| Ln | ligand(s) (n = number of ligands) |
| m | multiplet |
| Me | Methyl |
| MVK | methyl vinyl ketone |
| n-Bu | n-butyl |
| NMI | N-methylimidazole |
| NMR | nuclear magnetic resonance |
| NOESY | nuclear Overhauser effect spectroscopy |
| NSPCs | neural stem cells |
| Ph | phenyl |
| PPARs | peroxisome proliferator-activated receptors |
| ppm | parts per million |
| PPRE | peroxisome proliferator response element |
| PPTS | pyridinium p-toluenesulfonate |

| | |
|---|---|
| q | quartet |
| r.t. | room temperature |
| RCM | ring closing metathesis |
| Red-Al | sodium bis(2-methoxyethoxy)aluminum hydride |
| ROMP | ring opening metathesis polymerization |
| RXR | retinoid X receptor |
| s | singlet |
| Ser | serine |
| t | triplet |
| TBA | tetra-n-butylammonium |
| TBDPS | tert-butyldiphenylsilyl |
| TEMPO | (2,2,6,6-tetramethylpiperidin-1-yl)oxidanyl |
| THF | tetrahydrofuran |
| TIPS | triisopropylsilyl |
| TLC | thin-layer chromatography |
| TMS | trimethylsilyl |
| TOCSY | total correlation spectroscopy |
| Ts | p-toluenesulfonyl |
| USD | United States dollar |
| UV | ultraviolet |

# 1. Introduction

## 1.1 Use of Natural Products in Drug Discovery

If a chemical exerts biological effects, it must have a molecular target in living organisms. The first step of drug discovery in a therapeutic area is usually to find a suitable drug target, such as receptors, enzymes or nucleic acids. These drug targets generally have complex roles, it is thus evidently important to have a thorough understanding of these biomacromolecules' cellular functions and physiological effects. With the advancement of various genome projects and the field of proteomics, an ever-increasing number of proteins are newly discovered as potential targets.[1] While it is encouraging that medicinal chemists now have many more targets to aim for, they do not have enough lead compounds to interact with the new targets.[2] The difficulty nowadays is to identify molecules that could interact with potential targets, and thus answer crucial questions such as their fundamental functions.

Since the dawn of the pharmaceutical industry, natural products have served as the single most important source for lead compounds. Before the era of high-throughput screening and genomics, more than 80% of drug molecules were either natural products or their derivatives.[3] More recently (1994 to 2007), natural products still accounted for around 50% of all drug molecules.[4,5] These natural products can come from a wide range of sources such as plants, animals and microbes, and they cover a broad spectrum of medical conditions.

Moreover, all forms of life are in an uphill battle in fighting thermodynamics, Erwin Schrödinger once defined life as a system that resists decaying to disorder and equilibrium,[6] such a battle costs energy. However, nature still spends much scarce energy in making many structurally elaborate molecules, from Darwin's point of view, these molecules would normally have some sort of biological activity. In contrast to totally laboratory-made molecules, naturals products have a much higher chance to be bioactive, and to resemble biosynthetic intermediates or metabolites.

Another reason why natural product holds promises in medicine is their enormous structural and chemical diversity, to a degree no synthetic library can surpass. For example, the antimalarial drug artemisinin extracted from sweet wormwood contains a trioxane ring, which appears to be extremely unstable (**Figure 1**), a structure that is very unlikely and beyond chemists' imagination for drug design. This large collection of extremely novel compounds is of course invaluable; however, their structural complexity also makes their syntheses very difficult. Instead, natural products are usually extracted from natural sources – a time-consuming, costly and unproductive process. Therefore, a tremendous amount of effort has been made into the total syntheses of natural compounds in academia and industry. Furthermore, total synthesis can potentially provide access to a library of natural product's analogues, which is extremely important in lead compound campaign and optimizing drug-target interactions.

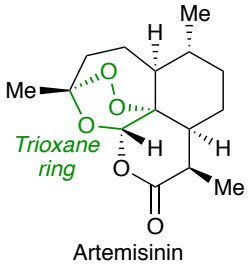


**Figure 1**. The structure of artemisinin, an antimalarial drug.

## 1.2 Biological Motivation for the Synthesis of (±) 7-HDHA Synthesis

PPARs (Peroxisome Proliferator-Activated Receptors) are a class of "adopted orphan" nuclear receptors that consist of PPAR$\alpha$, PPAR$\delta$, and PPAR$\gamma$. It is believed that the PPARs family of receptors plays a major regulatory role in energy homeostasis and metabolic function,[7] such as the metabolism of carbohydrates, lipids, and proteins.[8] Also, various studies have shown that PPARs regulates cellular differentiation and development, and tumorigenesis etc.[9–11] PPARs function as ligand-dependent transcription factors, namely, all PPARs heterodimerize with a retinoid X receptor (RXR), these heterodimers then bind to PPREs (PPAR Response Elements) within promoter regions of the target

genes, realizing the regulation of target gene expression.[12] In the absence of a PPARs ligand, these heterodimers are associated with co-repressor complex and block the target gene transcription,[13] whereas upon binding to an agonist ligand (**Figure 2**), the conformation of a PPAR is changed so that a new binding domain is created, allowing the recruitment of transcriptional co-activators that ultimately results in an increase in gene transcription.[10]

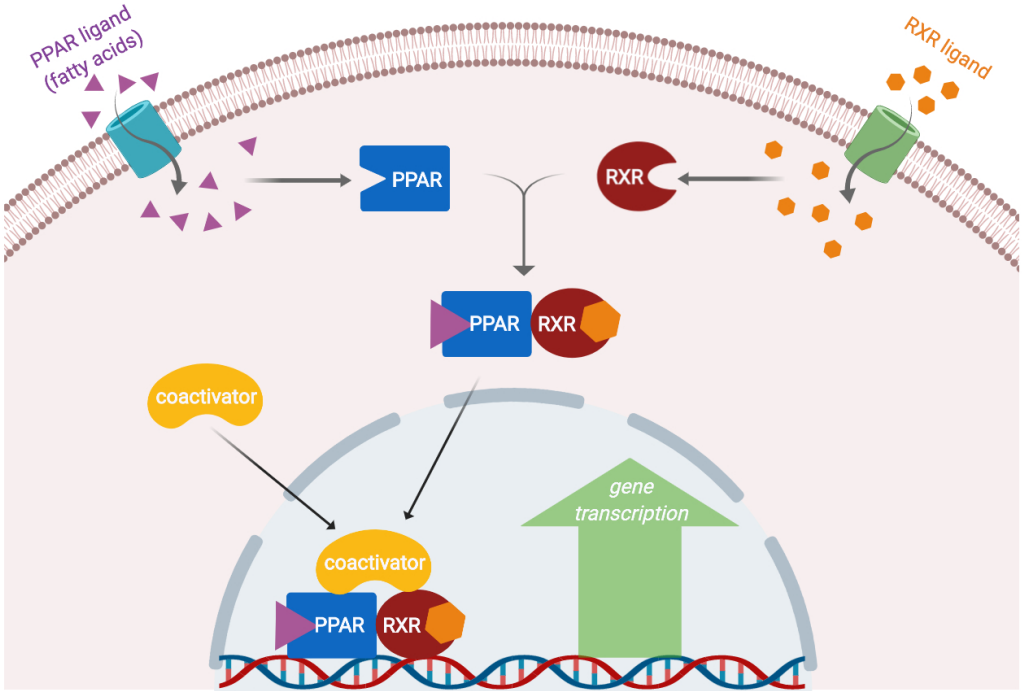


**Figure 2**. The mode of action for PPARs family of nuclear receptors. The ligand-bound PPARs heterodimerize with an RXR receptor, which then recruits a transcriptional co-activator. This complex then binds to the promoter regions of the target genes, realizing the regulation of target gene expression.

PPARα is highly expressed in brown adipose tissue and the liver,[14,15] where it responds to various free fatty acids in different sensitivities and thus increases or decreases energy metabolism rates. For example, studies showed that PPARα is a positive regulator for fatty acid oxidation,[16] lipid transport and metabolism, ketogenesis and gluconeogenesis.[17–19] Also, gene expression studies revealed that PPARα is distributed in cerebral cortex, hippocampus, brain stem and retina.[20,21] Another study suggested that hippocampus PPARα is essential to memory formation *via* transcriptional

upregulation of CREB (cAMP response element-binding protein), a transcription factor capable of binding DNA and regulating gene expression.[22] Subsequently, several novel potential endogenous ligands extracted from the hippocampus have been identified and shown to stimulate synapse formation by hippocampal neurons,[23] these new additions of ligand have furthered our understanding of hippocampal neurogenesis. The neurogenic capacity of hippocampal neural stem/progenitor cells (NSPCs) depends on a balance between quiescent and proliferative states, where the activity of NSPCs is regulated by the rate of fatty acid oxidation that requires PPAR$\alpha$, which is highly upregulated in quiescent.[24] Hence, the understanding of PPAR$\alpha$ is also important for hippocampal neurogenesis studies since failing neurogenesis has been implicated in many neuropsychiatric diseases.

The attention of PPAR$\gamma$ has been focused on its relation to the promotion of adipogenesis in white and brown adipose tissue.[25] Moreover, PPAR$\gamma$ contributes to insulin sensitivity,[26] and is important for anti-inflammatory in macrophages[27] and other tissues such as the colon.[28] Two recent reports demonstrated the crucial roles of PPAR$\gamma$ in the brain that affect feeding, insulin sensitivity, and energy metabolism.[29,30] Furthermore, PPAR$\gamma$ has potential neuroprotective in various pathological states, such as cerebral ischemia and Alzheimer's disease.[31] Since it seems that PPAR$\alpha$ and PPAR$\gamma$ together play very important yet very different molecular and physiological roles in the central nervous system (CNS) comparing to their roles in other tissues, it is reasonable to assume the brain-expressed PPARs would have different ligands than their counterparts in peripheral tissues, not to mention the brain's vastly different environment. Therefore, previously identified ligands and described PPARs-ligand interactions might have a little basis in the CNS, which calls the discovery of novel endogenous ligands and sequential study on PPAR-ligand interactions.

As a group of treatable targets, a number of potent agonists and antagonists for PPARs have been identified from small molecule libraries,[32] yet the PPARs are generally viewed as "sensors" for a variety of less potent but crucial endogenous ligands, particularly polyunsaturated fatty acids.[33–35] However, the variety of lipids and potential endogenous ligands in different tissues has not been fully established. Moreover, there is still debate

on the values of many previously identified PPARs natural ligands. For example, 1) many showed low affinities to PPARγ, including 13-hydroxyoctadecadienoic acid (13-HODE), 9-HODE, 15-hydroxyeicosatetraenoic acid (15-HETE), 5-hydroxyeicosapentaenoic acid (5-HEPA), etc.;[36] 2) although oleoylethanolamide is a potent ligand for PPARα, there is no evidence supporting its direct binding to PPARα;[37,38] 3) PPARγ ligand, 15-deoxy-Δ-$^{12,14}$-prostaglandin $J_2$ (15d-$PGJ_2$), has much a lower physiological concentration than required for actual PPARs activation;[39,40] and 4) nitroalkene derivatives of oleic acid (OA-$NO_2$) and linoleic acid ($LNO_2$) have the half-lives too short in our body to be the actual ligands.[41]

Our collaborator at the University of Toronto, Dr. Henry Krause group recently isolated an omega-3 fatty acid, 7-hydroxyl docosahexaenoic acid (7-HDHA, **Figure 3**), from zebrafish brain and eyes, and mouse hippocampus and cerebellum. They demonstrated that 7-HDHA is an endogenous ligand for both PPARα and PPARγ. In human neutrophils, 7-HDHA was biosynthesized from the oxidation of docosahexaenoic acid (DHA), mediated by 5-lipoxygenase (ALOX-5). When neutrophils were treated with an ALOX-5 inhibitor, the formation of 7-oxo-DHA and its hydroxy precursor 7-HDHA was completely suppressed.[42] *In vivo* and *in vitro*-based assays were used to show that 7-HDHA binds directly to both said receptors' ligand binding sites, as a potent agonist for PPARα and a partial agonist for PPARγ. More preliminary studies from Dr. Krause group indicated that in the brain, 7-HDHA stimulates the actions of PPARα in promoting hippocampal neuronal growth and synapse formation, which are associated with memory formation and regeneration. As for PPARγ, 7-HDHA's partial agonist ability was still able to stop the cyclin-dependent kinase 5 (Cdk-5) mediated phosphorylation at Ser273 in PPARγ, which lowers both inflammatory and lipogenic activities.

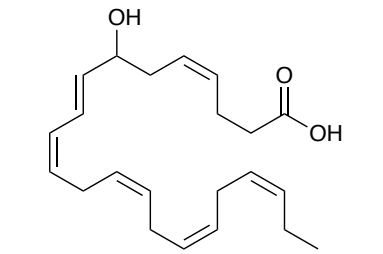


7-hydroxyl docosahexaenoic acid
***(±) 7-HDHA***

**Figure 3.** The structure of (±) 7-HDHA

These early results showcase many possible physiological roles for 7-HDHA in the brain, eye, and metabolism. They would help our understanding of corresponding diseases such as cerebral ischemia, Alzheimer's disease, diabetes, obesity, etc., which in turn helps the development of possible therapeutic treatments. The planned study on PPARs-7-HDHA interactions requires a steady and substantial supply of 7-HDHA, which has been hampered by its extremely high price and limited commercial supply. For instance, one commercial supplier prices the racemic 7-HDHA at 65 USD per 25 μg, and it has only 2.2 milligrams in stock. The completion of the total synthesis of 7-HDHA will now enable extensive studies of this system, and will prove useful in drug discovery efforts targeting the PPAR family of nuclear receptors.

## 1.3 Retrosynthetic Analysis of (±) 7-HDHA

Despite its linear structure and the presence of only one stereogenic center, 7-HDHA presents significant synthetic challenges. For instance, the -OH group at the 7-position quickly became a disadvantage during the first and seemingly most straightforward synthesis plan. Moreover, 7-HDHA possesses six olefin moieties, including skipped, isolated and conjugated alkenes, five of which are in Z configuration and are prone to isomerization and conjugation.

The retrosynthetic analysis of (±) 7-HDHA began with recognizing that the carboxylic acid group on C-1 can be revealed by hydrolysis reaction of the corresponding

ester (**Scheme 1**). Similarly, the hydroxyl group on C-7 can be exposed by the deprotection of its silyl ether assisted by a fluoride source. The protection of the alcohol and acid group could potentially reduce their acidic proton's interference in many reactions and thus prevent unwanted side reactions. Next, in the protected 7-HDHA **1,** there are two conjugated double bonds between C-8 and C-11. The olefin between C-10 and C-11 is in Z-configuration and could be accessed by Z-selective semi-hydrogenation reactions from corresponding alkyne **2**, such methods have significant precedent in the literature, especially in the realm of heterogeneous hydrogenations.

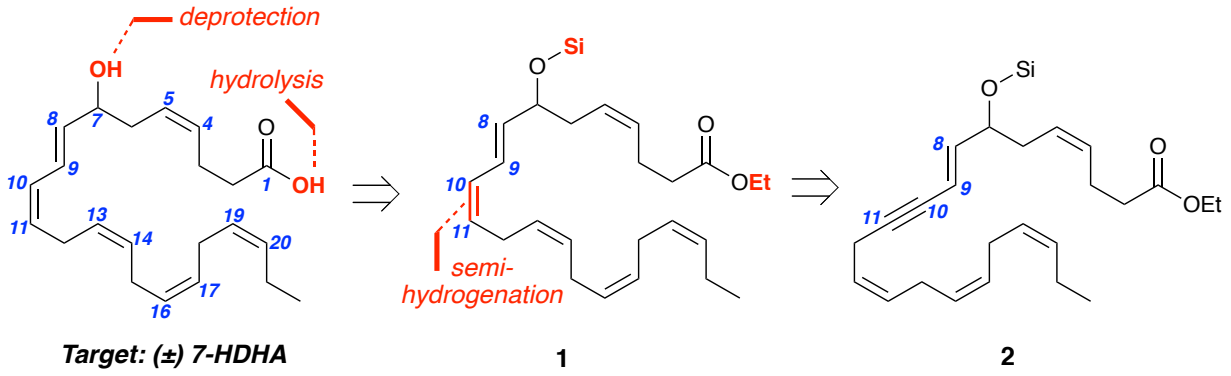


**Scheme 1.** The first part of the retrosynthetic analysis for (±) 7-HDHA.

In compound **2**, the $sp^2$-sp bond between C-9 to C-10 can be forged by a Sonogashira coupling reaction. The two coupling partners are a vinyl iodide (C-1 to C-9 fragment) and a terminal alkyne (C-10 to C-22 fragment) (**Scheme 2**). For the vinyl iodide fragment, we devised two strategies to access it Z-olefin between C-4 and C-5. The first strategy involves an 8-membered lactone formation (compound **3**), this method relies on locking the double bond Z-configuration by confining it within a ring structure. Normally in a chain structure, simple Z-double bond is less stable more its E counterpart, however, double bond Z-geometry is vastly more preferred when present in a small or medium-sized ring. Thus, we envisioned that the Z-olefin between C-4 and C-5 can be readily formed selectively if we enclose it into a ring. There are several methods to realize the simultaneous formations of the ring and the olefin, with ring closing metathesis being the most straightforward one.

The other strategy to access the Z-double bond in the C-1 to C-9 fragment relies on a direct and Z-selective olefination method to give a chain structure (compound **4**). Without the thermodynamic drive created in the first "ring strategy", this "chain strategy" requires a method that kinetically favors the formation of a Z-double bond. A well-studied and reliable example for such Z-selective olefination is Wittig reaction, using a non-stabilized phosphonium ylide.

On the other hand, the C-10 to C-22 fragment (compound **5**) also presents some challenges. First of all, the olefin synthesis needs to be Z-selective, and mild enough to accommodate the skipped olefins, since harsh conditions might isomerize the skipped olefins into either E-olefins or conjugated systems. Transition metal-catalyzed, heterogeneous semi-hydrogenation of alkynes is one of the most canonical methods for Z-olefin synthesis. More importantly, it should allow us to form all three Z-olefins in a single step from corresponding skipped tetrayne. Another challenge is that the semi-hydrogenation needs to be selective so that the terminal alkyne is unaffected. Fortunately, this can be achieved simply by replacing the terminal alkynyl proton with a silyl protecting group.

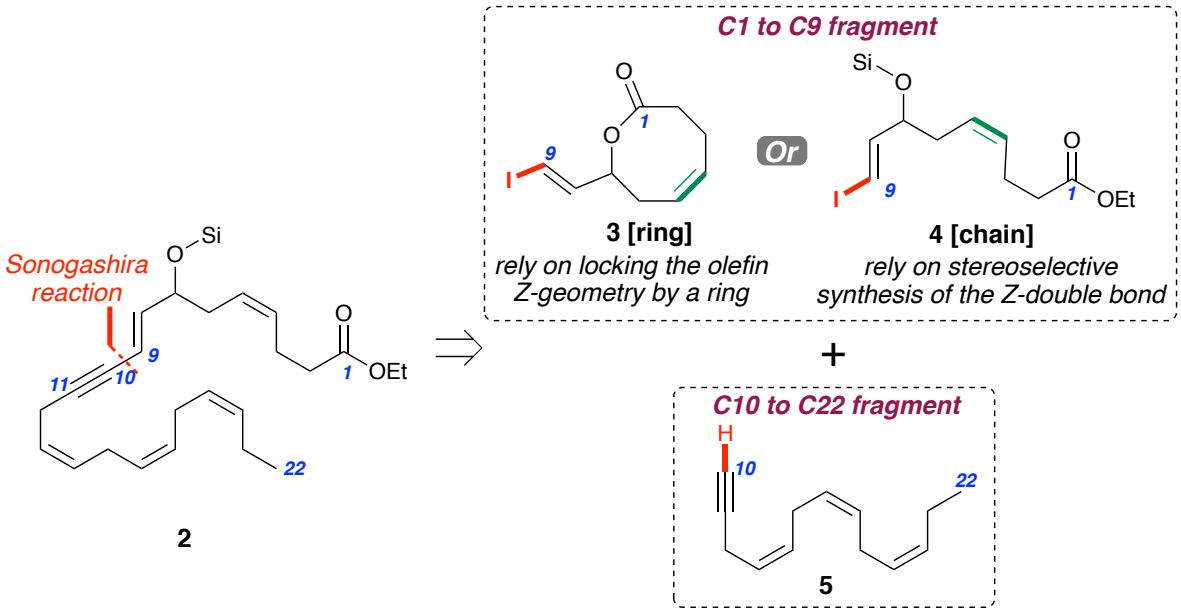


**Scheme 2.** The second part of the retrosynthetic analysis for (±) 7-HDHA.

# 2. Total Synthesis of (±) 7-HDHA

## 2.1 First Synthetic Approach Towards Fragment S1

The planned synthesis of fragment **3** required an efficient method to construct an eight-membered ring, and ideally, the ring formation would simultaneously install the *Z*-olefin between C-4 and C-5. This approach features a ring-closing metathesis (RCM) to accomplish this goal. A fast route to access the RCM precursor diene **7** was executed.

Compound **8** was initially made by two sequential reactions (**Scheme 3**); 1) standard silylation of propargyl alcohol **6** by chlorotrimethylsilane to give **7** and 2) transfer of the silyl group from the oxygen atom to the terminal *sp*-hybridized carbon atom to give the volatile alcohol **8**. Although these two sequential reactions were smooth transformations, the combined yield over two steps was only about 50%. The yield was improved by first treating compound **6** with 3.0 equivalents of the strong base, ethylmagnesium bromide, to result in the formation of a dianionic species, which was then quenched with TMSCl. Therefore compound **8** was realized in a single step with an almost 2-fold increase in yield.[43]


**Scheme 3.** The two synthetic methods to alcohol **3.**

The alkyne moiety in propargyl alcohol **8** was reduced by sodium bis(2-methoxyethoxy) aluminum hydride (Red-Al) to give *trans*-hydrogenated allylic alcohol **9** (**Scheme 4**), which was then oxidized to aldehyde **10** using the Cu-TEMPO catalytic system developed by Stahl and co-workers.[44]

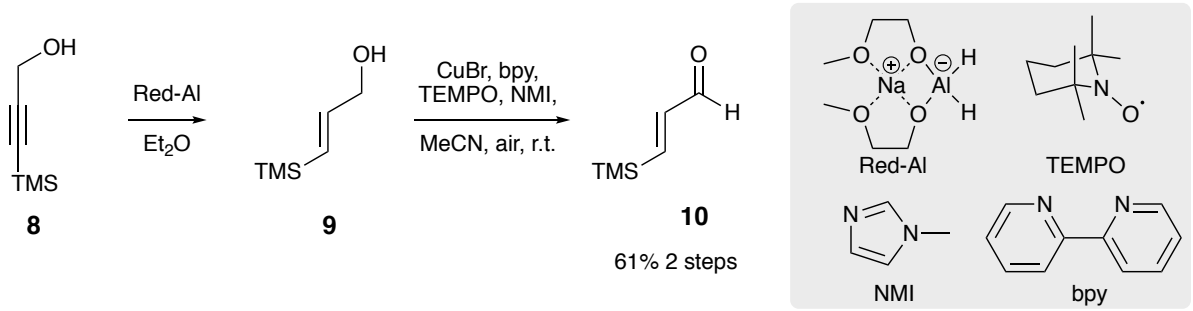


**Scheme 4**. The synthesis of aldehyde **5**.

The alkyne reduction with Red-Al depends critically on the presence of the neighboring OH group. First, Red-Al deprotonates the alcohol to give intermediate **11** (**Scheme 5**), then a hydride is delivered to the β carbon in an intramolecular fashion to result in a five-membered vinylaluminum ring **12**. Then the *trans*-olefin **9** is formed by stereospecific substitution of a proton for aluminum upon quenching the intermediate with acid. It is worth noting that by applying this organoaluminium intermediate, other electrophiles (such as $I_2$) have been used for functionalized olefin synthesis. [45]

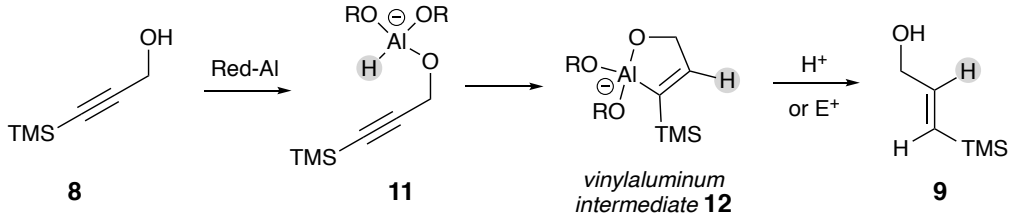


**Scheme 5.** Mechanism of Red-Al reduction of **8**.

The (bpy)$Cu^{I}$/TEMPO catalytic system developed by Stahl and co-workers oxidizes primary alcohols to the corresponding aldehydes under extremely mild conditions.[44] Similar methods that use catalytic amount of TEMPO for alcohol oxidations were reported previously with various stoichiometric oxidants including electric current,[46] NaOCl,[47] peroxy acid,[48,49], etc. A more relevant alcohol oxidation method by using $CuCl_2$/TEMPO/$O_2$ system was also reported in the 1980s by Semmelhack and co-workers.[50] They proposed that their reaction proceeds through an oxoammonium cation intermediate ($TEMPO^+$) that forms by $Cu^{II}$ oxidation of TEMPO,[51,52] the $TEMPO^+X^-$ species then oxidizes alcohol to aldehyde (**Scheme 6**).[53–55]

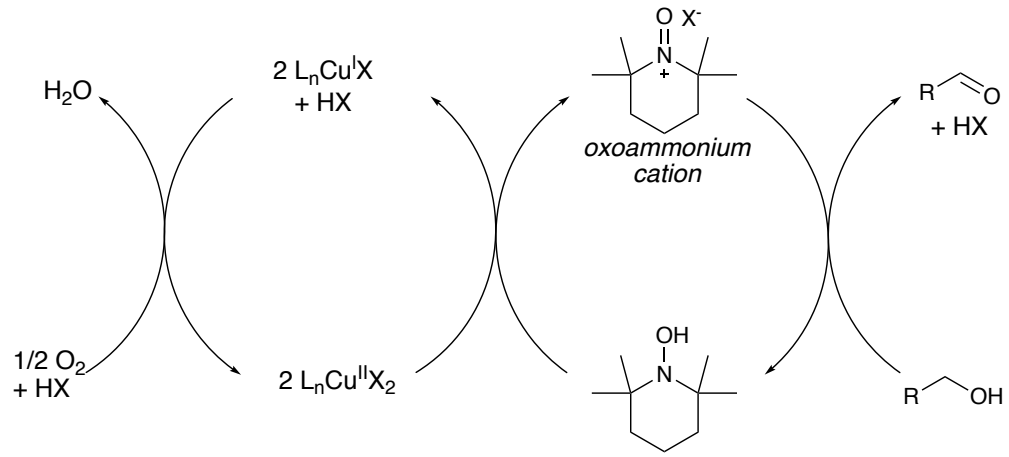


**Scheme 6.** Semmelhack's mechanism for TEMPO-catalyzed aerobic alcohol oxidation.

However, it is unlikely that (bpy)$Cu^{I}$/TEMPO catalytic system follows the above mechanism. Stahl and co-workers suggested that $TEMPO^{+}$ is not involved as an active oxidant under their reaction conditions. Based on experimental evidence 1) $Cu^{II}$ is incapable of oxidizing TEMPO to $TEMPO^{+}$ under the reaction condition, especially when bound to bipyridyl ligand, and 2) $TEMPO^{+}$ is not nearly kinetically competent enough to perform such fast oxidation. In turn, they suggested a pathway that involves $Cu^{II}$ and TEMPO acting in concert to deliver a net two-electron alcohol oxidation. [56] Also, Stahl showed that the alcohol is oxidized by intramolecular concerted hydrogen atom transfer *via* a six-membered ring transition state, involving a $\eta^1$-nitroxyl-Cu adduct (**Scheme 7**).[57]

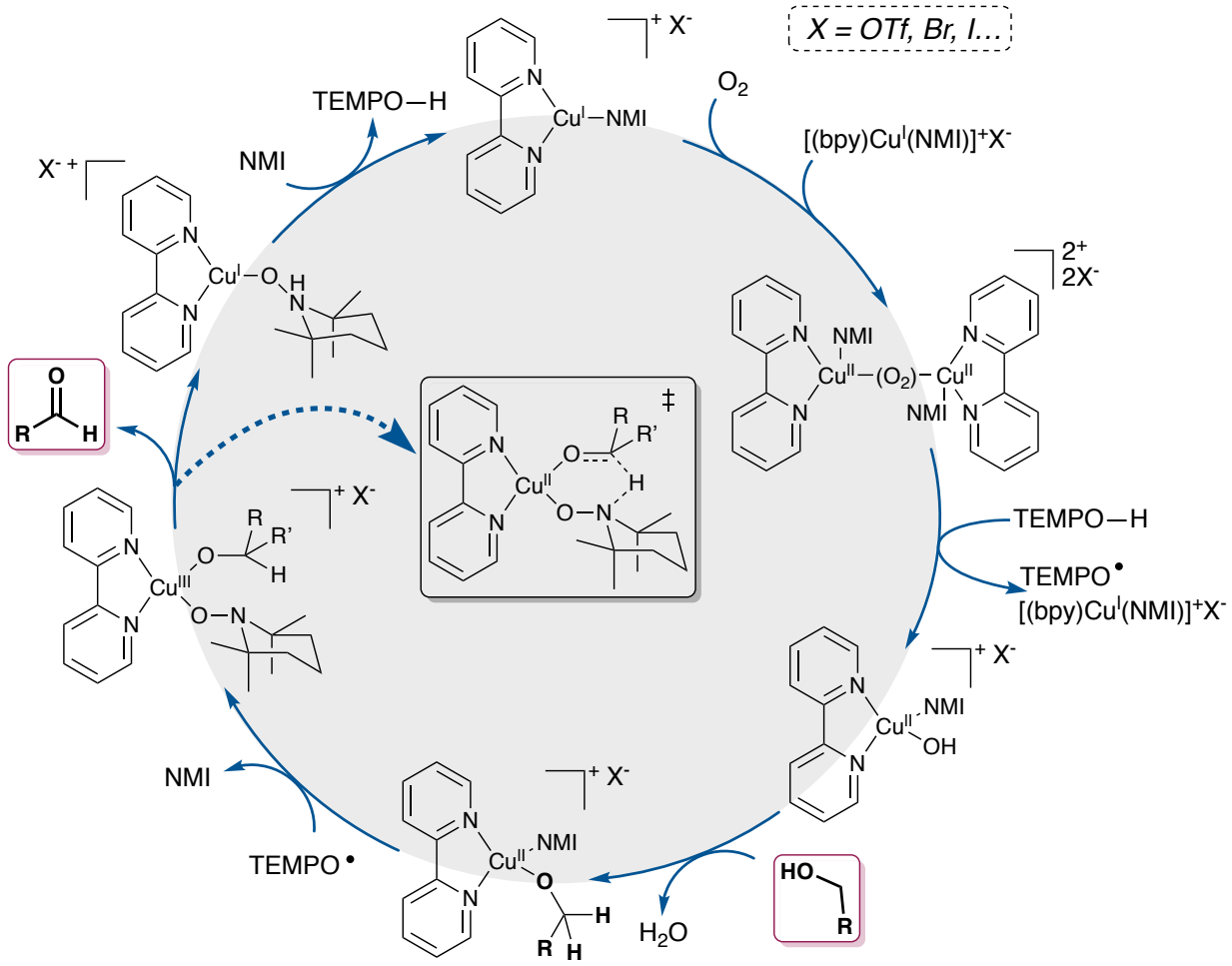


**Scheme 7.** The mechanism for Cu/TEMPO-catalyzed aerobic alcohol oxidation suggested by Stahl and co-workers.

Aldehyde **10** was treated with allylmagnesium bromide and delivered alcohol **13** (**Scheme 8**). Then Steglich esterification between **13** and 4-pentenoic acid **14** mediated by DCC and a catalytic amount of DMAP furnished **7**, the ring closing metathesis precursor.

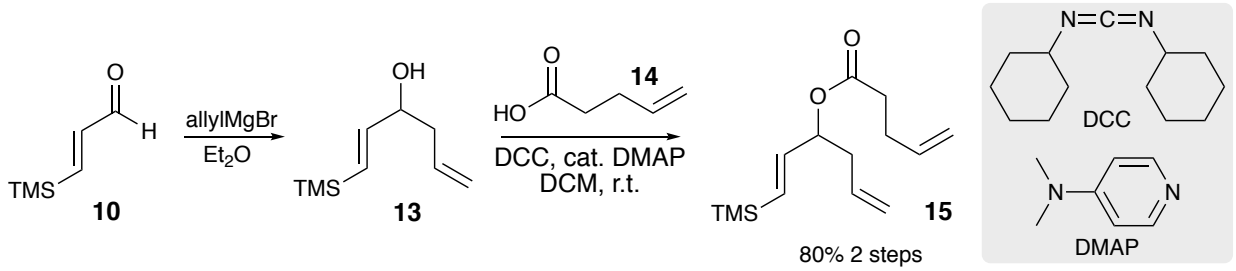


**Scheme 8.**The synthesis of diene **15**.

It is worth mentioning that allylmagnesium bromide can only be formed in diethyl ether. It has been reported that allyl bromide reacts quantitatively with magnesium in THF to give 1,5-hexadiene through Würtz-type reaction.[58] N,N'-Dicyclohexylcarbodiimide (DCC) was one of the first carbodiimides developed as a dehydration reagent to mediate ester and amide formation.[59] The reaction's neutral and mild reaction conditions have made it very popular especially in peptide synthesis,[60] since the direct conversion from carboxylic acid to amide is difficult because the basic amine group tends to convert the acid into unreactive carboxylate. An efficient Steglich esterification requires the use of a catalytic amount of nucleophilic catalyst, usually DMAP, which acts as an acyl transfer agent because of its higher nucleophilicity than that of alcohols (**Scheme 9**). Dicyclohexylurea is always the stoichiometric byproduct in the DCC coupling reaction, and it cannot be visualized by UV light or staining the TLC plate, thus its removal is frequently problematic and requires multiple careful filtrations of the crude product before flash column purification.

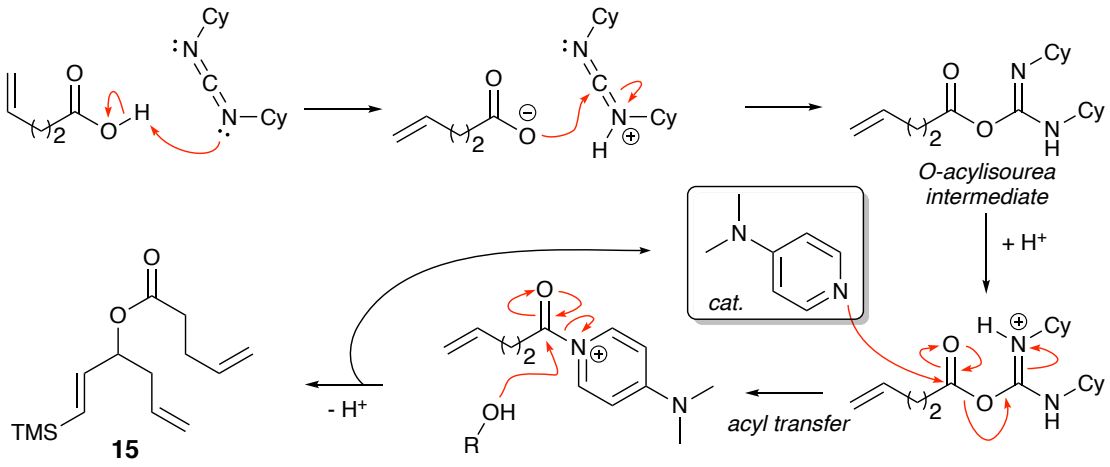


**Scheme 9.** The mechanism of Steglich esterification.

With ester **15** in hand, we attempted ring-closing metathesis (RCM) with Hoveyda-Grubbs 2nd generation catalyst, however, neither TLC and crude NMR analysis showed product formation. Different ruthenium-based metathesis catalysts and various reaction conditions were used, unfortunately, none of them gave the desired product **16** (**Scheme 10**).

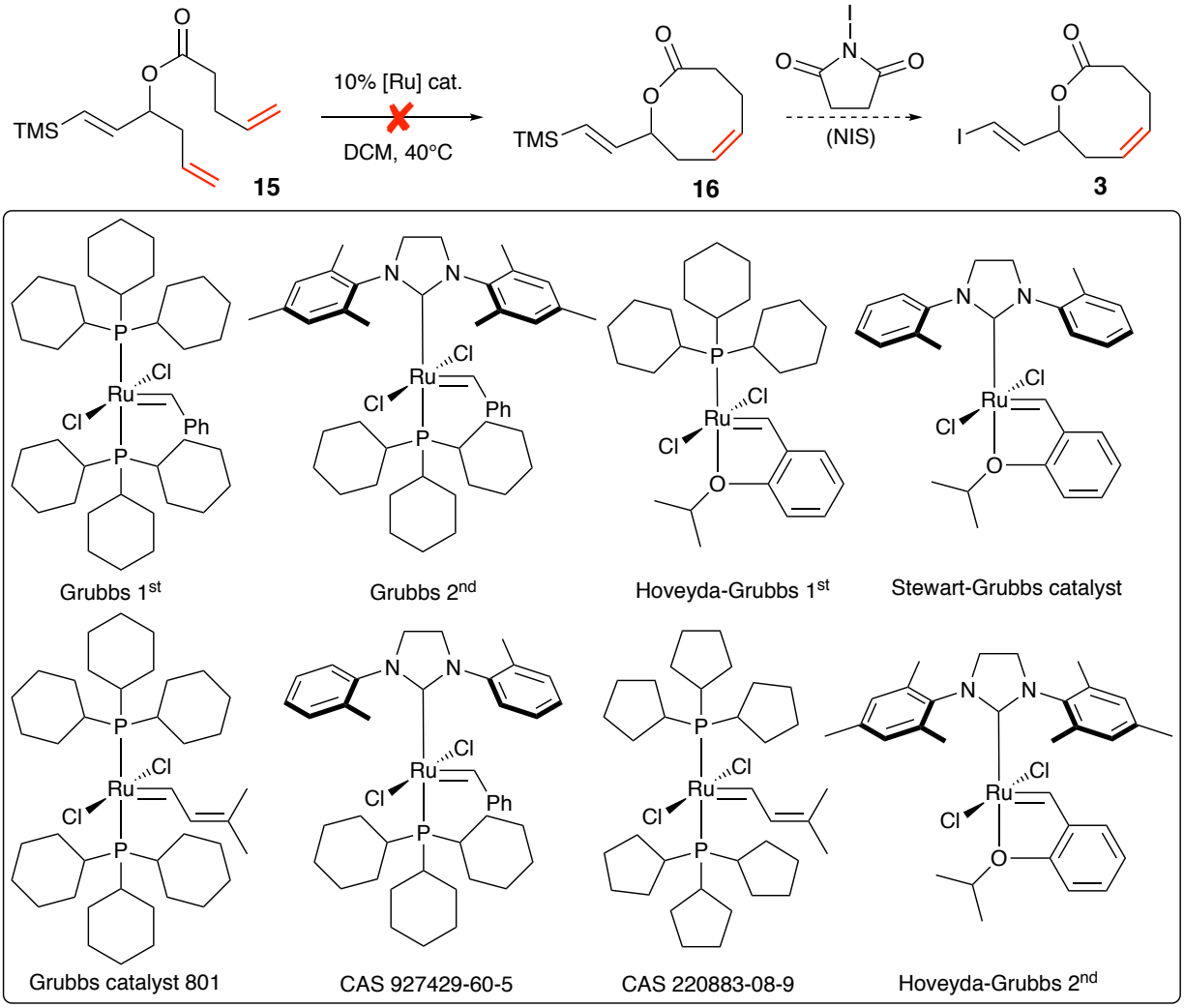


**Scheme 10.** Attempted ring-closing metathesis and all ruthenium-based catalysts that were used.

RCM reactions to access 5-, or 6-membered rings with very high yields are well documented. However, the formation of a medium-sized ring is challenging and often fails.[61,62] It is safe to say that the majority of RCM reactions are largely governed by thermodynamics since every step in the mechanism is in principle reversible.[63]

Two types of strains in a ring contribute to the overall ring strain, they are angle strain and transannular strain. Although larger-sized rings release angle strain, the transannular strain could increase due to the imperfect staggering of the substituents. This explains why the ring strains increase from seven- to nine-membered cyclic olefins

(**Figure 4. A**) and supports the fact that RCM often encounters problems for the formation of medium-sized rings.[64] This notion is also supported by studies that explore the correlations between ring sizes and cyclization rates in stoichiometric lactonization reactions for saturated lactones.[65,66] Although the values in **Figure 4. B** are for saturated lactones, they provide a useful illustration of the correlation between ring sizes and formation rates. In **Figure 4. B**, the entropic cost ($\Delta S^{\neq}$, purple line) in a lactonization generally increases with increasing ring size, which can translate into the decrease of encounter probability of two ends of a chain required for cyclization. The enthalpic cost ($\Delta H^{\neq}$, red line) reflects the lactone ring strain. Noticeably, eight- and nine-membered rings have the largest ring strain that offsets their reasonably high encounter probabilities, granting eight- and nine-membered rings the lowest rates of formation (green line). This rate retardation in metathesis is problematic because it increases the opportunity for competing catalyst decomposition, therefore, reduces yields or promotes side reactions.[67]

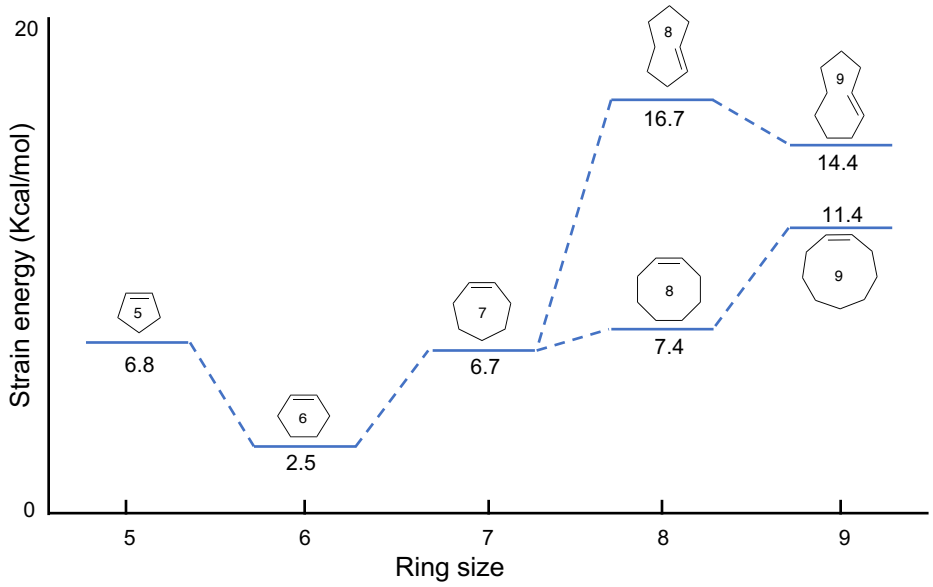


**(A)**

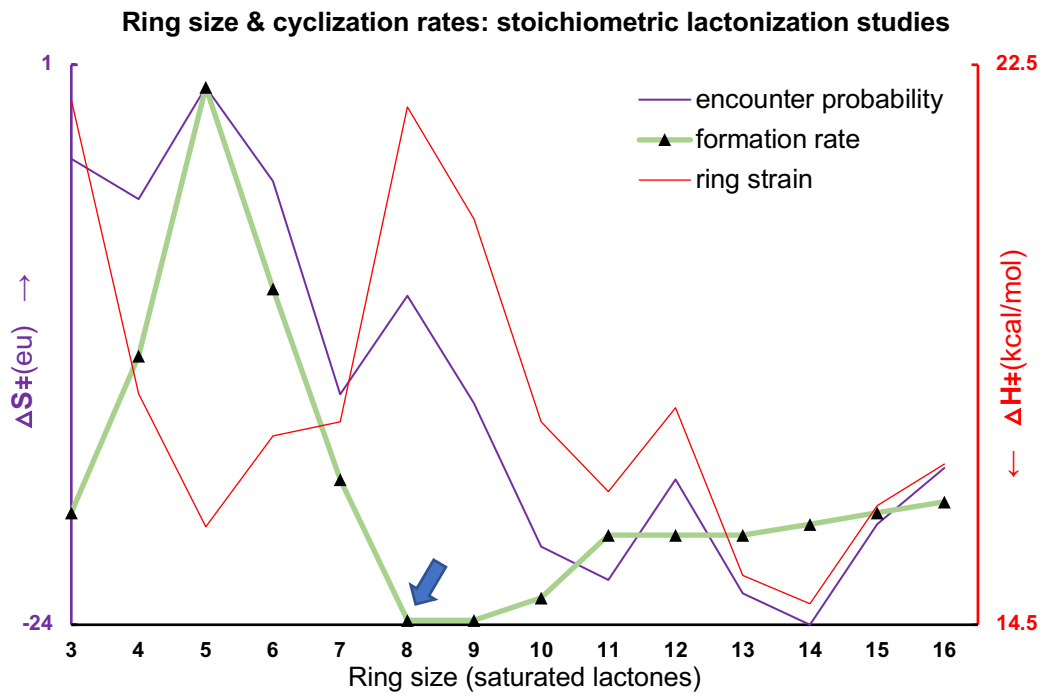


**(B)**

**Figure 4**. A. Calculated strain energies for unsaturated, carbocyclic olefins of five to nine members;[64] B. $\Delta S^{\neq}$ profile (purple line, the entropic cost), $\Delta H^{\neq}$ profile (red line, the enthalpic cost) and the formation rate (green line) of various sizes of saturated lactones in stoichiometric lactonization studies.[65,66] Note: the formation rate (green line) is not referred by a Y-axis, only to show its general trend.

However, it is not to say 8- or 9- (may include 10-) membered rings are impossible to form *via* RCM, there are indeed many reported successful examples.[68–73] Besides the catalyst design, one of the ways to achieve RCM for these "tough" ring sizes is to use high dilution of the reaction mixture.[74] It is known that intermolecular metathesis (acyclic diene metathesis, ADMET) is a competing bimolecular process in RCM reactions, fortunately, this process can be kinetically suppressed by high dilution to avoid diene oligomerization. An intrinsic problem with high dilution is that the catalyst-substrate reaction is still bimolecular, whose rate will also be lowered by lowering the reaction concentration, giving time for catalyst decomposition. In our efforts, with Hoveyda-Grubbs 2$^{nd}$ and Grubbs 2$^{nd}$ catalysts, diene **15** was subjected to the concentrations of 5 mM, 3 mM, 2 mM and 1 mM in either DCM or toluene. Unfortunately, none of these conditions gave the desired RCM

product. To achieve 1 mM substrate concentration, 50 milligrams of diene **15** requires 200 milliliters of solvent. Concentrations lower than 1 mM would be highly impractical but might be needed. In practice, we achieved the most vigorous dilution by adding both substrate and the catalyst solutions dropwise into the reaction mixture with the help of two syringe pumps. this protocol provides substrate concentration that is significantly lower than 1 mM. Unfortunately, it also did not give the desired product, even though high dilution reportedly worked in some challenging macrocyclizations.[74]

Fortunately, there is a way to circumvent the oligomerization problem in RCM reactions. Other than cross-metathesis and RCM, ruthenium-based catalysts can also perform ring-opening metathesis polymerization (ROMP): also an equilibrium process between diene polymer/oligomer and cyclized product (RCM product). Therefore, if oligomers are inevitably formed during RCM reactions, they could in principle still be converted to cyclized products *via* ROMP equilibrium (**Scheme 11**).[75,76] Although metathesis often is described as a fully reversible process, the loss of volatile ethylene molecules is irreversible under normal operating conditions, making the oligomerization and RCM irreversible processes. Fortunately, ROMP is fully reversible because it does not release ethylene, providing an indirect way to access RCM products. Applying the logic in **Scheme 11**, there are examples in the literature that use oligomers or dimers of a diene as the precursors to RCM when direct RCM failed to work.[62]

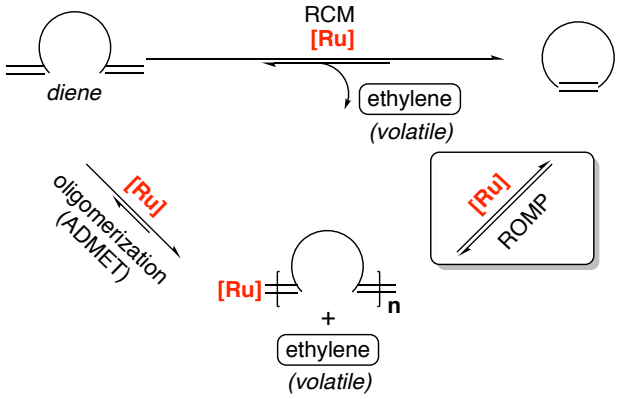


**Scheme 11.** A general scheme of ring closing metathesis of a diene, including the direct RCM pathway and indirect ADMET-ROMP pathway. ADMET: acyclic diene metathesis; ROMP: ring-opening metathesis polymerization.

Since ROMP is an equilibrium process, without redesigning the diene substrate or the catalyst, operational manipulations could be made to lead the equilibrium to shift towards either direction (ring or chain). Thus, it is important to know what governs the equilibrium constant in a ROMP reaction, and one can borrow from a related theoretical study by Jacobson and Stockmayer that considers the distribution of cyclic and linear polymers present at equilibrium in concentrated solutions.[77] Ring formation by intramolecular reactions was a long-standing problem in linear polymer condensations. The study predicted a concentration-dependent ring-chain equilibrium in a reversible polymerization process, where high dilution would favor the ring formation and the high concentration would favor the polymer/oligomer formation. Because Jacobson-Stockmayer theory makes a couple of ideal assumptions, such as it treats all rings as strainless and the cyclization as athermal, it is more of a general prediction, so each RCM case in real life will need specific measures.

Based on the Jacobson-Stockmayer theory, one can predict that there is no need to perform a cyclization reaction under extreme dilution throughout the whole course, as long as the final concentration reaches the "critical concentration" that leads the equilibrium to ring formation. Danishefsky and co-workers tested the use of Ziegler "infinite dilution"[65] methods in RCM with Grubbs 2$^{nd}$ catalyst. Compared to reactions in which all reagents were added at once, the dropwise addition of diene (over a 7-hour period) to the catalyst solution in refluxing benzene had no influence on the RCM product yield.[78] In his examinations, the final RCM yield solely depended on the final concentration, which confirms Jacobson-Stockmayer theory's prediction, at least in some cases. This is very useful information because we do not have to use a highly diluted reaction mixture in the beginning. If oligomerization is kinetically favored, one could start the reaction at a much higher concentration so that oligomer-ring (ROMP) equilibrium quickly establishes, then one can dilute the reaction *X* times to reach the favored dilution for RCM product. the initial high reaction concentration would help catalyst-substrate reaction rate and reduce catalyst decomposition. We performed such a procedure, however, no desired product was seen after many attempts with different catalysts (Grubbs 2$^{nd}$ and Hoveyda-Grubbs 2$^{nd}$) and solvents (DCM and toluene, 40°C and 80°C).

At this point, catalyst decomposition or deactivation in the reaction condition has to be considered. The most obvious catalyst deactivation is through the chelation of polar functionalities to the catalyst's ruthenium metal center, this is a very common issue that has a minimal effect on readily-cyclized dienes, but can be extreme for more demanding substrates (**Scheme 12**).[79]

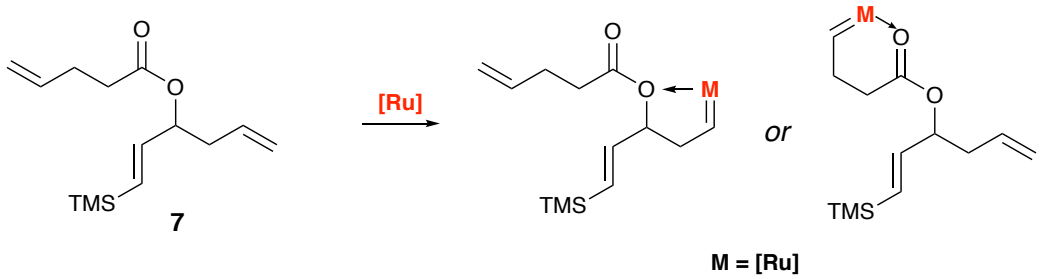


**Scheme 12**. Two possible chelation modes for ruthenium with the polar functional groups in diene **15**.

To inhibit this poisoning chelating effect, Lewis acids have been often used as co-catalysts in RCM. In the case of an oxygen atom being a chelating element, an oxyphilic transition metal Lewis acid can be used, such as titanium isopropoxide,[80–83] that could out-compete [Ru] and occupy the Lewis basic functionalities. However, upon treating our RCM reactions with either 0.3 equivalent, 1.0 equivalent or 2.0 equivalents of titanium isopropoxide, no beneficial effect was observed.

There were some other efforts we made for this RCM reaction. They are: 1) A range of temperatures from room temperature (in DCM or toluene) to 110°C (in toluene); 2) addition of extra catalysts after the reaction showed no more change on TLC plates; 3) carrying out the reaction at static vacuum using 1,3,5-trimethylbenzene as solvent, to maximize the ethylene extrusion and, 4) vigorous degassing of the solvent (multiple freeze-pump-thaw cycles). None of the adjustments showed any promise, it seems that diene **7** is not compatible with our current RCM protocols, certainly not with Grubbs-class ruthenium catalysts in our system. Complications could come from the possibility of vinyl silane moiety participating in the catalytic cycle, or other ruthenium catalysts decomposition pathways, which is a very active research area. There are other metal complexes that can be used for metathesis, although Schrock's molybdenum-based

catalysts are much more reactive metathesis catalysts than Grubbs'. It was avoided in our synthesis due to the extremely high cost and air/moisture sensitivity. We decided to explore other routes to access fragment **3**.

## 2.2 Second Synthetic Approach Towards Fragment 3

To access a strained ring using RCM reaction from an acyclic diene is usually both entropically and enthalpically disfavored, which is the major problem in our hands. Instead of building from an acyclic system, ring expansion provides an alternative way for larger ring formation, and this process should be largely entropically neutral. The second approach to fragment **16** features a two-atom ring expansion *via* Claisen rearrangement, from a 6-membered to the target 8-membered ring (**Scheme 13**).

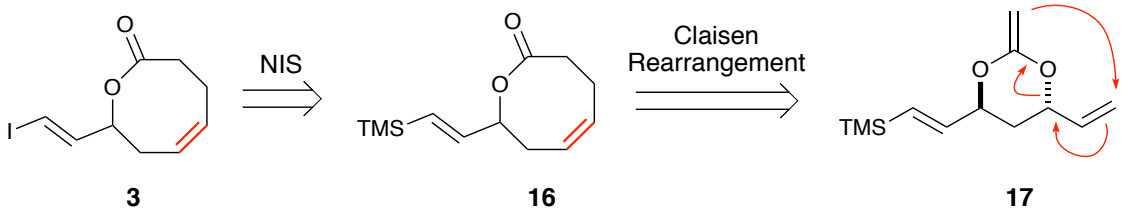


**3** **16** **17**

**Scheme 13.** The retrosynthetic analysis of fragment **3** featuring a Claisen rearrangement.

β-Hydroxyl ketone **19** was synthesized from an aldol condensation between aldehyde **5** and methyl vinyl ketone **18** (MVK) (**Scheme 14**).

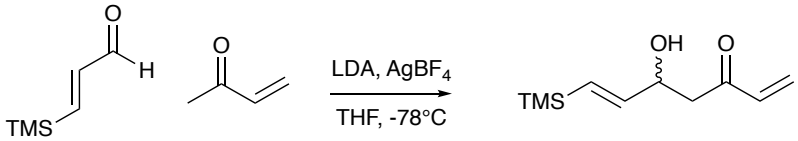


**10** *MVK* **18** **19**
30%

**Scheme 14.** Synthesis of β-hydroxyl ketone **19** *via* aldol condensation between aldehyde **10** and methyl vinyl ketone (MVK).

Although it seems to be straightforward and classic aldol reaction, the use of MVK as nucleophile is very rarely described in the literature. The reaction is very sensitive to

the order of addition of reagents. First of all, MVK was added dropwise to LDA solution to ensure complete formation of MVK enolate without self-condensation; secondly, the formed MVK enolate was added dropwise to the solution of aldehyde **10** and $AgBF_4$. In the literature, unfortunately, aldol condensation involving MVK **18** enolate either was very low yielding (addition to benzaldehyde at -78 °C, without any additive, 8% yield)[84], or used inaccessible additives. Hong and co-workers described the aldol condensations between MVK enolate and aldehydes by using superstoichiometric amount of various exotic lanthanide(III) Lewis acids, with up to 69% isolated yield (Lewis acid: $TbCl_3$).[84]

Another concern is that this aldol reaction produces the only stereogenic center present in the final product 7-HDHA. However, a literature search was disappointing for the possible enantioselective variant of the aldol reaction. The only example was a direct asymmetric Zn-aldol reaction of MVK using a catalytic amount of a dinuclear Zn-complex reported by Trost (**Figure 5**), with an average yield about 50% and moderate enantioselectivity.[85,86]

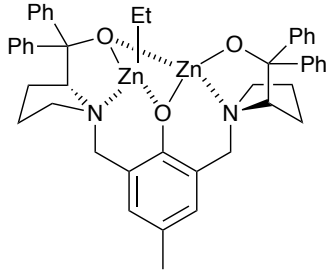


**Figure 5.** The catalytic zinc complex used in Trost's direct asymmetric Zn-aldol reactions of MVK.

There are also some methods that could be potentially used to achieve this aldol condensation. They include the use of arginine,[87] immobilized oligopeptides on magnetic particles,[88] and the pre-formation of silyl enol ether,[89,90], *etc*. These methods all have limited substrate scopes and inaccessible materials.

Nevertheless, β-hydroxyl ketone **19** was treated with tetramethylammonium triacetoxyborohydride [$Me_4N{\bullet}BH(OAc)_3$] to produce diol **20** diastereoselectively (**Scheme 15**). The use of triacetoxyborohydride to perform *anti*-reduction of β-hydroxyl ketones was

first described by Saksena and co-workers in 1983.[91] They employed sodium triacetoxyborohydride [Na•BH(OAc)$_3$], and envisioned an intramolecular hydride delivery directed by the β-hydroxyl group. The method was further developed and improved by Evans in 1987,[92] and has been used widely and reliably in many syntheses.[93,94]

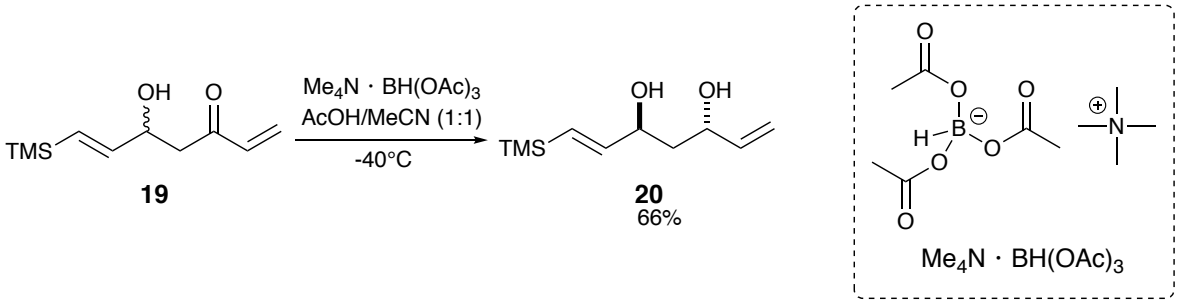


**Scheme 15.** The synthesis of cyclic carbonate **20**.

Triacetoxyborohydride itself can reduce aldehyde in the presence of ketone,[95] this weak reactivity comes from the electron-withdrawing effect of the three acetoxy groups as well as the steric shielding of the B-H bond. The low hydride reduction potential is needed to minimize the interference of completing bimolecular reductions. However, the acetoxy group is a readily exchangeable ligand. The hydroxyl group could pre-associate with the reducing agent. This leads to a relatively more electron-rich boron species that then reduces carbonyl group *via* a well-defined transition state, in an intramolecular fashion (**Scheme 16**).

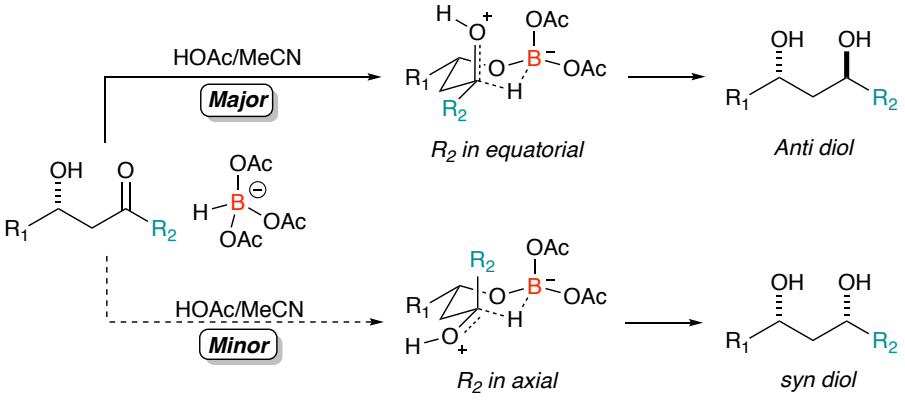


**Scheme 16.** β -hydroxyl directed anti-reduction of a ketone *via* well-defined six-membered ring transition state.

Although both $Me_4N\bullet BH(OAc)_3$ and $Na\bullet BH(OAc)_3$ were available, we chose the former to avoid any coordinating counter ions (such as $Na^+$) that might interfere with the reaction. From a practical point of view, this reaction required -35°C to -40°C temperature overnight, a well-insulated bath equipped with a chiller was needed.

Diol **20** was then converted to a cyclic carbonate **21**, with N,N'-carbonyl diimidazole (CDI), a far safer alternative to phosgene (**Scheme 17**). Carbonate **21** was then treated with freshly prepared $Cp_2TiMe_2$ to give cyclic ketene acetal **17.** We expected **17** to undergo [3,3]-sigmatropic rearrangement to afford desired 8-membered lactone in the same pot.

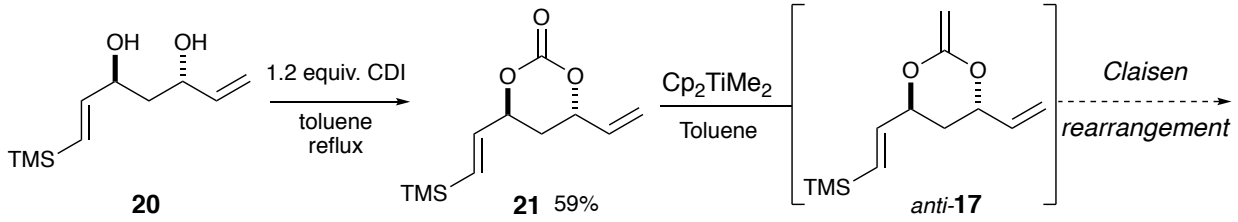


**Scheme 17.** The synthesis of carbonate **11** and the sequential *in situ* generation of the ketene acetal **12** by $Cp_2TiMe_2$.

The Petasis reagent $Cp_2TiMe_2$ was freshly prepared by salt metathesis reaction between methylmagnesium bromide with titanocene dichloride ($Cp_2TiCl_2$). The reaction was clean and $Cp_2TiMe_2$ was quantified by quantitative $^1$HNMR.[96] As an analog to Wittig reagents, $Cp_2TiMe_2$ can be used for methylenation of most types of neutral carbonyl functionalities including aldehydes, ketones, esters, anhydrides, carbonates, amides, imides, silyl esters, thioesters, selenoesters and acylsilanes, this robust reactivity is driven by Ti(IV)'s high oxophilicity.[97–101] The mechanism of the olefination involves the formation of a carbene complex ($Cp_2Ti{=}CH_2$) *via* thermal $\alpha$-elimination of $Cp_2TiMe_2$ (**Scheme 18**), which is followed by a [2+2] cycloaddition between the carbene and carbonyl group to afford an oxatitanacyclobutane intermediate, a sequential cyclo-reversion then delivers the cyclic ketene acetal **17** with the byproduct $Cp_2Ti{=}O$.

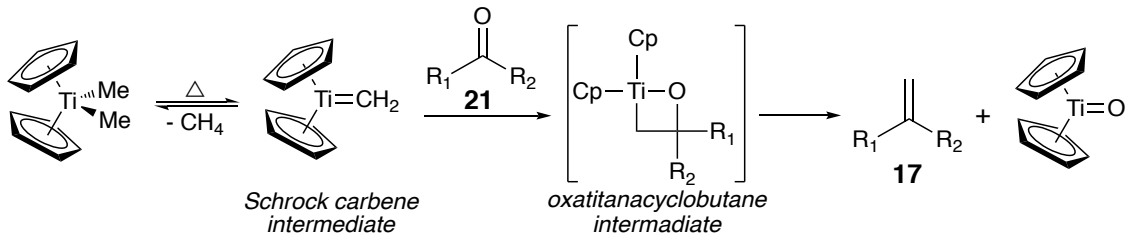


**Scheme 18.** The mechanism for the methylenation of carbonyl compounds using $Cp_2TiMe_2$.

The ring expansion method *via* Claisen rearrangement from cyclic ketene acetal has been explored extensively by Holmes and co-workers.[102–110] The transition state conformation analysis of the Claisen rearrangement provides an answer to why *anti*-diol configuration was needed in compound **20**: if ***syn*-20** was used, the resulting cyclic ketene acetal would have to adopt an unfavored 6-membered ring transition state with two substituents in axial positions (**Scheme 19**).

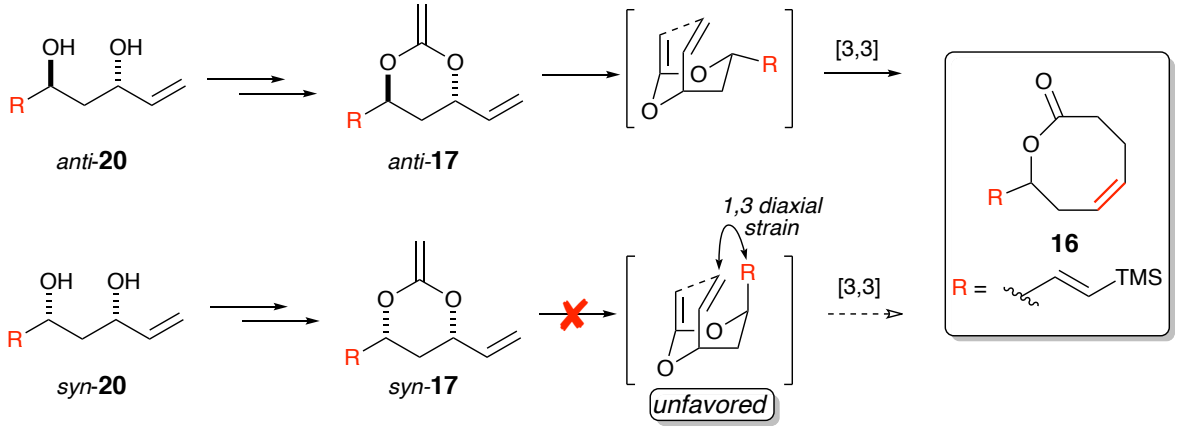


**Scheme 19.** Transition states of cyclic ketene acetal during Claisen rearrangement.

Apart from the fact that 8-membered rings favor internal Z-double bonds instead of the E configuration, the proposed transition state in **Scheme 19** also explains why the formation of Z-olefin is preferred to E-olefin from a kinetic point of view. Claisen rearrangement of **17** could either proceed through a chair-like or a boat-like transition state. The former would deliver a Z-olefin (compound **16**) while the latter will give an E-olefin[102,104](**Scheme 20**). Molecules that could adopt both transition state geometries will prefer the chair-like geometry. This argument is supported by strong evidence from Paquette's study on their Claisen-mediated formation of cyclooctenone.[111]

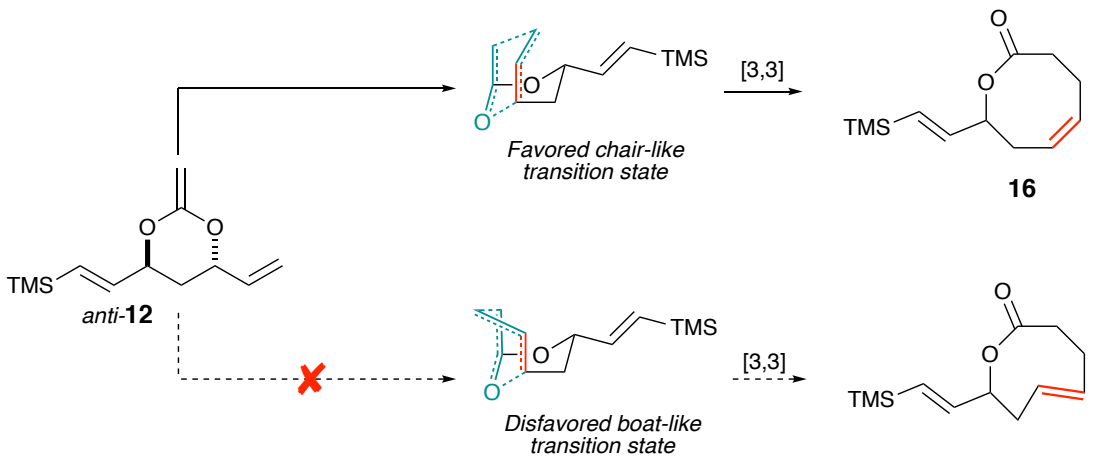


**Scheme 20.** The chair-like transition state during [3,3]-sigmatropic rearrangement explains the formation of Z-olefin.

Unfortunately, the one-pot methylenation-Claisen rearrangement of **21** only yielded a trace amount of product **16**. However, the 10-membered cyclic ketone **22** was formed as the major product. We reasoned that the desired product **16** was indeed formed, but in the presence of $Cp_2TiMe_2$, **16** quickly undergoes another methylenation-Claisen rearrangement sequence and thus results in cyclic ketone **22** (**Scheme 21**).

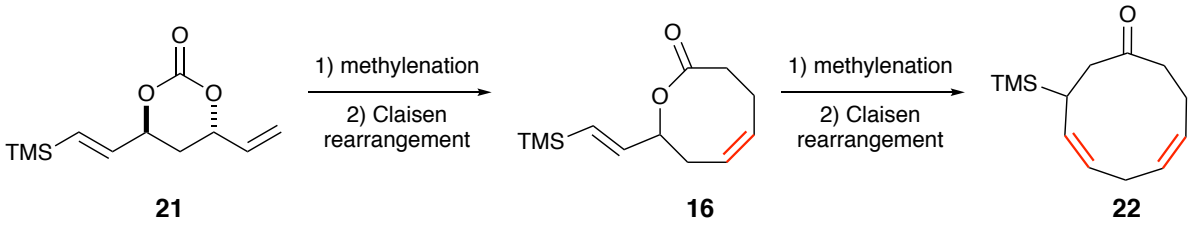


**Scheme 21**. The formation of cyclic ketone **22**.

The major product **22**'s NMR data corresponds perfectly with the proposed structure. First of all, $^{13}$C-NMR shows a characteristic ketone carbonyl carbon peak at 211.76 ppm. Secondly, it showed 11 carbon peaks, while the starting material **21** has 9 distinct carbon atoms; this supports the conclusion that the methylenation occurred twice because every methylenation would add one more carbon to the molecule. Thirdly, DEPT-135 showed that **22** has one quaternary carbon (C=O), 5 methine groups (-CH), 4 methylene groups (-$CH_2$) and 1 type of methyl groups (3 x -$CH_3$ in -TMS group). Lastly,

$^1$H-NMR suggests 4 alkenyl protons, 9 alkyl protons and 9 protons in the TMS group, 22 protons in total.

We concluded that $Cp_2TiMe_2$ was too reactive, and desired product **16** was likely more reactive than starting material **21** towards $Cp_2TiMe_2$, thus the reaction cannot stop at **16** under the reaction conditions.

## 2.3 Third Synthetic Approach Towards Fragment 3

To overcome the over methylenation issue in the previous attempt, we devised another method to access the Claisen rearrangement precursor **17**, it features the double bond formations *via* selenoxide elimination instead of $Cp_2TiMe_2$.

*Anti*-diol **32** was synthesized by the similar reaction sequence that led to *Anti*-diol **20** (**Scheme 22, B**) with the main difference being the aldol reaction. The aldol starting materials **26** and **30** were designed so that MVK was not involved. Therefore β-hydroxyl ketone **31** was formed with a much better yield than **19**. Also, aldehyde **26** was synthesized as the electrophile in the aldol reaction (**Scheme 22, A**), as here it served as an acrolein equivalent, acrolein being difficult to handle and thus should be avoided.

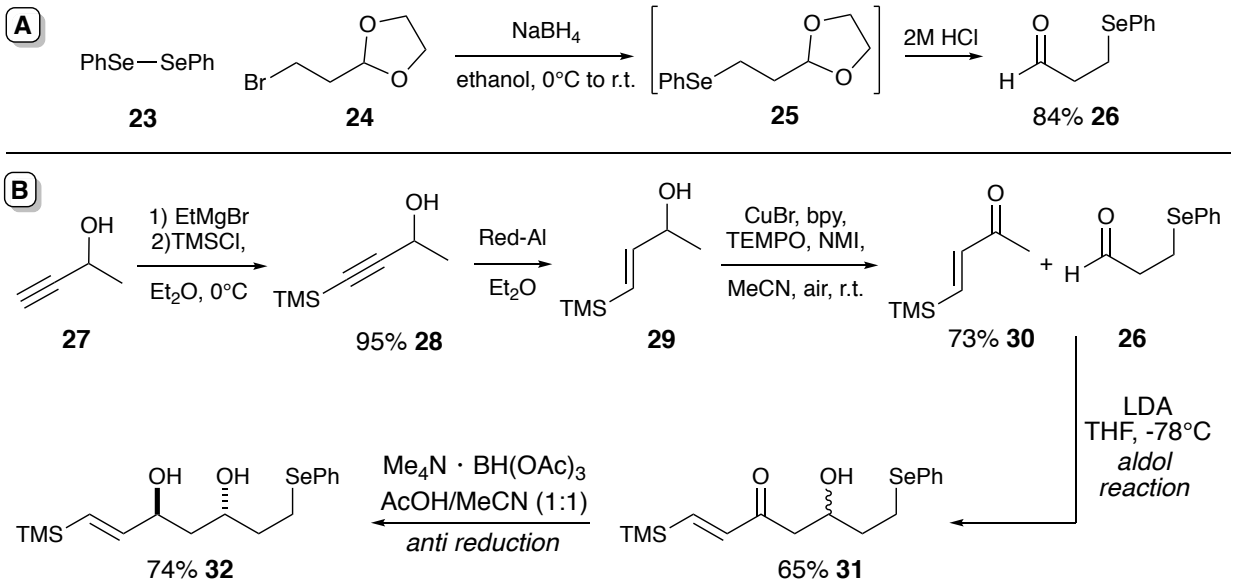


**Scheme 22.** The syntheses of aldehyde **26** and anti-diol **32**.

Acetal **35** was first synthesized quantitatively from electrophilic phenylselenyl chloride and ethyl vinyl ether in ethanol (**Scheme 23, A**). **35** serves as an acetal transfer reagent for the acetalization of diol **23** under acidic condition, furnishing cyclic acetal **36**. Since we designed **36** to contain two phenylselenide functionalities, upon treatment of a suitable oxidizing agent such as $NaIO_4$, we envisioned both phenylselenides should be oxidized to selenoxide, and then undergo fast thermal *syn*-elimination to deliver cyclic ketene acetal **17**.[112] In the same pot, we envisioned **17** would undergo a sequential Claisen rearrangement and deliver the desired lactone **16** (**Scheme 23, B**).[102–104,107,109]

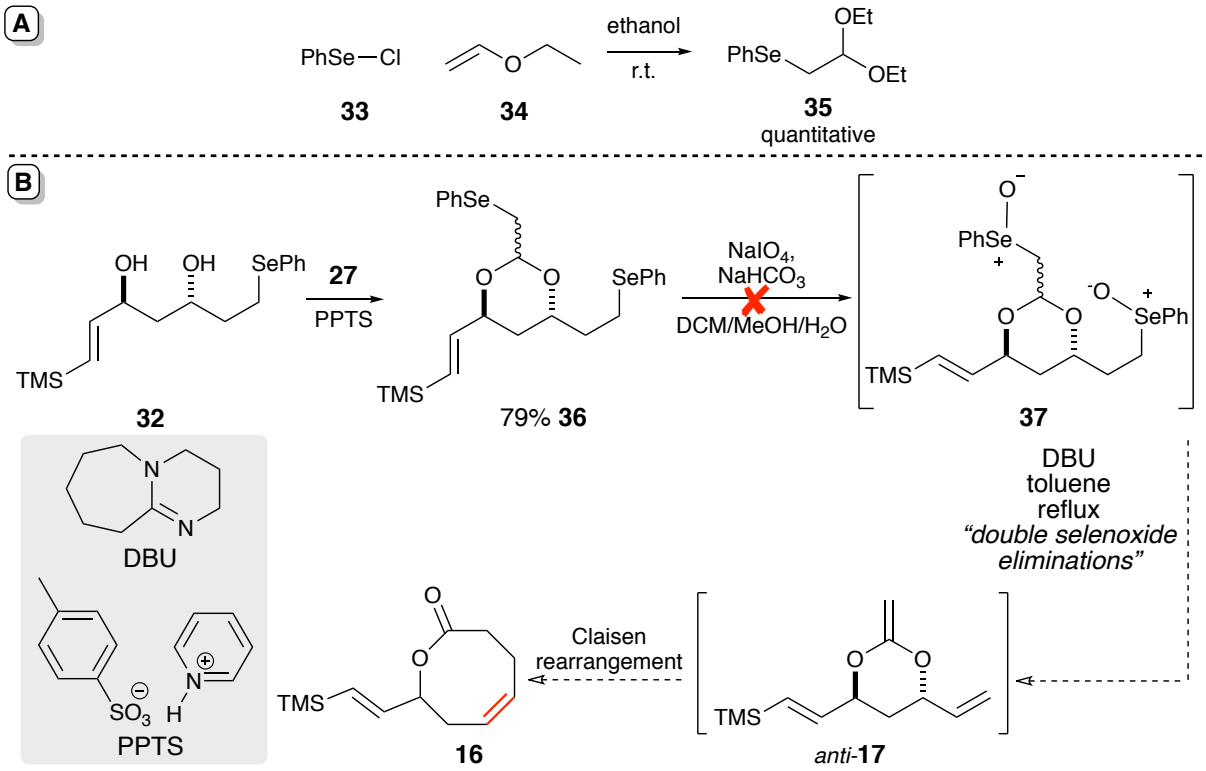


**Scheme 23.** The proposed alternative synthesis of lactone **8**.

However, after **36** was treated with the oxidation-Claisen sequence, no desired product **16** was observed. Only one selenide group underwent oxidation to give the only product **38** (**Figure 6**), even with a superstoichiometric amount of oxidant and elevated temperature.

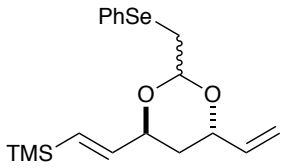


**38**

**Figure 6.** The only product **38** observed after treating **36** with oxidation-Claisen conditions described in **Scheme 23, B**.

The incompetent selenium oxidation under similar reaction conditions was also witnessed by Holmes and co-workers.[104,105] Perhaps it can be explained by the disproportionation of the elimination byproduct benzeneselenenic acid (**40**, PhSe-OH)

under the reaction condition (**Scheme 24**).[105] Assuming $Se^1$ undergoes β-elimination faster than $Se^2$, the selenoxide elimination byproduct, benzeneselenenic acid **40**, has been shown to disproportionate to benzeneseleninic acid **41** and diphenyl diselenide **42**. The latter can be a reducing agent and is hypothesized to transform selenoxide **39** back to **38**.

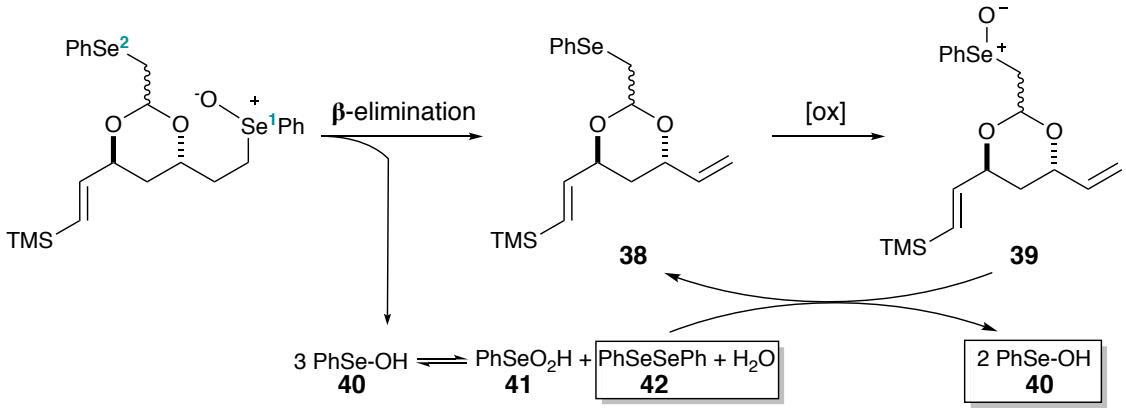


**Scheme 24.** Selenoxide **41** can be reduced back to selenide **39** because of the disproportionation of benzeneselenenic acid **41**.

Before exploring more reaction conditions to overcome the selenide oxidation problem, some other concerns about this olefination-Claisen method surfaced. First of all, ketene acetal intermediate **17** has two vinyl substituents branching off the ring, both of them could potentially undergo Claisen rearrangement with the ketene acetal group, although we anticipate the mono-substituted olefin to be more reactive. The same Claisen rearrangement with a vinyl silane (-$SiMe_2Ph$) also has been reported before.[110]

Our second concern was the iodination reaction from vinyl silane **16** to vinyl iodide **3** (**Scheme 10**). We performed many experiments to test the feasibility of the iodination with substrates similar to **16** (**Scheme 25**). After extensive experimentation, we failed to iodinate ester **15** as the reactions gave inseparable mixtures of products, and the best yield obtained with alcohol **13** was only 25%.

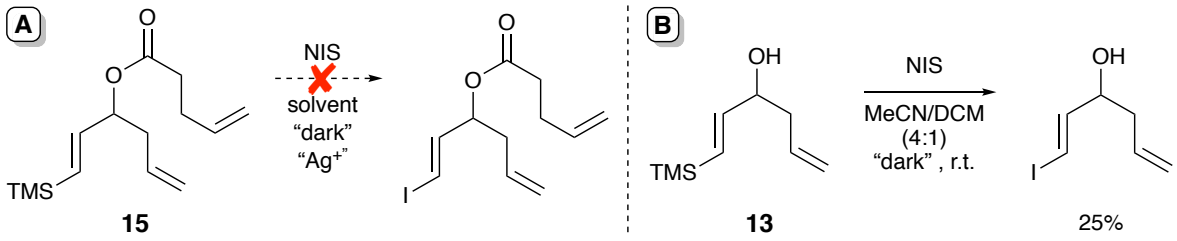


**Scheme 25.** Results of the desilyliodination reactions of **15** and **13**.

Facing these difficulties and limitations we experienced for the synthesis of vinyl iodide lactone **3**, we decided to start exploring the synthesis of **4**. The synthesis of **4** was also designed to bypass the problematic or low-yielding reactions we learned during the synthesis of **3,** such as the aldol condensation involving MVK and the desilyliodination reaction.

## 2.4 Synthetic Approach to Fragment 4

The synthesis of **4** can be accomplished by a Wittig reaction between aldehyde **43** and phosphonium ylide **44** (**Scheme 26**). Luckily, **44** is an unstabilized ylide which is required for the formation of Z-olefin. Although **43** seems to be a simple molecule, it contains a β-hydroxyl aldehyde, which is usually inaccessible by classic aldol. Moreover, in this case, the aldol reaction to form **43** would require an acetaldehyde that is particularly problematic because of its self-condensation. Alternatively, a Stork reaction could be employed to tackle this issue. However, the corresponding enamine from acetaldehyde is sensitive and requires distillation to purify, which is challenging without a proper setup.

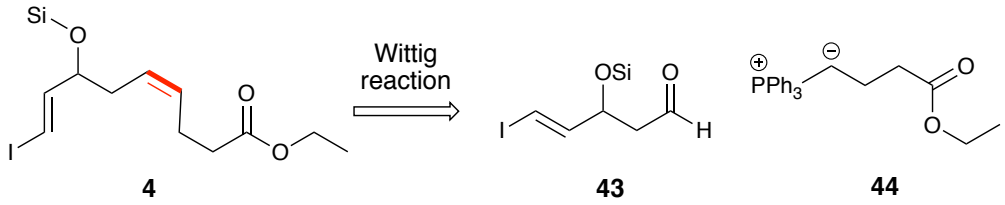


**Scheme 26.** Retrosynthetic analysis of **4**.

Therefore, we designed a synthesis of **43** that does not involve aldol-type reactions. Commercially available acetylene **45** was formylated with DMF to give aldehyde **46** in quantitative yield (**Scheme 27**). Aldehyde **46** was then treated with Grignard reagent **47** to deliver alcohol **48**. This reaction was performed at 60°C in THF. The high temperature required is unconventional for Grignard reactions. The acetylenic TIPS group was then removed by TBAF to give acetal **49**. Compound **49** is a masked β-hydroxyl aldehyde, the acetal group will be eventually removed to reveal the aldehyde, thus we decided to protect the -OH group with an acid-robust silyl group (TBDPS) and arrived at acetal **50**. Otherwise under the deacetalization conditions, the unprotected -OH tends to be eliminated and give exclusively the conjugated aldehyde, a problem we experienced in some early test experiments for acetal hydrolysis

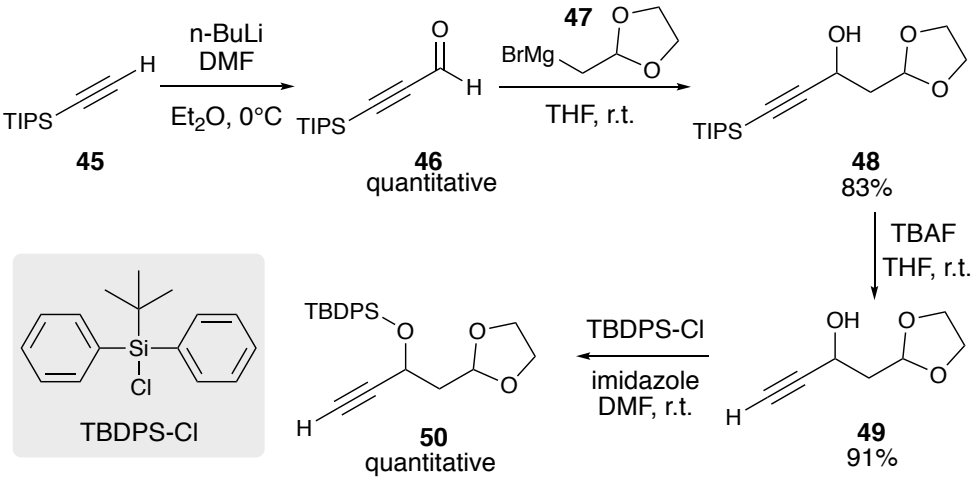


**Scheme 27**. The synthesis of **50**.

The significance of zirconocene hydrochloride ($HCp_2ZrCl$) in organic synthesis is well-established,[113–117] including in hydrozirconation or halogenation of alkenes and alkynes,[118,119] reductions of various organic functional groups such as amides and oxazolidinones (Evans' auxiliary),[118,120] as well as application in transition metal-catalyzed coupling reactions.[119] However, $HCp_2ZrCl$ suffers from a short shelf life due to its unstable nature. Therefore a number of efforts have been made to generate it *in situ*, which largely involves treating zirconocene dichloride ($Cp_2ZrCl_2$) with a reducing agent such as a metal hydride[118,119] or an alkylmagnesium bromide.[121]

Alkyne **50** was treated first with $HCp_2ZrCl$ generated *in situ* from $Cp_2ZrCl_2$ and DIBAL-H, then the reaction was quenched with $I_2$ to furnish vinyl iodide **51** (**Scheme 28**).[119] The *trans* double bond geometry was confirmed by the large coupling constant between the two alkenyl protons ($^3J_{HH}$ = 14.44 Hz). The aldehyde group in **52** was then revealed by hydrolyzing the acetal with a mild Lewis acid $PdCl_2(MeCN)_2$.

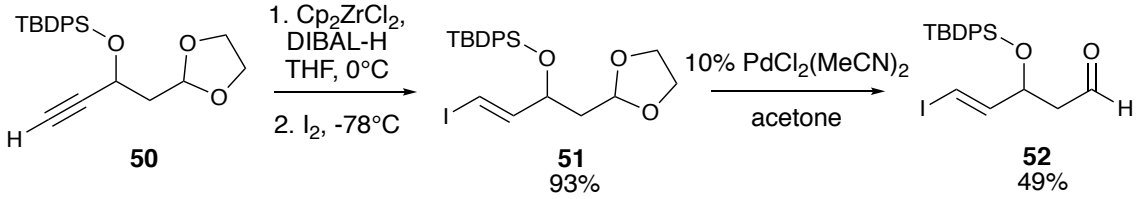


**50** **51** 93% **52** 49%

**Scheme 28.** The synthesis of aldehyde **52**.

The hydrozirconation of an alkyne with $HCp_2ZrCl$ is stereospecific, *cis* addition of Zr–H across the triple bond is almost always observed,[122] giving two possible vinyl zirconium intermediates **53** or **54** (**Scheme 29**). However, the zirconocene moiety is bulky and thus sensitive to steric congestion. It would preferably position itself away from the larger vinyl substituent, making **53** the dominant intermediate. Upon quenching **53** with $I_2$, a vinyl iodide **51** with E configuration was formed. In the last iodination step, the mechanism could be a direct electrophilic attack of the $-ZrCp_2Cl$ moiety, or a $\sigma$-bond metathesis, since an oxidative insertion pathway was impossible for an electropositive, $d^0$ metal center.

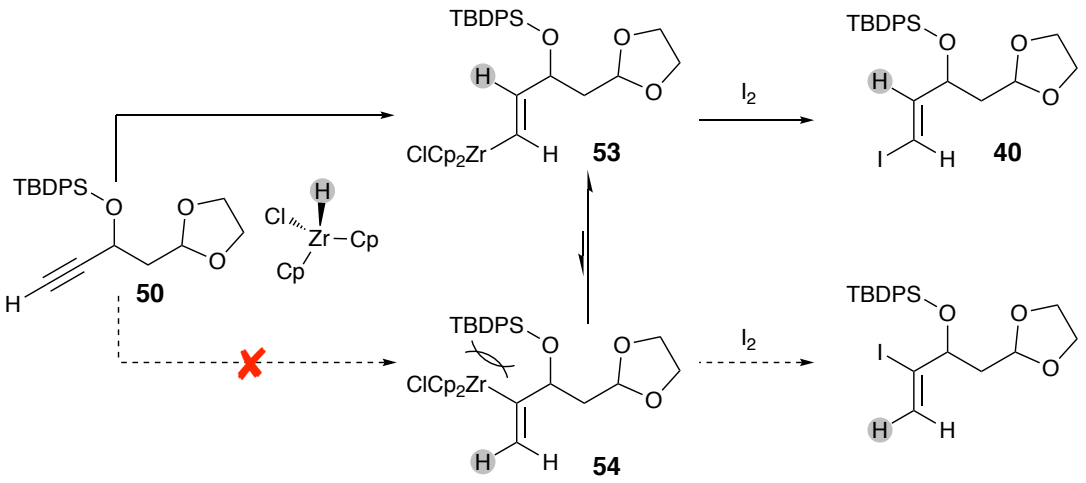


**Scheme 29.** Regioselectivity of the iodination of **50** *via* vinyl zirconium intermediate.

Before using $PdCl_2(MeCN)_2$, several methods to hydrolyze the acetal group in **51** were examined. When simple Bronsted acids were used, the hydrolysis was extremely slow, with very low conversion even after prolonged reaction time. Lewis acid-catalyzed transacetalization seemed to be more suitable in this case, with 10% $PdCl_2(MeCN)_2$ and a large excess of acetone, aldehyde **52** was obtained in 49% yield, the rest was almost all recovered **51**. It is worth mentioning that the much stronger Lewis acid $FeCl_3$ also gave a similar yield in much shorter reaction time, but no acetal **51** could be recovered due to other side reactions.

The desired compound **4** was synthesized by a Wittig reaction between the unstabilized phosphonium ylide **44** and aldehyde **52** in 58% yield (**Scheme 30**). To ensure its Z-olefin selectivity, the reaction temperature was strictly controlled below -78°C.

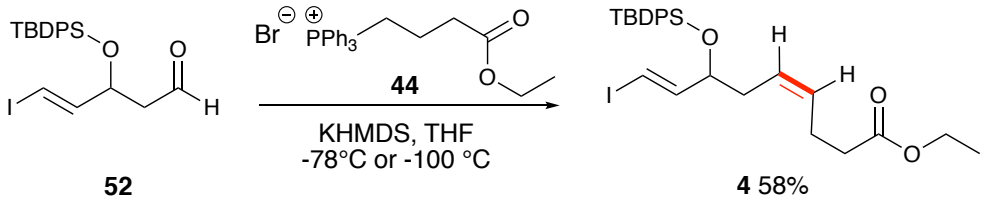


**Scheme 30.** The synthesis of fragment **4**.

The mechanism of the Wittig reaction has been the subject of substantial speculation and debate.[123] Proposed mechanisms include several different betaine

pathways,[124] [2+2] cycloaddition pathways,[125,126] single electron transfer pathway[127], *etc.* Also, the mechanism is likely to change with the reaction conditions and the reactants involved. Nevertheless, the formation of an oxaphosphetane intermediate during Wittig reaction is generally accepted. Under kinetic control in the transition state (TS) of the oxaphosphetane intermediate formation (**Scheme 31**), $R^2$ is positioned away from $R^1$ and the bulky triphenylphosphonium group to minimize steric interaction. The resulting oxaphosphetane intermediate would have two R groups in *a syn* relationship, which would naturally produce Z-olefin upon oxaphosphetane decomposition, with triphenylphosphine oxide as a byproduct, the thermodynamic driving force.

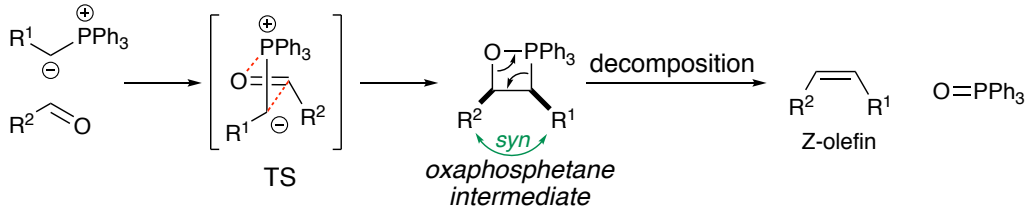


**Scheme 31.** The mechanism and stereoselectivity of Wittig reaction using non-stabilized phosphonium ylide.

The two alkenyl protons (H-4 and H-5) in product **4** gave an overlapping and complex multiplet on the $^1$HNMR spectrum, thus their coupling constants cannot be extracted directly to confirm the double bond geometry. Fortunately, H-4 and H-5's six neighboring protons (H-2, H-3, H-6) also appeared together between 2.1 to 2.2 ppm, ideal for a homo-decoupling NMR experiment (spectra: page 89). In the decoupled $^1$H-NMR spectrum of **4**, H-4 appeared as a doublet and H-5 became a doublet of doublets (H-5 is $^4J_{HH}$ coupled to H-7). The vicinal $^3J_{HH}$ between H-4 and H-5 can be determined to be 10.7 Hz, which falls into the range of typical $^3J_{HH}$ of two *cis* alkenyl protons (10-12 Hz).[128] Furthermore, the $^3J_{HH}$ of two alkenyl protons is 15.09 Hz in *trans*-2-butene, and 10.88 Hz in *cis*-2-butene,[129] with the latter is very close to that of **4** (**Scheme 32**).

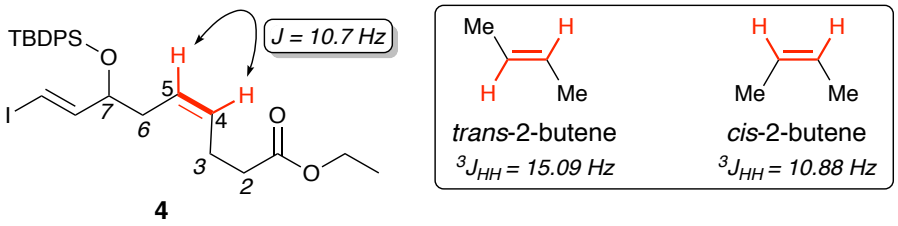


**Scheme 32**. The confirmation of the double bond geometry between C4 and C5 *via* H-H coupling constant.

## 2.5 Synthetic Approach to Fragment 5

Commercially available alcohol **55** was converted to the corresponding tosylate **56** by treating with tosyl chloride (**Scheme 33**).[130] The Cu-mediated coupling reaction between **56** and propargyl alcohol afforded alcohol octa-2,5-diyn-1-ol **57** in good yield.[131] The -OH group in **57** was then converted to a bromide (**58**) by an Appel reaction using triphenylphosphine and $CBr_4$. In the Appel reaction, $CBr_4$ can be substituted with $Br_2$ and result in the formation of **58** with the same yield. Next, the direct propargylic substitution of **58** with commercially available skipped diyne **59,** under the same CuI-mediated conditions, gave TMS-protected skipped tetrayne **60**. The skipped tetrayne **60** is unstable and decomposes quickly during flash column chromatography. However, the crude product was very clean judging by its NMR, therefore the crude **60** was carried to the next step without further purification.

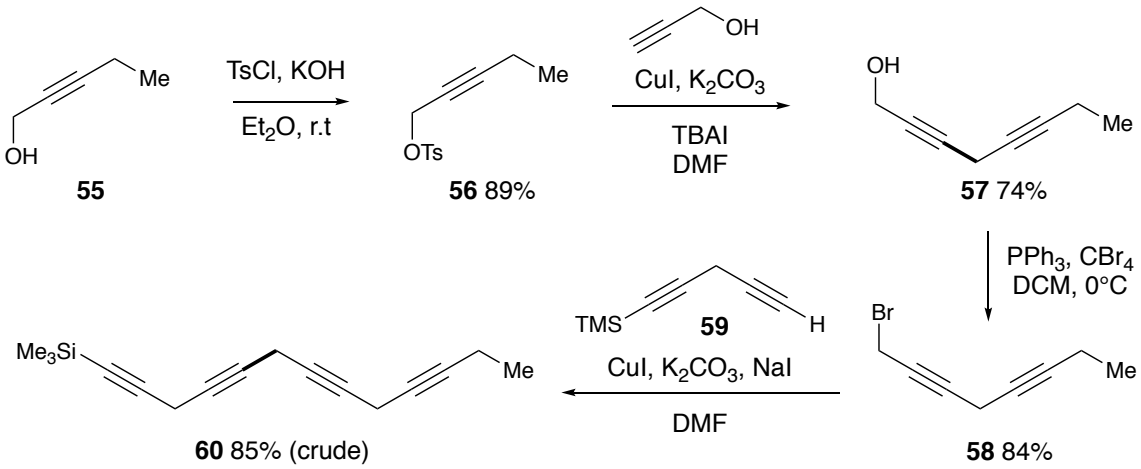


**Scheme 33.** The synthesis of skipped tetrayne **60**.

The copper-mediated substitution of propargylic halide or tosylate by terminal alkynes provides a mild way to quickly assemble skipped poly-yne systems. This method was described almost at the same time by Jeffery,[132] Pivnitsky,[133] and Huang.[134] The reaction mechanism is generally accepted to be an $S_N2$ mechanism (**Scheme 34**). The acetylenic proton on the terminal alkyne is significantly acidified by the coordination of $Cu^I$ to the triple bond. After deprotonation, a copper(I) acetylide nucleophile is produced. In comparison, other methods usually involve the use of a strong base to create the acetylenic nucleophile, and the resulting highly basic and nucleophilic conditions are obliviously incompatible with many sensitive functional groups.

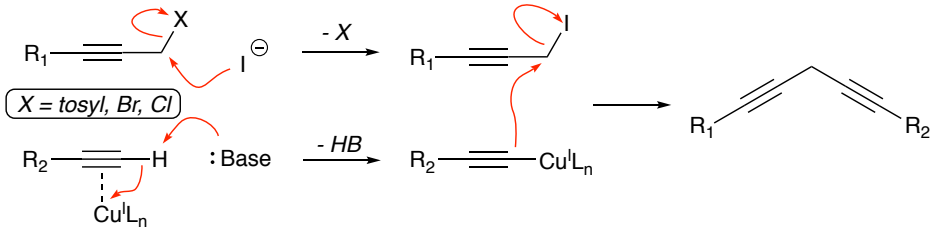


**Scheme 34.** The mechanism for the $Cu^I$-mediated propargylic substitution of a leaving group by a terminal alkyne.

The selective semi-hydrogenation of **60** to **61** was more challenging than expected. Initially attempts using Lindlar catalyst with 1.1 equivalents of quinoline additive under $H_2$ atmosphere failed. Varying the temperature, solvent and catalyst loading, the amount of

quinoline and the $H_2$ pressure did not lead to any improvement. The Rosenmund catalyst (Pd on $BaSO_4$) also failed to give any conversion under various conditions (**Scheme 35**). Although the hydrogenation of alkynes seems like a trivial matter and it was perceived as such in most student books, a literature survey suggests that the semi-reduction of alkynes becomes challenging in poly-yne systems. Especially when other functional groups are present, semi-hydrogenation reactions are usually highly dependent on conditions.[135] In some unfortunate cases, several alkyne substrates simply do not undergo hydrogenation using Lindlar or other Pd-based catalysts.[136]

Luckily there are many semi-hydrogenation methods in the chemist's toolbox. We decided to employ the P2-Ni heterogenous catalyst, although it was less practical compared to Lindlar or Rosenmund. During World War II, Brown and Schlesinger observed granular black precipitates when some first-row metal salts (cobalt, iron, nickel or copper) were treated with sodium borohydride. In aqueous media, they found out that when nickel acetate was treated with sodium borohydride, the resulting fine black power can be used to reduce olefins. Later this system was termed P1-Nickel. Subsequently, after extensive experimentations, a derivative of the P1-Nickel system was finally discovered to semi-hydrogenate alkynes to *cis*-alkenes, with excellent stereo- and chemoselectivity. This novel catalytic system was referred to as P2-Nickel, made under standardized conditions that include the use of $Ni(OAc)_2$, ethylenediamine as catalyst modifier and ethanol as solvent.

Even though the P2-Ni catalyst is extremely sensitive to oxygen and cannot be stored, it has emerged as one of the most used reducing reagents for the semi-hydrogenation of alkynes, probably only second to Lindlar catalyst, because of its mild reaction condition and extremely wide functional group compatibility. In our hands, the semi-hydrogenation of tetrayne **60** using P2-Ni catalyst provided **61** in 26% yield despite our best efforts (**Scheme 35**). It is worth noting that **60** was subjected to hydrogenation reaction as a crude product. Thus an impurity might have hampered the hydrogenation reaction. Lastly, the trimethylsilyl group was cleaved in $K_2CO_3$/methanol to furnish fragment **5**.

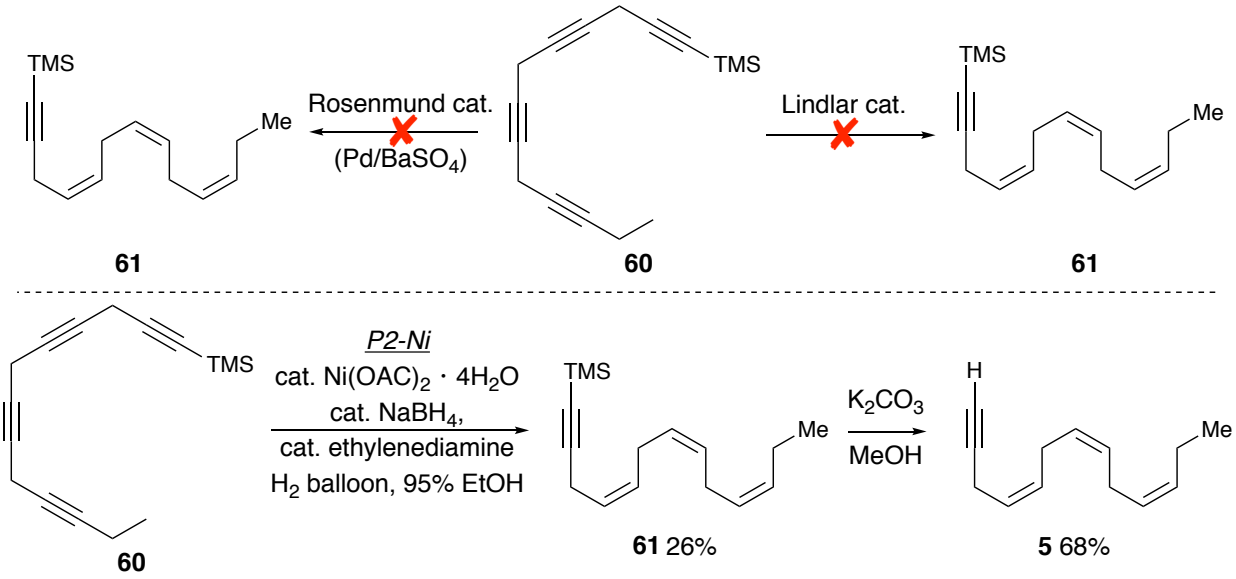


**Scheme 35.** Synthesis of **S3** *via* P2-Ni-catalyzed poly yne semi-hydrogenation.

## 2.6 Completion of the Synthesis of (±) 7-HDHA

With the fragment vinyl iodide **4** and terminal alkyne **5** in hand, we were ready to join these two pieces and complete the synthesis of our final target (±) 7-HDHA in a few more steps. Firstly, the complete carbon assembly of 7-HDHA can be furnished by a Sonogashira reaction between **4** and **5**.

The Sonogashira coupling is a palladium-catalyzed C-C bond forming reaction that couples a terminal sp-hybridized carbon atom with an $sp^2$ carbon atom of a vinyl or aryl halide or pseudo-halide. Since its development in 1975 by Sonogashira,[137] it has become one of the most robust ways to construct C-C bonds. A report in 2011 concluded that in medicinal chemistry, in terms of C-C formation, the Sonogashira reaction was the second most used reaction in the pursuit of drug candidates.[138] The mechanism of the Sonogashira reaction is generally believed to involve two independent catalytic cycles (**Scheme 36**). While the palladium cycle follows a classic mechanism of a palladium-catalyzed coupling reaction. The exact mechanism of the copper cycle is still poorly understood.[139] It is believed that the $Cu^I$ species coordinates to the terminal alkyne to give

a π-alkyne copper complex, that significantly increases the acidity of the acetylenic proton. A weak base is then able to remove the acetylenic proton and give a neutral copper acetylide, which can be transferred to the palladium cycle *via* transmetalation.[140]

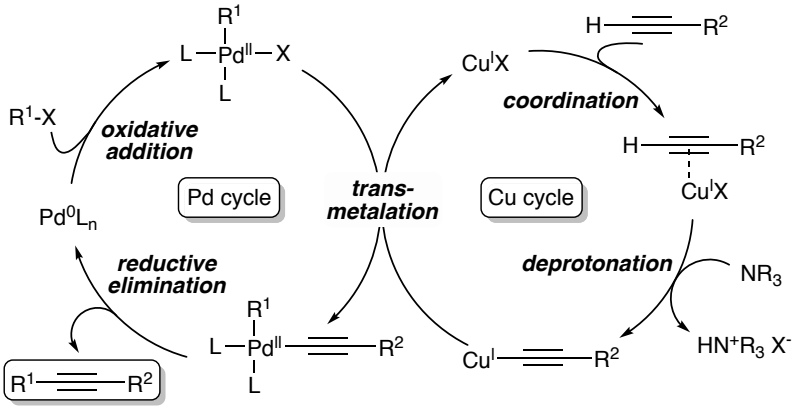


**Scheme 36.** The catalytic mechanism of Sonogashira coupling reaction.

The Sonogashira coupling reaction between **4** and **5** was very smooth (**Scheme 37**) and gave compound **2** (96%) as a 7-HDHA derivative.

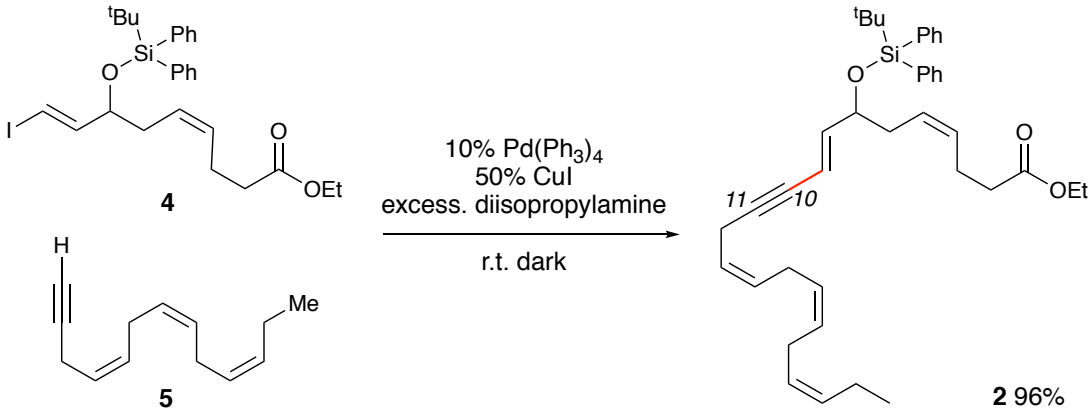


**Scheme 37**.The synthesis of **2** by Sonogashira coupling reaction.

The next step would be a *cis* semi-hydrogenation of **2** to furnish the final Z-double bond in the molecule between C10 and C11. The method needed to be very mild to avoid any possibilities of double bond isomerization. A survey of the literature confirmed some of our concerns associated with popular Pd-based catalysts. For example, Batista-Pereira and co-workers experienced an unexpected isomerization of a conjugated Z-double bond

to its more stable E configuration when Lindlar's catalyst was used (**Scheme 38, A**).[141] In the synthesis of lipoxin A4 (**Scheme 38, B**), Nicolaou and co-workers also reported the isomerization of the desired (7E,9E,11Z,13E)-tetraene to its more stable all-*trans* isomer during Lindlar semi-hydrogenation (DCM, r.t., quinoline). Although the isomerization only occurred to a small extent, the purification of the product tetraene was hampered, and ultimately required reverse-phase HPLC separation.[142] In another report that examed a series Pd-based semi-hydrogenation catalysts, the authors concluded that the extent of this *cis-trans* stereomutation was unpredictable.[143]

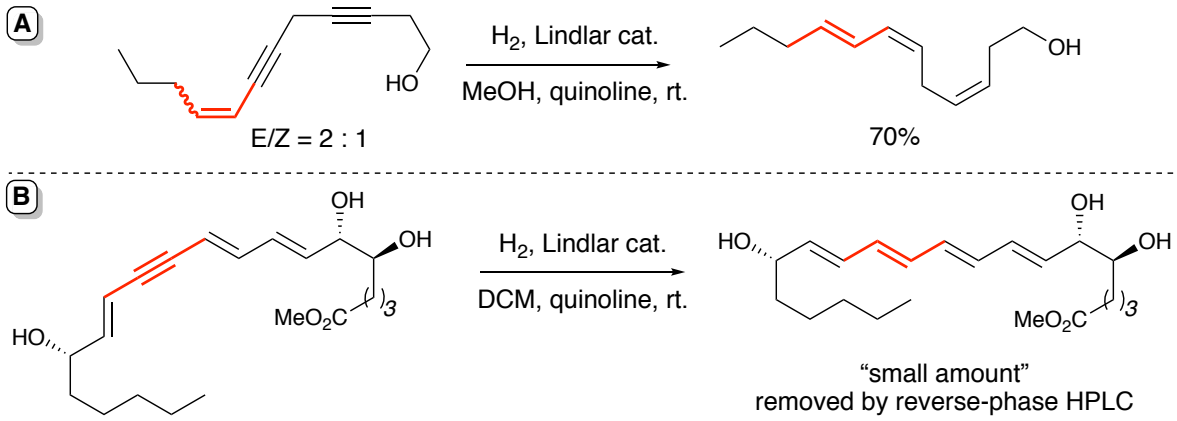


**Scheme 38**. Two examples of double bonds undergoing *cis-trans* isomerization under semi-hydrogenation using Lindlar catalyst.

With the concerns of olefin *cis-trans* isomerization and the consequential problematic separation, we decided to steer away from Pd-based semi-hydrogenation methods. During our literature search, a heterogeneous semi-hydrogenation method that uses a mixture of Zn(0), $Cu(OAc)_2$, and $AgNO_3$ reagents came to light. The Zn(Cu/Ag) semi-hydrogenation protocol was reported by Boland and co-workers[144] in the 1980s. In essence, this Zn-based semi-hydrogenation method features very mild reaction conditions, high reproducibility, excellent Z-selectivity, and fortunately in our favour, it is only reactive towards conjugated C-C triple bonds like the one in substrate **2**.

Initially, we followed the same reaction conditions as Boland and co-workers reported but always arrived at an incomplete conversion. Although no side product was formed, the separation of **1** and **2** was very difficult by flash column chromatography. To

achieve the full conversion of **2**, we first realized that the reaction solvent (water or methanol) cannot dissolve **2**, which made the introduction of a small amount of **2** into the reaction mixture impossible. Fortunately, one report used dioxane/water mixture as the reaction solvent and obtained a good yield and Z-selectivity.[145] Thus a solution of **2** in dioxane was prepared and efficiently transferred to the Zn(Cu/Ag) mixture. Secondly, the conversion increased when zinc dust was freshly activated by 1M HCl before use. Lastly and most importantly, we found that after the reaction stalled, spiking the reaction mixture with a few drops of aqueous 1M HCl can promote the reaction further to some extent.[145] The addition of small amounts of 1M HCl every 24 hours eventually pushed the reaction to completion in two days, and furnished **1** in quantitative yield (**Scheme 39**).

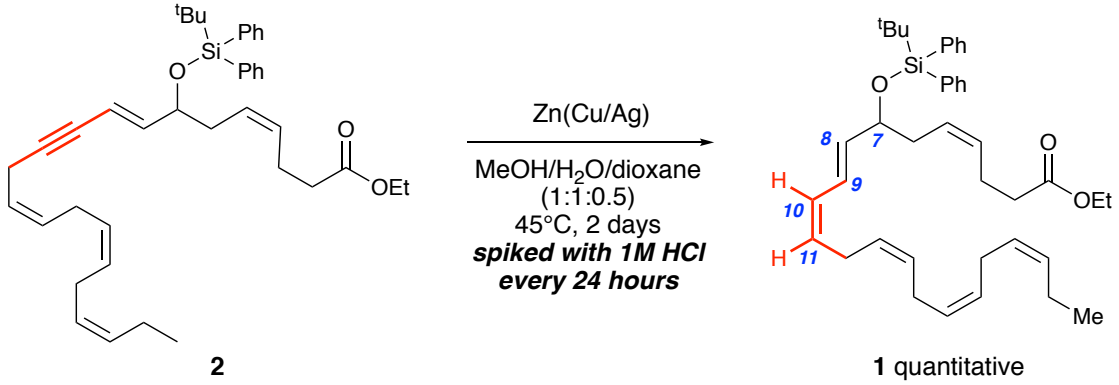


**2** **1** quantitative

**Scheme 39.** The synthesis of **1**.

In the $^{1}$H-NMR spectrum of product **1**, the signals of H-8, H-9, and H-10 were well resolved, however, H-11's peak completely overlaps with the other alkenyl protons. The H-10 signal was a doublet of doublets with coupling constants of 10.82 Hz and 10.82 Hz (apparent triplet), which falls into the range of typical $^{3}J_{HH}$ of two *cis* alkenyl protons. On the other hand, the *trans*-$^{3}J_{HH}$ between H-8 and H-9 was 15.11 Hz.

To complete the synthesis of (±) 7-HDHA, the TBDPS protecting group in **1** was removed with TBAF to reveal the alcohol **62** with 78% yield (**Scheme 40**). Next, the ester group in **62** was converted to a carboxylic acid group under ester hydrolysis condition (LiOH in THF/$H_2O$), delivering the final target (±) 7-HDHA in 80% yield.

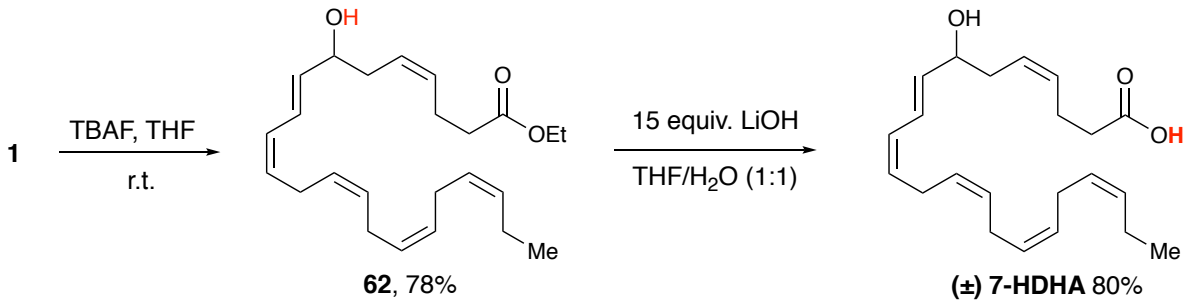


**Scheme 40.** Completion of the synthesis of (±) 7-HDHA.

To our best knowledge, there is no reported NMR data for (±) 7-HDHA in the literature. Thus, we acquired a collection of 1D and 2D NMR spectra from a 700 MHz NMR spectrometer, to confirm the structure of our synthesized (±) 7-HDHA. Using 2D COSY, 2D TOCSY, 2D HSQC, 2D HMBC, 2D HSQC-TOCSY, and 2D-HSQC-DEPT spectra, the connectivity of atoms of (±) 7-HDHA was proven, and all the carbon and proton signals were assigned. The *cis*-geometry of the double bonds can be confirmed by the 2D-NOESY spectrum, as the allylic protons on the opposite sites of a *cis* double bond show NOESY correlation.

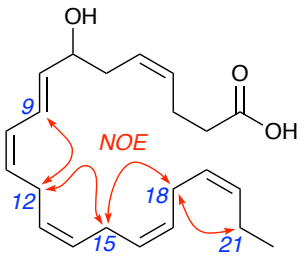


**Figure 7.** NOESY correlations are used to confirm the double bonds' *cis*-geometry.

# 3. Conclusion

In conclusion, convergent total synthesis of (±) 7-HDHA was completed with the longest linear reaction sequence of 11 steps from commercially available (triisopropylsilyl)acetylene. The overall yield of the final product is 12% (calculated based on the longest linear reaction sequence). This concise route mainly relies on the simultaneous formation of multiple Z-double bonds with the semi-hydrogenation catalyst P2-Nickel, and a late-stage semi-hydrogenation with Zn(Cu/Ag) reagent. Using this route, large quantities of (±) 7-HDHA were prepared rapidly with high quality (compared to commercial supply), and we are able to supply our collaborator generously. As a result, more comprehensive studies on (±) 7-HDHA in relations to PPAR nuclear receptors were initiated. Moreover, this synthetic route paved the way for the syntheses of enantiopure (+) 7-HDHA and (-) 7-HDHA that are currently in progress.

# 4. Experimental Section

## 4.1 General Experimental

All reactions were conducted in flame- or oven-dried glassware under an atmosphere of argon unless specified otherwise. All solvents were freshly distilled or obtained from solvent purification system (Inert® PureSolv MD5) prior to use unless specified otherwise. Triethylamine and diisopropylamine were distilled from $CaH_2$. Commercial reagents were used as received. Thin-layer chromatography was performed on SiliCycle® silica gel 60 F254 plates. Visualization was carried out using UV light (254 nm) and/or $KMnO_4$, $(NH_4)_2Ce(NO_3)_6$, vanillin, or anisaldehyde solution. Hexanes (ACS grade) and ethyl acetate (ACS grade) were used as received. Flash column chromatography was carried out using SiliCycle® *SiliaFlash*® silica gel (230-400 mesh, 40-63 μm, 60 Å pore size). All NMR spectra were recorded on a Bruker 300 AV, Bruker 400 AV, Bruker DRX 600 or Bruker Ascend 700 spectrometer in chloroform-d (99.8% deuterated), using TMS in chloroform-d as an external standard. Spectral recorded using chloroform were calibrated to 7.26 ppm $^{1}H$ and 77.16 ppm $^{13}C$. Chemical shifts ($\delta$) are reported in ppm and multiplicities are indicated by s (singlet), d (doublet), t (triplet), q (quartet), p (pentet), sext (sextet), td (triplet of doublets), dd (doublet of doublets), dddd (doublet of doublet of doublet of doublets), m (multiplet), or br (broad). Coupling constants *J* are reported in Hertz (Hz).

## 4.2 Experimental Procedures of the Synthesis of (+) 7-HDHA: Final Route

3-(triisopropylsilyl)propiolaldehyde (**46**)

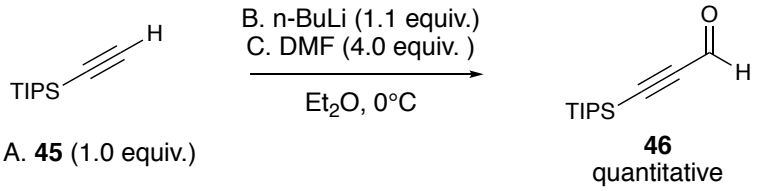


A. **45** (1.0 equiv.)

**46**
quantitative

An oven-dried 200 mL round-bottom flask was filled with argon, and charged with a magnetic stirring bar and A (**45**, 5.00 g, 27.42 mmol, 1.0 equiv.) in 30 mL dry $Et_2O$. The solution was cooled to 0°C, n-BuLi (1.6 M in hexane, 18.85 mL, 30.16 mmol, 1.1 equiv.) was added dropwise to the flask at 0°C, and the reaction was stirred at 0°C for 30 min. DMF in 20 mL $Et_2O$ was then added dropwise to the reaction mixture at 0°C. The reaction mixture was stirred at 0°C for 2 hours and was then quenched at 0°C by slow addition of 1M HCl until a slightly acidic pH was reached. After 1 hour of stirring at room temperature. the organic phase was separated, and the aqueous phase was extracted exhaustively with ether. The organic layers were combined, washed over brine and dried over MgSO4, filtered and concentrated under reduced pressure. The residual oil was purified by flash chromatography using ethyl acetate and hexane (10:90) as eluent to afford 1-(triisopropylsilyl)-1-propynal (**46**) as a pale-yellow oil (5.73 g, 99% yield). The $^1$H-NMR and $^{13}$C-NMR data is in accordance with that previously reported in the literature.[146]

**$^1$H-NMR** (400 MHz, $CDCl_3$), see page 74

δ 9.21 (s, 1H), 1.13-1.09 (m, 21H)

**$^{13}$C-NMR** (100 MHz, $CDCl_3$), see page 75

δ 176.80, 104.60, 101.06, 18.55, 11.08

1-(1,3-dioxolan-2-yl)-4-(triisopropylsilyl)but-3-yn-2-ol **(48)**

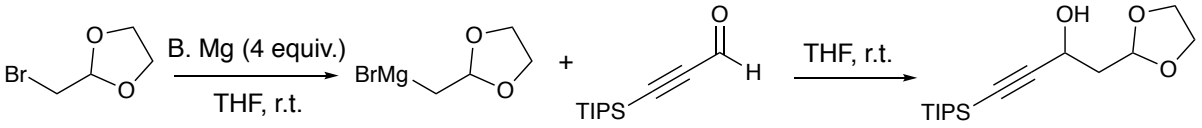


A. 2 equiv. C **47** D. **46** (1.0 equiv.) **48** 83%

An oven-dried 200 mL round-bottom flask was filled with argon, charged with a magnetic stirring bar and equipped with a condenser. B (458.47 mg, 19.00 mmol, 4 equiv.) and 20 mL THF was first added to the flask, followed by the addition of A (1.59 g, 9.5 mmol, 2 equiv.) and a crystal of $I_2$. The reaction mixture was stirred for 2 hours at room temperature, then D (1.0 g, 4.75 mmol, 1 equiv.) in 5 mL THF was added dropwise to the Grignard reagent. The reaction mixture was stirred at room temperature overnight, and then cooled to 0°C. 20 mL of water was added to the reaction, which was followed by the addition of saturated aqua. $NH_4Cl$. The organic phase was separated, and the aqueous phase was extracted with ether (X3). The organic layers were combined, washed over brine and dried over $MgSO_4$, filtered and concentrated under reduced pressure. The residual oil was purified by flash chromatography using ethyl acetate and hexane (30:70) as eluent to afford **48** as a colorless oil (1.18 g, 83% yield).

**$^1$H-NMR** (300 MHz, $CDCl_3$), see page 76

δ 5.17 (dd, *J* = 5.43 Hz, 4.41 Hz, 1H), 4.66 (m, 1H), 4.03-3.86 (m, 4H), 2.89 (d, *J* = 4.89 Hz, 1H), 2.21-2.02 (m, 2H), 1.07-1.05 (m, 20H)

**$^{13}$C-NMR** (75 MHz, $CDCl_3$), see page 77

δ 107.61, 102.68, 85.82, 64.98, 59.58, 41.15, 18.68, 11.21

**HRMS** (EI) mass $[M+NH_4^+]$+ calculated: 316.23025 *Da*; found: 316.23107 *Da*

1-(1,3-dioxolan-2-yl)but-3-yn-2-ol **(49)**

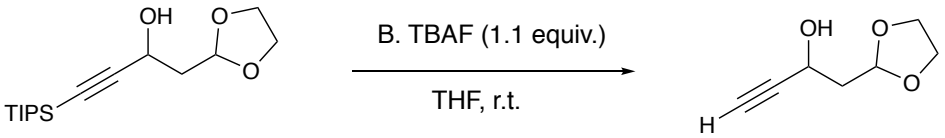


A. **48** (1 equiv.) **49** 91%

A 50 mL round-bottom flask was charged with a magnetic stirring bar, and A (500.0 mg, 1.68 mmol, 1 equiv.) in 20 mL THF. B (483.3 mg, 1.85 mmol, 1.1 equiv.) was added to the reaction mixture portion-wise. The mixture was stirred at room temperature for 3 hours. Next, the reaction mixture was concentrated using a rotary evaporator. The residual mixture was dissolved in ethyl acetate. This organic phase was then washed over brine, and dried over $MgSO_4$, filtered and concentrated under reduced pressure. The residual oil was purified by flash chromatography using ethyl acetate and hexane (50:50) as eluent to afford **49** as a colorless oil (217.13 mg, 83% yield). The $^{1}$H-NMR and $^{13}$C-NMR data is in accordance with that previously reported in the literature.[147]

**$^{1}$H-NMR** (300 MHz, $CDCl_3$), see page 78

δ 5.16 (dd, *J* =4.86 Hz, 4.68 Hz, 1H), 4.67 (m, 1H), 4.05-3.87 (m, 4H), 3.07 (d, *J* = 5.34 Hz, 1H), 2.48 (d, *J* = 2.22 Hz, 1H), 2.22-2.04 (m, 2H)

**$^{13}$C-NMR** (75 MHz, $CDCl_3$), see page 79

δ 102.53, 83.86, 73.17, 65.03, 58.86, 40.52

((1-(1,3-dioxolan-2-yl)but-3-yn-2-yl)oxy)(tert-butyl)diphenylsilane **(50)**

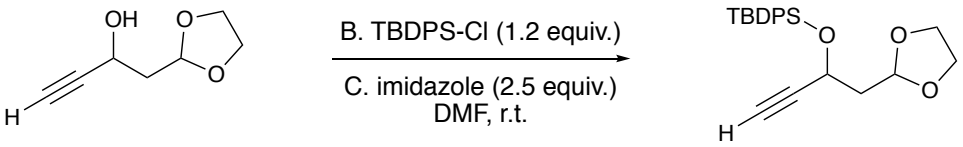


A. **49** (1.0 equiv.)

**50** quantitative

A 25 mL round-bottom flask was charged with a magnetic stirring bar and filled with argon. 5 mL of DMF was added to the flask, followed by the addition of A (214.00 mg, 1.51 mmol, 1 equiv.) and C (257.34 mg, 3.78 mmol, 2.5 equiv.). B (496.23 mg, 1.81 mmol, 1.2 equiv.) in 2 mL of DMF was added to the reaction mixture dropwise at room temperature. the reaction was stirred overnight. Next, the mixture was diluted with $Et_2O$, and water was added. The organic phase was separated, and the aqueous phase was extracted with ether (X3). The organic layers were combined, washed over brine and dried over $MgSO_4$, filtered and concentrated under reduced pressure. The residual oil was purified by flash chromatography using ethyl acetate and hexane (20:80) as eluent to afford **50** as a colorless oil (570.20 mg, 99% yield).

**$^1$H-NMR** (600 MHz, $CDCl_3$), see page 80

δ 7.75 (d, *J* = 6.72 Hz, 2H), 7.70 (d, *J* = 7.35 Hz, 2H), 7.44-7.36 (m, 6H), 5.02 (t, *J* = 5.1 Hz, 1H), 4.57 (td, *J* = 6.78 Hz, 1.92 Hz, 1H), 3.88-3.74 (m, 4H), 2.32 (d, *J* = 1.92 Hz, 1H), 2.10-2.03 (m, 2H), 1.08 (s, 9H)

**$^{13}$C-NMR** (150 MHz, $CDCl_3$), see page 81

δ 136.22, 136.06, 133.53, 129.89, 129.80, 127.72, 127.53, 101.77, 84.34, 73.55, 64.87, 64.76, 60.740, 42.94, 27.03, 19.44

**HRMS** (EI) mass $[M+H^+]+$ calculated: 381.18805 *Da*; found: 381.18857 *Da*

(E)-((1-(1,3-dioxolan-2-yl)-4-iodobut-3-en-2-yl)oxy)(tert-butyl)diphenylsilane **(51)**

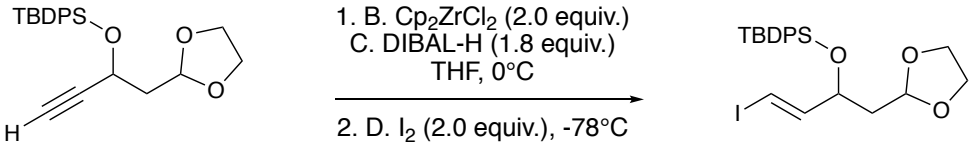


A. **50** (1.0 equiv.)

**51** 93%

A 25 mL round-bottom oven-dried flask was charged with a magnetic stirring bar and filled with argon. In the flask, B (602.16 mg, 2.06 mmol, 2.0 equiv.) was dissolved in 2.5 mL of THF, and the solution was cooled to 0°C. DIBAL-H (1.0 M in toluene, 1.85 mL, 1.85 mmol, 1.8 equiv.) was added dropwise into the reaction flask. The reaction was left stirring for 30 minutes. A (392.2 mg, 1.03 mmol, 1 equiv.) in 1.5 mL of THF was added dropwise to the reaction mixture at 0°C. After 1 hour of stirring, the reaction was cooled to -78°C, and D (522.85 mg, 2.06 mmol, 2.0 equiv.) in 1.5 mL of THF was added dropwise (very slowly) to the reaction mixture. After 20 minutes stirring, the reaction was quench with 1 M HCl. The organic phase was separated, and the aqueous phase was extracted with ether (X3). The organic layers were combined, washed successively with saturated $Na_2S_2O_3$, $NaHCO_3$ and brine, dried over $MgSO_4$, filtered and concentrated under reduced pressure. The residual oil was purified by flash chromatography using ethyl acetate and hexane (5:95) as eluent to afford **51** as a colorless oil (485.5 mg, 93% yield).

**$^1$H-NMR** (400 MHz, $CDCl_3$), see page 82

δ 7.66-7.61 (m, 4H), 7.43-7.36 (m, 6), 6.48 (dd, *J* = 14.44 Hz, 7.40 Hz, 1H), 5.88 (dd, *J* =14.24 Hz, 0.84 Hz, 1H), 4.87 (t, *J* = 5.16 Hz, 1H), 4.31 (q, *J* = 6.56 Hz, 1H), 3.87-3.72 (m, 4H), 1.92 (m, 1H), 1.80 (m, 1H), 1.05 (s, 9H)

**$^{13}$C-NMR** (100 MHz, $CDCl_3$), see page 83

δ 147.58, 135.94, 133.57, 129.76, 127.59, 101.53, 77.89, 73.01, 64.69, 64.64, 41.69, 26.99, 19.37

**HRMS** (EI) mass $[M+Na^+]+$ calculated: 531.0823 *Da*; found: 531.0816 *Da*

(E)-3-((tert-butyldiphenylsilyl)oxy)-5-iodopent-4-enal **(52)**

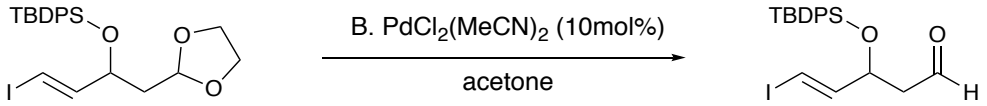


A. **51** (1.0 equiv.) **52** 49%

A 50 mL round-bottom flask was charged with a magnetic stirring bar, filled with argon and added 20 mL of acetone. A (50.00 mg, 0.1 mmol, 1.0 equiv.) was added to the flask, which was followed by the addition of B (2.60 mg, 0.01 mmol, 0.1 equiv.). the reaction mixture was stirred at room temperature, in the dark for two days. The solvent was then removed, and the residual mixture was dissolved in $Et_2O$, dried over $MgSO_4$, filtered and concentrated under reduced pressure. The residual oil was purified by flash chromatography using hexane and toluene (10:90) as eluent to afford **52** as a colorless oil (22.75 mg, 49% yield).

**$^1$H-NMR** (300 MHz, $CDCl_3$), see page 84

δ 9.67 (t, *J* = 2.19 Hz, 1H), 7.65-7.60 (m, 4H), 7.45-7.37 (m, 6H), 6.54 (dd, *J* = 14.48 Hz, 6.57 Hz, 1H), 6.12 (dd, *J* = 14.46 Hz, 0.99 Hz, 1H), 4.58 (q, *J* = 5.73 Hz, 1H), 2.59-2.44 (m, 2H), 1.05 (s, 9H)

**$^{13}$C-NMR** (176 MHz, $CDCl_3$), see page 85

δ 200.34, 146.45, 135.96, 133.07, 130.21, 127.93, 78.74, 71.77, 50.41, 27.04, 19.42

**HRMS** (EI) mass $[M+NH_4^+]$+ calculated: 482.10068 *Da*; found: 482.10053 *Da*

(4Z,8E)-ethyl 7-((tert-butyldiphenylsilyl)oxy)-9-iodonona-4,8-dienoate **(4)**

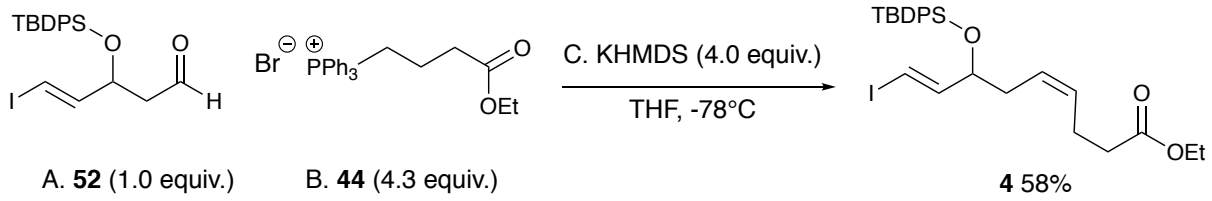


A. **52** (1.0 equiv.) B. **44** (4.3 equiv.) **4** 58%

A 25 mL round-bottom oven-dried flask was charged with a magnetic stirring bar and filled with argon. B (667.73 mg, 1.46 mmol, 4.3 equiv.) in 3 mL of THF was introduced into the flask, which was then cooled to -78°C. C (0.5 M in toluene, 2.72 mL, 1.36 mmol, 4.0 equiv.) was added dropwise into the flask, a yellow suspension was resulted. After 1 hour of stirring at -78°C. A (106 mg, 0.34 mmol, 1.0 equiv.) in 3 mL of THF was added dropwise (very slowly) to the reaction mixture. After 1 hour stirring at -78°C, the reaction was quenched by saturated $NH_3Cl$, and diluted with $Et_2O$. The organic phase was separated, and the aqueous phase was extracted with ether (X3). The organic layers were combined, washed with brine, dried over $MgSO_4$, filtered and concentrated under reduced pressure. The residual oil was purified by flash chromatography using ethyl acetate and hexane (5:95) as eluent to afford **4** as a colorless oil (110.84 mg, 58% yield).

**$^1$H-NMR** (400 MHz, $CDCl_3$), see page 86

δ 7.67-7.61 (m, 4H), 7.44-7.35 (m, 6H), 6.47 (dd, *J* = 14.40 Hz, 6.56 Hz, 1H), 5.98 (dd, *J* = 14.40 Hz, 1.04 Hz, 1H), 5.42-5.28 (m, 2H), 4.14-4.08 (m, 3H), 2.28-2.16 (m, 6H), 1.25 (t, *J* = 7.12 Hz, 3H), 1.06 (s, 9H)

**$^{13}$C-NMR** (100 MHz, $CDCl_3$), see page 87

δ 173.17, 147.86, 136.01, 133.89, 133.58, 130.39, 129.92, 127.75, 125.44, 75.70, 60.46, 35.25, 34.27, 27.12, 22.99, 19.46, 14.01

**HRMS** (EI) mass $[M+NH_4^+]$+ calculated: 580.17384 *Da*; found: 580.17322 *Da*

pent-2-yn-1-yl 4-methylbenzenesulfonate **(56)**

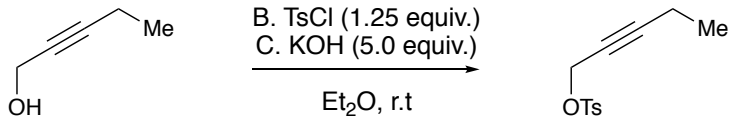


A. **55** (1.0 equiv.) **56** 89%

In a 100 mL round-bottom flask, A (1.00 g, 11.89 mmol, 1.0 equiv.) was dissolved in 25 mL $Et_2O$. B (2.83 g, 14.86 mmol, 1.25 equiv.) and C (3.34 g, 59.45 mmol, 5.0 equiv.) were added into the solution. after the mixture was stirred at room temperature overnight, 20 mL $Et_2O$ was added. The reaction mixture was washed with saturated $NaHCO_3$, brine, dried over $MgSO_4$, filtered and concentrated under reduced pressure to afford **4** as a pale yellow oil (2.51 g, 89% yield), no further purification was needed. The $^1$H-NMR and $^{13}$C-NMR data is in accordance with that previously reported in the literature.[131]

**$^1$H-NMR** (400 MHz, $CDCl_3$), see page 89

δ 7.82 (d, *J* = 8.28 Hz, 2H), 7.34 (d, *J* = 8.22 Hz, 2H), 4.70 (t, *J* = 2.16 Hz, 2H), 2.45 (s, 3H), 2.12-2.06 (m, 2H), 1.02 (t, *J* = 7.52 Hz, 3H)

**$^{13}$C-NMR** (100 MHz, $CDCl_3$), see page 90

δ 144.99, 133.60, 129.86, 128.29, 91.90, 71.35, 58.89, 21.78, 13.30, 12.49

octa-2,5-diyn-1-ol **(57)**

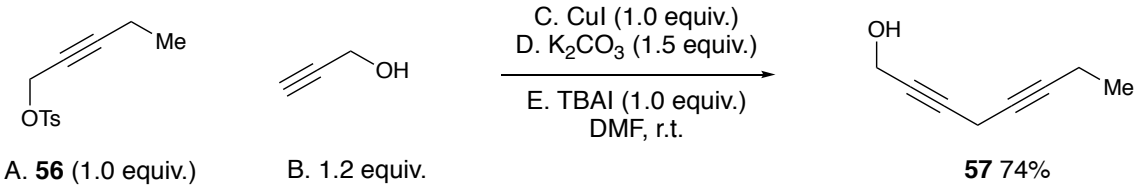


A. **56** (1.0 equiv.) B. 1.2 equiv. **57** 74%

In a 100 mL round-bottom flask, A (2.51 g, 10.53 mmol, 1 equiv.) was dissolved in 25 mL of DMF. C (2.01 g, 10.53 mmol, 1.0 equiv.), D (2.18 g, 15.80 mmol, 1.5 equiv.), and E (3.89 g, 10.53 mmol, 1.0 equiv.) were then added into the flask. The reaction mixture was cooled to 0°C, and B (708.60 mg, 12.64 mmol, 1.2 equiv.) was added dropwise. The reaction mixture was returned to room temperature, and stirred overnight. Next, the reaction mixture was cooled to 0°C, 20 mL cold water and 150 mL of saturated $NH_4Cl$ was added sequentially. The mixture was extracted three times with $Et_2O$. The organic layers were combined, washed with brine, dried over $MgSO_4$, filtered and concentrated under reduced pressure. The residual oil was purified by flash chromatography using ethyl acetate and hexane (30:70) as eluent to afford **57** as a yellow oil (816.20 mg, 76% yield). The $^1$H-NMR and $^{13}$C-NMR data is in accordance with that previously reported in the literature.[131]

**$^1$H-NMR** (400 MHz, $CDCl_3$), see page 91

4.27 (m, 2H), 3.19 (m, 2H), 2.18 (m, 2H), 1.12 (t, *J* = 2.16 Hz, 3H)

**$^{13}$C-NMR** (100 MHz, $CDCl_3$), see page 92

δ 82.58, 80.93, 78.48, 72.81, 51.36, 13.92, 12.45, 9.92

1-bromoocta-2,5-diyne **(58)**

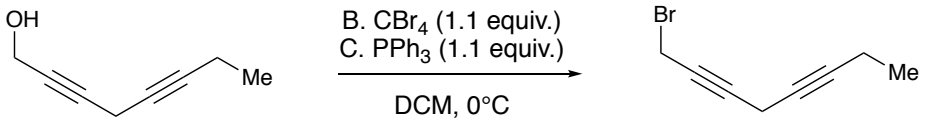


A. **57** (1.0 equiv) **58** 84%

A 100 mL round-bottom oven-dried flask was charged with a magnetic stirring bar and filled with argon. A (1.00 g, 8.19 mmol, 1.0 equiv.) and B (2.99 g, 9.01 mmol, 1.1 equiv.) were dissolved in 20 mL of DCM in the flask. C (2.36 g, 9.01 mmol, 1.1 equiv.) in 10 mL of DCM was then added dropwise to the reaction mixture. After overnight stirring at room temperature, the solvent was removed by using rotary evaporator, the residual mixture was purified directly using flash chromatography with ethyl acetate and hexane (5:95) as eluent to afford **58** as a pale yellow oil (1.27 g, 84% yield). The $^{1}$H-NMR and $^{13}$C-NMR data is in accordance with that previously reported in the literature.[148]

**$^{1}$H-NMR** (600 MHz, $CDCl_3$), see page 93

δ 3.92 (m, 2H), 3.21 (m, 2H), 2.17 (m, 2H), 1.12 (td, *J* = 7.44 Hz, 1.67 Hz, 3H)

**$^{13}$C-NMR** (150 MHz, $CDCl_3$), see page 94

δ 82.83, 82.25, 75.40, 72.32, 14.97, 13.94, 12.49, 12.49, 10.22

trimethyl(trideca-1,4,7,10-tetrayn-1-yl)silane **(60)**

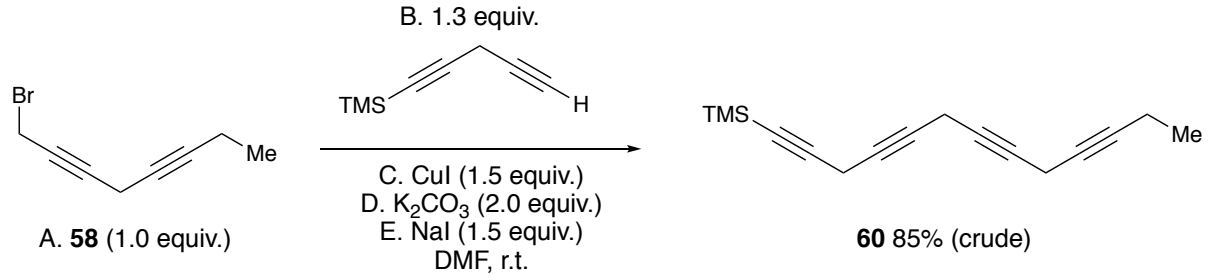


In a 200 mL round-bottom flask, A (1.29 g, 6.87 mmol, 1 equiv.) was dissolved in 60 mL of DMF. C (1.99 g, 10.46 mmol, 1.5 equiv.), D (1.93 g, 13.94 mmol, 2.0 equiv.), and E (1.57 g, 10.46 mmol, 1.5 equiv.) were then added into the flask. The reaction mixture was cooled to 0°C, and B (1.23 g, 9.06 mmol, 1.3 equiv.) was added dropwise. The reaction mixture was returned to room temperature and stirred overnight. Next, the reaction mixture was cooled to 0°C, 20 mL cold water and 150 mL of saturated $NH_4Cl$ was added sequentially. The mixture was extracted three times with $Et_2O$. The organic layers were combined, washed with brine, dried over $MgSO_4$, filtered and concentrated under reduced pressure to afford **60** as a red oil (1.43 g, 85% yield). The crude **60** was unstable and used for the next step immediately.

**$^1$H-NMR** (300 MHz, $CDCl_3$), see page 95

3.22 - 3.13 (m, 6H), 2.22 – 2.13 (m, 6H), 1.12 (t, *J* = 7.50 Hz, 3H)

trimethyl((4Z,7Z,10Z)-trideca-4,7,10-trien-1-yn-1-yl)silane **(61)**

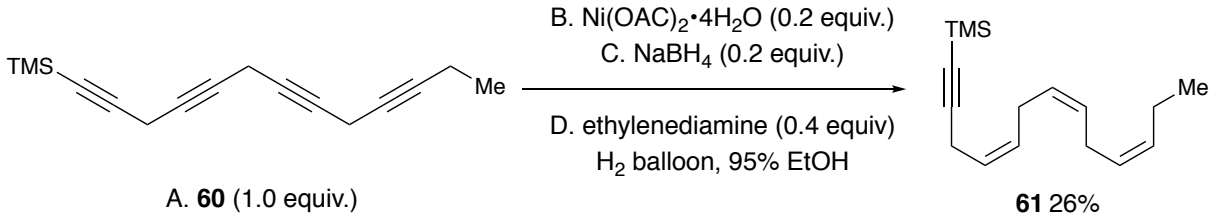


A. **60** (1.0 equiv.)

**61** 26%

A 125 mL round-bottomed flask was charged a magnetic stirring bar and B (301.1 mg, 1.21 mmol, 0.2 equiv.). The flask was purged with $H_2$ gas three times by vacuum-$H_2$ cycle. 20 mL of 95% EtOH (all EtOH used was degassed by freeze-pump-thaw method) was introduced into the flask under constant supply of $H_2$ gas flow. C (45.77 mg, 1.21 mmol, 0.2 equiv.) was pre-dissolved in 5 mL of 95% EtOH, and introduced into the reaction flask dropwise, and the reaction mixture turned to black. After 30 minutes of stirring, D (109.38 mg, 1.82 mmol, 0.4 equiv.) in 1 mL of 95% EtOH was then added into the reaction mixture. Next, A (1.46 g, 6.07 mmol, 1.0 equiv.) in 2 mL of 95% EtOH was introduced into the reaction mixture, and the flask was then sealed and equipped with an $H_2$ balloon. After overnight stirring, the reaction mixture was filtered through a pad of Celite and rinsed with ether. The filtrate was concentrated under reduced pressure, and purified by flash chromatography with pentane as eluent to afford **61** as a colorless oil (388.50 mg, 26% yield).

**$^1$H-NMR** (600 MHz, $CDCl_3$), see page 96

δ 5.48-5.29 (m, 6H), 3.02 (d, *J* = 4.74 Hz, 2H), 2.84-2.79 (m, 4H), 2.06 (m, 2H), 0.98 (t, *J* = 7.56 Hz, 3H), 0.15 (s, 9H)

**$^{13}$C-NMR** (150 MHz, $CDCl_3$), see page 97

δ 132.28, 130.02, 129.11, 127.38, 127.07, 124.44, 105.20, 84.48, 25.72, 25.70, 20.72, 18.56, 14.41, 0.24

**HRMS** (EI) mass $[M+H^+]+$ calculated: 247.2 *Da*; found: 247.2 *Da*

(4Z,7Z,10Z)-trideca-4,7,10-trien-1-yne **(5)**

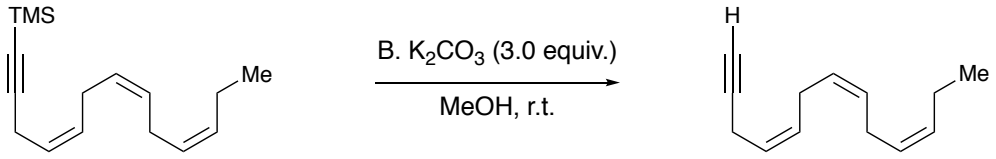


A. **61** (1.0 equiv.) **5** 68%

A 25 mL round-bottomed flask was charged with a magnetic stirring bar and 5 mL of THF/MeOH (1:1), A (100.0 mg, 0.41 mmol, 1.0 equiv.), and B (170.0 mg, 1.23 mmol, 3.0 equiv.). After the reaction mixture was stirred at room temperature for three hours, it was filtered through a pad of Celite. The filtrate was concentrated under reduced pressure, and purified directly by flash chromatography with pentane as eluent to afford **5** as a colorless oil (48.8 mg, 68% yield).

**$^1$H-NMR** (600 MHz, $CDCl_3$), see page 98

δ 5.55-5.30 (m, 6H), 3.00 (m, 2H), 2.88-2.82 (m, 4H), 2.10 (pentet, *J* = 7.57 Hz, 2H), 2.01 (t, *J* = 2.72 Hz, 1H), 1.00 (t, *J* = 7.54 Hz, 3H)

**$^{13}$C-NMR** (150 MHz, $CDCl_3$), see page 99

δ 132.39, 130.42, 129.29, 127.33, 127.11, 124.22, 82.84, 68.35, 25.78, 20.81, 17.12, 14.50

**HRMS** (EI) mass [M+H] calculated: 175.14813 *Da*; found: 175.14802 *Da*

(4Z,8E,13Z,16Z,19Z)-ethyl 7-((tert-butyldiphenylsilyl)oxy)docosa-4,8,13,16,19-pentaen-10-ynoate **(2)**

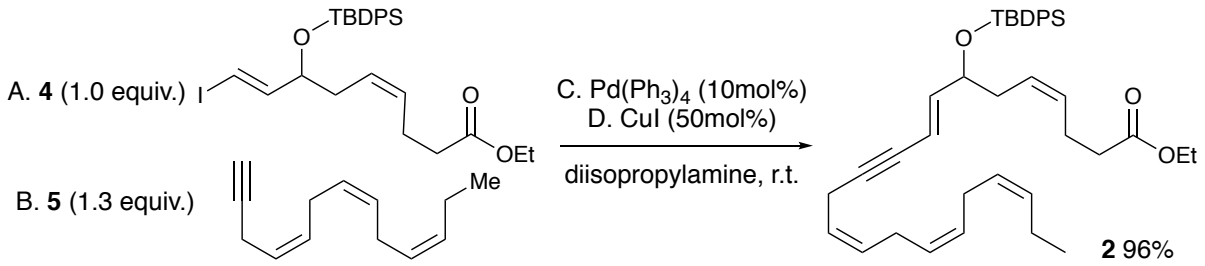


A 10 mL oven-dried round-bottomed flask was filled with argon. Two mL of freshly-distilled diisopropylamine, A (67.51 mg, 0.12 mmol, 1.0 equiv.) and C (13.87 mg, 0.012 mmol, 0.1 equiv.) were added into the flask. The resulting solution was stirred for 30 minutes. Next, D (11.43 mg, 0.06 mmol, 0.5 equiv.) and B (30.0 mg, 0.16 mmol, 1.3 equiv.) were added. After overnight stirring, the mixture was diluted with $Et_2O$, followed by adding saturated $NH_4Cl$. The aqueous layer was extracted with $Et_2O$ (X 3). The organic layers were combined, washed with brine, dried over $MgSO_4$, filtered and concentrated. The residual oil was purified by flash chromatography using ethyl acetate and hexane (5:95) as eluent to afford **2** as a colorless oil (69.9 mg, 96% yield).

**$^1$H-NMR** (400 MHz, $CDCl_3$), see page 100

δ 7.68 – 7.61 (m, 4H), 7.43 – 7.34 (m, 6H), 6.01 (dd, *J* = 15.84 Hz, 5.74 Hz, 1H), 5.54 (dd, *J* = 15.83 Hz, 1.51 Hz, 1H), 5.50 – 5.26 (m, 8H), 4.20 (m, 1H), 4.10 (q, *J* = 7.13 Hz, 2H), 3.09 – 3.08 (m, 2H), 2.86 – 2.80 (m, 2H), 2.28 – 2.04 (m, 2H), 1.24 (t, *J* = 7.13 Hz, 3H), 1.06 (s, 9H), 0.98 (t, *J* = 7.53 Hz, 3H)

**$^{13}$C-NMR** (150 MHz, $CDCl_3$), see page 101

173. 21, 144.09, 136.06, 136.04, 134.30, 133.81, 132.29, 130.00, 129.84, 129.79, 129.12, 127.72, 127.69, 127.42, 127.07, 125.80, 124.69, 110.05, 88.58, 78.73, 73.22, 60.40, 35.63, 34.24, 29.86, 27.18, 25.70, 22.99, 20.72, 18.50, 18.06, 14.41.

**HRMS** (EI) mass [M+H] calculated: 609.37585 *Da*; found: 609.37614 *Da*

(4Z,8E,10Z,13Z,16Z,19Z)-ethyl 7-((tert-butyldiphenylsilyl)oxy)docosa-4,8,10,13,16,19-hexaenoate **(1)**

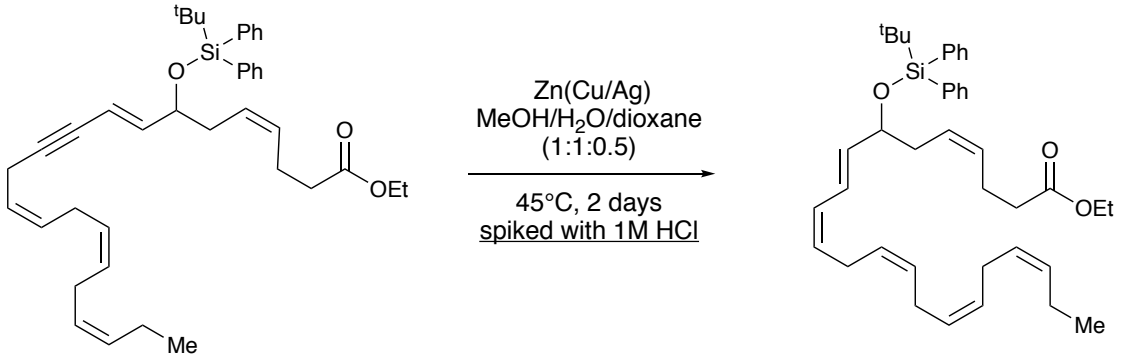


A. **2** (1.0 equiv.) **1** quantitative

**The Preparation of Zn(Cu/Ag)** 3.0 g of Zn dust was freshly purified by washing sequentially with 1 M HCl twice, distilled water, EtOH, and $Et_2O$ (the wash solutions were removed each time by filtration). The purified zinc dust was transferred into a 100 mL round-bottomed flask that was charged with a magnetic stirring bar and filled with argon. 30 mL of distilled water was added, and 300 mg of $Cu(OAc)_2 \cdot H_2O$ was added to the vigorously stirred suspension. After 15 minutes of stirring, 300 mg of $AgNO_3$ was added to the suspension. After another 30 minutes stirring, the water was filtered off under strict argon atmosphere, the wet Zn(Cu/Ag) cake was washed sequentially with acetone and $Et_2O$, the solvents were removed each time by filtration. The fresh Zn(Cu/Ag) was then dried under vacuum.

**The Synthesis of 1** The fresh Zn(Cu/Ag) was transferred to a 100 mL argon-filled round-bottom flask. 50 mL of MeOH: H2O (1:1) was added into the flask. A (150.0 mg, 0.25 mmol) in 1.5 mL of dioxane was added to the suspension of Zn(Cu/Ag). The reaction mixture was stirred at 45°C for 6 hours, then 0.2 mL of 1 M HCl was added to the reaction mixture. After overnight stirring, another 0.2 mL of 1 M HCl was added to the reaction. Aliquots were taken to check the consumption of A by $^1$H-NMR. Until the reaction reached full conversion, 0.2 mL of 1 M HCl was added to the reaction mixture every 16 to 24 hours. After the completion, the reaction mixture was filtered through Celite, the cake was rinsed with MeOH and then $Et_2O$ thoroughly. The filtrate was concentrated under reduced

pressure until most of the organic solvent was removed. The residual mixture was diluted with $Et_2O$, the organic layer was washed with water, then brine (X2), dried over $MgSO_4$, filtered and concentrated under reduced pressure. The residual oil was purified by flash chromatography using ethyl acetate and hexane (5:95) as eluent to afford **1** as a colorless oil (154.1 mg, 100% yield).

**$^1$H-NMR** (600 MHz, $CDCl_3$), see page 102

δ 7.69 – 7.64 (m, 4H), 7.42 – 7.33 (m, 6H), 6.22 (dd, *J* = 15.11 Hz, 11.09 Hz, 1H), 5.89 (t, *J* = 10.82 Hz, 1H), 5.61 (dd, *J* = 15.12 Hz, 6.54 Hz, 1H), 5.41 – 5.28 (m, 9H), 4.23 (m, 1H), 4.11 (q, *J* = 7.14 Hz, 2H), 2.83 – 2.78 (m, 6H), 2.32 – 2.28 (m, 1H), 2.25 – 2.22 (m, 3H), 2.20 – 2.16 (m, 2H), 2.05 (m, 2H), 1.24 (t, *J* = 7.22 Hz, 3H), 0.97 (t, *J* = 7.53 Hz, 3H)

**$^{13}$C-NMR** (150 MHz, $CDCl_3$), see page 103

δ 173. 25, 136.14, 136.08, 135.90, 134.48, 134.21, 132.20, 129.73, 129.66, 129.62, 128.78, 128.62, 128.34, 127.98, 127.64, 127.54, 127.17, 126.45, 125.39, 73.87, 60.40, 36.09, 34.32, 29.85, 27.19, 26.14, 25.76, 25.69, 23.06, 20.70, 19.49, 14.40

**HRMS** (EI) mass [M+H] calculated: 611.39150 *Da*; found: 611.39185 *Da*

(4Z,8E,10Z,13Z,16Z,19Z)-ethyl 7-hydroxydocosa-4,8,10,13,16,19-hexaenoate **(62)**

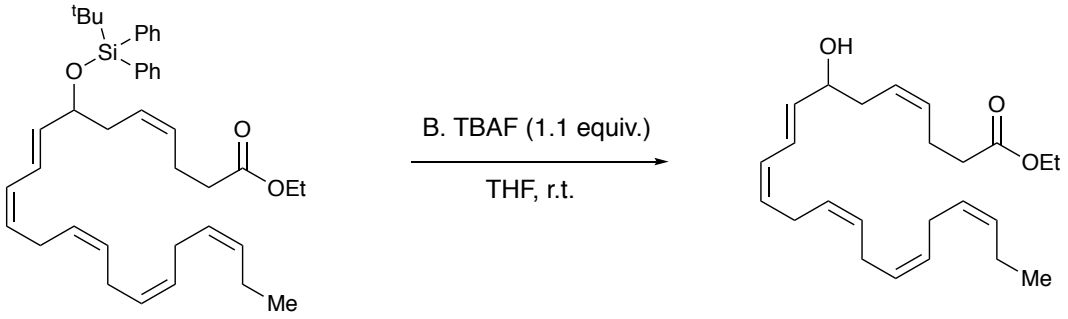


A. **1** (1 equiv.) **62** 78%

A 25 mL round-bottom flask was charged with a magnetic stirring bar, and A (130.0 mg, 0.21 mmol, 1 equiv.) in 10 mL THF, B (1M in THF, 0.24 mL, 0.23 mmol, 1.1 equiv.) was added to the solution drop-wise. The mixture was stirred at room temperature overnight. Next, the reaction mixture quenched by the addition of water, the aqueous layer was separated and extracted with ethyl acetate (X 3). The organic phase was then washed over brine, and dried over $MgSO_4$, filtered and concentrated under reduced pressure. The residual oil was purified by flash chromatography using ethyl acetate and hexane (15:85) as eluent to afford **62** as a colorless oil (61.4 mg, 78% yield).

**$^1$H-NMR** (700 MHz, $CDCl_3$), see page 104

δ 6.56 (dd, *J* = 15.07 Hz, 11.23 Hz, 1H), 6.02 – 5.99 (m, 1H), 5.73 (dd, *J* = 14.71 Hz, 6.44 Hz, 1H), 5.55 – 5.46 (m, 2H), 5.43 – 5.36 (m, 6H), 5.34 – 5.30 (m, 1H), 4.24 (m, 1H), 4.13 (q, *J* = 7.21 Hz, 2H), 2.97 (m, 2H), 2.85 (m, 2H), 2.81 (m, 2H), 2.42 – 2.33 (m, 6H), 2.08 (m, 2H), 1.25 (t, *J* = 7.03 Hz, 3H), 0.98 (t, *J* = 7.54 Hz, 3H)

**$^{13}$C-NMR** (150 MHz, $CDCl_3$), see page 105

δ 173.37, 135.88, 132.25, 131.23, 130.48, 128.81, 128.17, 127.96, 127.78, 127.17, 126.32, 125.61, 72.05, 60.59, 35.57, 34.13, 26.27, 25.82, 25.72, 23.02, 20.72, 14.41, 14.39

**HRMS** (EI) mass [M+$NH_4$] calculated: 390.30027 *Da*; found: 390.30028 *Da*

(4Z,8E,10Z,13Z,16Z,19Z)-7-hydroxydocosa-4,8,10,13,16,19-hexaenoic acid **(±) 7-HDHA**

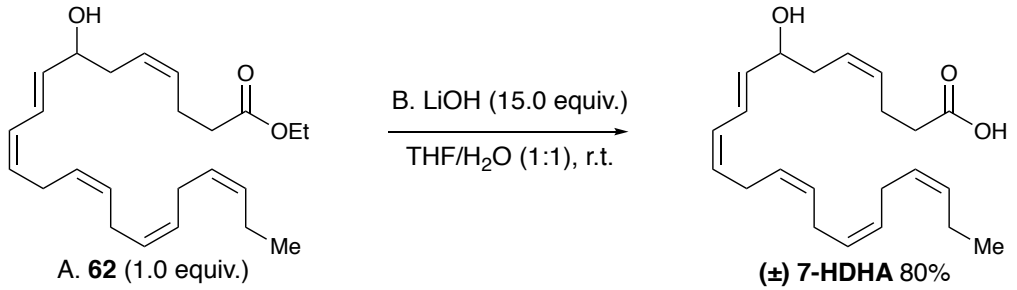


A. **62** (1.0 equiv.) **(±) 7-HDHA** 80%

In a 10 mL argon-filled round-bottomed flask, A (41.0 mg, 0.11 mmol, 1.0 equiv.) was dissolved in 3 mL of $H_2O$: THF (1:1), B (39.5mg, 1.65 mmol, 15.0 equiv.) was then added to the flask. The reaction was stirred at room temperature overnight. The reaction mixture was then cooled to 0°C, 1 M HCl was then added dropwise until the aqueous layer was acidified. The aqueous layer was extracted with ethyl acetate exhaustively. The organic phase was then washed over brine, and dried over $MgSO_4$, filtered and concentrated. The residual oil was purified by flash chromatography using ethyl acetate and hexane (50:50) as eluent to afford **(±) 7-HDHA** as a colorless oil (30.4 mg, 80% yield).

**$^1$H-NMR** (700 MHz, $CDCl_3$), see page 106

δ 6.55 (dd, *J* = 15.13 Hz, 11.06 Hz, 1H), 6.00 (t, *J* = 10.86 Hz, 1H), 5.72 (dd, *J* = 15.16 Hz, 6.41 Hz, 1H), 5.53 (m, 1H), 5.48 (m, 1H), 5.43 – 5.35 (m, 6H), 5.32 (m, 1H), 4.25 (m, 1H), 2.97 (t, *J* = 6.93 Hz, 2H), 2.85 (t, *J* = 6.41 Hz, 2H), 2.81 (t, *J* = 6.51 Hz, 2H), 2.45 – 2.33 (m, 6H), 2.09 – 2.06 (m, 2H), 0.97 (t, *J* = 7.84 Hz, 3H), the carboxylic acid proton was not observed in this spectrum.

**$^{13}$C-NMR** (176 MHz, $CDCl_3$), see page 107

δ 177.67, 135.65, 132.25, 130.93, 130.58, 128.80, 128.10, 127.94, 127.74, 127.14, 126.56, 125.69, 72.10, 35.46, 33.60, 26.25, 25.80, 25.70, 22.75, 20.71, 14.42

**HRMS** (ESI) mass [M-H]- calculated: 343.2268 *Da*; found: 343.2278 *Da*

## 4.3 COSY and HMBC Correlations of (±) 7-HDHA

(4Z,8E,10Z,13Z,16Z,19Z)-7-hydroxydocosa-4,8,10,13,16,19-hexaenoic acid **(±) 7-HDHA**

**COSY correlations**

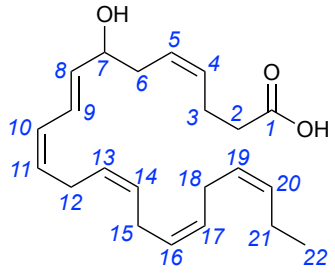


| Proton No. | $^1$H δ (ppm) (mult, *J* (Hz))[a,b] | COSY Correlations[c] |
|---|---|---|
| H-2 | part of the m at 2.45 – 2.33 | |
| H-3 | part of the m at 2.45 – 2.33 | |
| H-4 | 5.48 (m, 1H) | H-5 |
| H-5 | 5.53 (m, 1H) | H-4 |
| H-6 | part of the m at 2.45 – 2.33 | |
| H-7 | 4.25 (m, 1H) | H-8 |
| H-8 | 5.72 (dd, *J* = 15.16 Hz, 6.41 Hz) | H-7, H-9 |
| H-9 | 6.55 (dd, *J* = 15.13 Hz, 11.06 Hz) | H-8, H-10 |
| H-10 | 6.00 (t, *J* = 10.86 Hz) | H-9, H-12 |
| H-11 | part of the m at 5.43 – 5.35 | |
| H-12 | 2.97 (t, *J* = 6.93 Hz) | |
| H-13 | part of the m at 5.43 – 5.35 | |
| H-14 | part of the m at 5.43 – 5.35 | |
| H-15 | 2.85 (t, *J* = 6.41 Hz) | |
| H-16 | part of the m at 5.43 – 5.35 | |
| H-17 | part of the m at 5.43 – 5.35 | |
| H-18 | 2.81 (t, *J* = 6.51 Hz) | H-19 |
| H-19 | 5.32 (m) | H-18 |
| H-20 | part of the m at 5.43 – 5.35 | |
| H-21 | 2.09 – 2.06 (m) | H-22 |
| H-22 | 0.97 (t, *J* = 7.84 Hz) | H-21 |

[a] Recorded at 700 MHz,
[b] Assignments based on COSY, HSQC, HMBC, and HSQC-TOCSY.
[c] Only those correlations which could be unambiguously assigned are recorded.

(4Z,8E,10Z,13Z,16Z,19Z)-7-hydroxydocosa-4,8,10,13,16,19-hexaenoic acid **(±) 7-HDHA**

## HMBC correlations

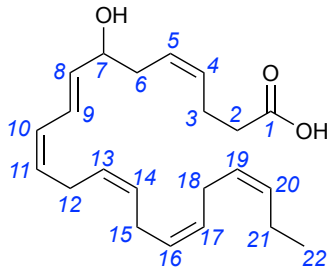


| Carbon No. | $^{13}$C δ (ppm) | $^{1}$H δ (ppm) (mult, *J* (Hz))[a,b] | HMBC Correlations[c] |
|---|---|---|---|
| 2 | 33.60 | H-2 : part of the m at 2.45 – 2.33 | H-3 |
| 3 | 22.75 | H-3 : part of the m at 2.45 – 2.33 | H-4 |
| 4 | 130.93 | H-4: 5.48 (m, 1H) | H-3 |
| 5 | 126.56 | H-5: 5.53 (m, 1H) | H-6, H-7 |
| 6 | 35.46 | H-6 : part of the m at 2.45 – 2.33 | H-5, H-7 |
| 7 | 72.10 | H-7: 4.25 (m, 1H) | H-9, H-8, H-6 |
| 8 | 135.65 | H-8 : 5.72 (dd, *J* = 15.16, 6.41 Hz) | H-10, H-7, H-6 |
| 9 | 125.69 | H-9 : 6.55 (dd, *J* = 15.13, 11.06 Hz) | H-8, H-7, |
| 10 | 128.10 | H-10 : 6.00 (t, *J* = 10.86 Hz) | H-8, H-9, H-12 |
| 11 | 130.58 | H-11 : part of the m at 5.43 – 5.35 | H-9, H-12 |
| 12 | 26.25 | H-12 : 2.97 (t, *J* = 6.93 Hz) | H-10 |
| 13 | 127.74 | H-13 : part of the m at 5.43 – 5.35 | H-12 |
| 14 | part of 128.80 | H-14 : part of the m at 5.43 – 5.35 | |
| 15 | 25.80 | H-15 : 2.85 (t, *J* = 6.41 Hz) | |
| 16 | 127.94 | H-16 : part of the m at 5.43 – 5.35 | H-15, H-18 |
| 17 | part of 128.80 | H-17 : part of the m at 5.43 – 5.35 | |
| 18 | 25.70 | H-18 : 2.81 (t, *J* = 6.51 Hz) | H-19 |
| 19 | 127.14 | H-19 : 5.32 (m) | H-18, H-21 |
| 20 | 132.25 | H-20 : part of the m at 5.43 – 5.35 | H-18, H-21, H-22 |
| 21 | 20.71 | H-21 : 2.09 – 2.06 (m) | H-22 |
| 22 | 14.42 | H-22 : 0.97 (t, *J* = 7.84 Hz) | H-21 |

[a] Recorded at 700 MHz,
[b] Assignments based on COSY, HSQC, HMBC, and HSQC-TOCSY,
[c] Only those correlations which could be unambiguously assigned are recorded.

# References


(1) Harvey, A. L.; Edrada-Ebel, R.; Quinn, R. J. *Nat. Rev. Drug Discov.* **2015**, *14*, 111.

(2) Blumberg, B.; Evans, R. M. *Genes Dev.* **1998**, *12*, 3149–3155.

(3) Harvey, A. L. *Drug Discov. Today.* **2008**, *13*, 894–901.

(4) Newman, D. J.; Cragg, G. M. *J. Nat. Prod.* **2007**, *70*, 461–477.

(5) Butler, M. S. *Nat. Prod. Rep.* **2008**, *25*, 475–516.

(6) Macklem, P. T. *J. Appl. Physiol.* **2008**, *104*, 1844–1846.

(7) Ferré, P. *Diabetes.* **2004**, *53* (suppl 1), S43 LP-S50.

(8) Dunning, K. R.; Anastasi, M. R.; Zhang, V. J.; Russell, D. L.; Robker, R. L. *PLoS One.* **2014**, *9*, 1–11.

(9) Belfiore, A.; Genua, M.; Malaguarnera, R. *PPAR Res.* **2009**, *2009*, 1–18.

(10) Berger, J.; Moller, D. E. *Annu. Rev. Med.* **2002**, *53*, 409–435.

(11) Feige, J. N.; Gelman, L.; Michalik, L.; Desvergne, B.; Wahli, W. *Prog. Lipid Res.* **2006**, *45*, 120–159.

(12) Michalik, L.; Wahli, W. *J. Clin. Invest.* **2006**, *116*, 598–606.

(13) Tyagi, S.; Sharma, S.; Gupta, P.; Saini, A.; Kaushal, C. *J. Adv. Pharm. Technol. Res.* **2011**, *2*, 236.

(14) Braissant, O.; Foufelle, F.; Scotto, C.; Dauça, M.; Wahli, W. *Endocrinology.* **1996**, *137*, 354–366.

(15) Issemann, I.; Green, S. *Nature.* **1990**, *347*, 645–650.

(16) Leghmar, K.; Cenac, N.; Rolland, M.; Martin, H.; Rauwel, B.; Bertrand-Michel, J.; Le Faouder, P.; Bénard, M.; Casper, C.; Davrinche, C.; Fournier, T.; Chavanas, S. *PLoS One.* **2015**, *10*, 1–19.

(17) Bernal-Mizrachi, C.; Weng, S.; Feng, C.; Finck, B. N.; Knutsen, R. H.; Leone, T. C.; Coleman, T.; Mecham, R. P.; Kelly, D. P.; Semenkovich, C. F. *Nat. Med.* **2003**, *9*, 1069–1075.

(18) Keller, H.; Dreyer, C.; Medin, J.; Mahfoudi, A.; Ozato, K.; Wahli, W. *Proc. Natl. Acad. Sci.* **1993**, *90*, 2160–2164.

(19) Reddy, J. K.; Hashimoto, T. *Annu. Rev. Nutr.* **2001**, *21*, 193–230.

(20) Bookout, A. L.; Jeong, Y.; Downes, M.; Yu, R. T.; Evans, R. M.; Mangelsdorf, D. J.

*Cell.* **2006**, *126*, 789–799.

(21) Gofflot, F.; Chartoire, N.; Vasseur, L.; Heikkinen, S.; Dembele, D.; Merrer, J. Le; Auwerx, J. *Cell.* **2007**, *13*, 405–418.

(22) Roy, A.; Jana, M.; Corbett, G. T.; Ramaswamy, S.; Kordower, J. H.; Gonzalez, F. J.; Pahan, K. *Cell Rep.* **2013**, *4*, 724–737.

(23) Roy, A.; Kundu, M.; Jana, M.; Mishra, R. K.; Yung, Y.; Luan, C.-H.; Gonzalez, F. J.; Pahan, K. *Nat. Chem. Biol.* **2016**, *12*, 1075.

(24) Knobloch, M.; Pilz, G.-A.; Ghesquière, B.; Kovacs, W. J.; Wegleiter, T.; Moore, D. L.; Hruzova, M.; Zamboni, N.; Carmeliet, P.; Jessberger, S. *Cell Rep.* **2017**, *20*, 2144–2155.

(25) Ahmadian, M.; Suh, J. M.; Hah, N.; Liddle, C.; Atkins, A. R.; Downes, M.; Evans, R. M. *Nat. Med.* **2013**, *19*, 557.

(26) Deeb, S. S.; Fajas, L.; Nemoto, M.; Pihlajamäki, J.; Mykkänen, L.; Kuusisto, J.; Laakso, M.; Fujimoto, W.; Auwerx, J. *Nat. Genet.* **1998**, *20*, 284–287.

(27) Ricote, M.; Li, A. C.; Willson, T. M.; Kelly, C. J.; Glass, C. K. *Nature.* **1998**, *391*, 79–82.

(28) Su, C. G.; Wen, X.; Bailey, S. T.; Jiang, W.; Rangwala, S. M.; Keilbaugh, S. A.; Flanigan, A.; Murthy, S.; Lazar, M. A.; Wu, G. D. *J. Clin. Invest.* **1999**, *104*, 383–389.

(29) Lu, M.; Sarruf, D. A.; Talukdar, S.; Sharma, S.; Li, P.; Bandyopadhyay, G.; Nalbandian, S.; Fan, W.; Gayen, J. R.; Mahata, S. K.; Webster, N. J.; Schwartz, M. W.; Olefsky, J. M. *Nat. Med.* **2011**, *17*, 618.

(30) Ryan, K. K.; Li, B.; Grayson, B. E.; Matter, E. K.; Woods, S. C.; Seeley, R. J. *Nat. Med.* **2011**, *17*, 623.

(31) Kapadia, R.; Yi, J.-H.; Vemuganti, R. *Front. Biosci.* **2008**, *13*, 1813–1826.

(32) Balakumar, P.; Rose, M.; Ganti, S. S.; Krishan, P.; Singh, M. *Pharmacol. Res.* **2007**, *56*, 91–98.

(33) Nolte, R. T.; Wisely, G. B.; Westin, S.; Cobb, J. E.; Lambert, M. H.; Kurokawa, R.; Rosenfeld, M. G.; Willson, T. M.; Glass, C. K.; Milburn, M. V. *Nature.* **1998**, *395*, 137–143.

(34) Xu, H. E.; Lambert, M. H.; Montana, V. G.; Plunket, K. D.; Moore, L. B.; Collins, J. L.; Oplinger, J. A.; Kliewer, S. A.; Gampe, R. T.; McKee, D. D.; Moore, J. T.; Willson, T. M. *Proc. Natl. Acad. Sci.* **2001**, *98*, 13919–13924.

(35) Xu, H. E.; Lambert, M. H.; Montana, V. G.; Parks, D. J.; Blanchard, S. G.; Brown, P. J.; Sternbach, D. D.; Lehmann, J. M.; Wisely, G. B.; Willson, T. M.; Kliewer, S. A.; Milburn, M. V. *Mol. Cell.* **1999**, *3*, 397–403.

(36) Itoh, T.; Fairall, L.; Amin, K.; Inaba, Y.; Szanto, A.; Balint, B. L.; Nagy, L.; Yamamoto, K.; Schwabe, J. W. R. *Nat. Struct. Mol. Biol.* **2008**, *15*, 924–931.

(37) Fu, J.; Gaetani, S.; Oveisi, F.; Lo Verme, J.; Serrano, A.; Rodríguez de Fonseca, F.; Rosengarth, A.; Luecke, H.; Di Giacomo, B.; Tarzia, G.; Piomelli, D. *Nature.* **2003**, *425*, 90–93.

(38) Cluny, N. L.; Keenan, C. M.; Lutz, B.; Piomelli, D.; Sharkey, K. A. *Neurogastroenterol. Motil.* **2009**, *21*, 420–429.

(39) Jiang, C.; Ting, A. T.; Seed, B. *Nature.* **1998**, *391*, 82–86.

(40) Kliewer, S. A.; Lenhard, J. M.; Willson, T. M.; Patel, I.; Morris, D. C.; Lehmann, J. M. *Cell.* **1995**, *83*, 813–819.

(41) Baker, L. M. S.; Baker, P. R. S.; Golin-Bisello, F.; Schopfer, F. J.; Fink, M.; Woodcock, S. R.; Branchaud, B. P.; Radi, R.; Freeman, B. A. *J. Biol. Chem.* **2007**, *282*, 31085–31093.

(42) Cipollina, C.; Salvatore, S. R.; Muldoon, M. F.; Freeman, B. A.; Schopfer, F. J. *PLoS One* **2014**, *9*, e94836–e94836.

(43) Mohamed, M.; Brook, M. A. *Helv. Chim. Acta* **2002**, *85*, 4165–4181.

(44) Hoover, J. M.; Stahl, S. S. *J. Am. Chem. Soc.* **2011**, *133*, 16901–16910.

(45) Hayashi, Y.; Shoji, M.; Ishikawa, H.; Yamaguchi, J.; Tamura, T.; Imai, H.; Nishigaya, Y.; Takabe, K.; Kakeya, H.; Osada, H. *Angew. Chemie - Int. Ed.* **2008**, *47*, 6657–6660.

(46) Semmelhack, M. F.; Chou, C. S.; Cortes, D. A. *J. Am. Chem. Soc.* **1983**, *105*, 4492–4494.

(47) Anelli, P. L.; Biffi, C.; Montanari, F.; Quici, S. *J. Org. Chem.* **1987**, *52*, 2559–2562.

(48) Cella, J. A.; Kelley, J. A.; Kenehan, E. F. *J. Org. Chem.* **1975**, *40*, 1860–1862.

(49) Celia, J. A.; McGrath, J. P.; Kelley, J. A.; ElSoukkary, O.; Hilpert, L. *J. Org. Chem.* **1977**, *42*, 2077–2080.

(50) Semmelhack, M. F.; Schmid, C. R.; Cortés, D. A.; Chou, C. S. *J. Am. Chem. Soc.* **1984**, *106*, 3374–3376.

(51) Dijksman, A.; Arends, I.; Sheldon, R. A. *Org. Biomol. Chem.* **2003**, *1*, 3232–3237.

(52) Bailey, W. F.; Bobbitt, J. M.; Wiberg, K. B. *J. Org. Chem.* **2007**, *72*, 4504–4509.

(53) Miyazawa, T.; Endo, T.; Shiihashi, S.; Okawara, M. *J. Org. Chem.* **1985**, *50*, 1332–1334.

(54) Bobbitt, J. M. *J. Org. Chem.* **1998**, *63*, 9367–9374.

(55) Qiu, J. C.; Pradhan, P. P.; Blanck, N. B.; Bobbitt, J. M.; Bailey, W. F. *Org. Lett.* **2012**, *14*, 350–353.

(56) Hoover, J. M.; Ryland, B. L.; Stahl, S. S. *J. Am. Chem. Soc.* **2013**, *135*, 2357–2367.

(57) Ryland, B. L.; McCann, S. D.; Brunold, T. C.; Stahl, S. S. *J. Am. Chem. Soc.* **2014**, *136*, 12166–12173.

(58) Mazerolles, P.; Boussaguet, P.; Huc, V. *Org. Synth.* **2003**, *76*, 221–221.

(59) B, N.; W, S. *Angew. Chemie Int. Ed. English.* **1978**, *17*, 522–524.

(60) Montalbetti, C. A. G. N.; Falque, V. *Tetrahedron.* **2005**, *61*, 10827–10852.

(61) Kirkland, T. A.; Grubbs, R. H. *J. Org. Chem.* **1997**, *62*, 7310–7318.

(62) Conrad, J. C.; Eelman, M. D.; Duarte Silva, J. A.; Monfette, S.; Parnas, H. H.; Snelgrove, J. L.; Fogg, D. E. *J. Am. Chem. Soc.* **2007**, *129*, 1024–1025.

(63) Dias, E. L.; Nguyen, S. B. T.; Grubbs, R. H. *J. Am. Chem. Soc.* **1997**, *119*, 3887–3897.

(64) Schleyer, P. V. R.; Wiliiams, J. E.; Blanchard, K. R. *J. Am. Chem. Soc.* **1970**, *9*, 2377–2386.

(65) Illuminati, G.; Mandolini, L. *Acc. Chem. Res.* **1981**, *14*, 95–102.

(66) Galli, C.; Mandolini, L. *Eur. J. Org. Chem.* **2000**, 3117–3125.

(67) Stewart, I. C.; Keitz, B. K.; Kuhn, K. M.; Thomas, R. M.; Grubbs, R. H. *J. Am. Chem. Soc.* **2010**, *132*, 8534–8535.

(68) Miller, S. J.; Kim, S. H.; Chen, Z. R.; Grubbs, R. H. *J. Am. Chem. Soc.* **1995**, *117*, 2108–2109.

(69) Delgado, M.; Martín, J. D. *J. Org. Chem.* **1999**, *64*, 4798–4816.

(70) Maier, M. E. *Angew. Chemie - Int. Ed.* **2000**, *39*, 2073–2077.

(71) Michalak, M.; Wicha, J. *Org. Biomol. Chem.* **2011**, *9*, 3439–3446.

(72) Volchkov, I.; Lee, D. *J. Am. Chem. Soc.* **2013**, *135*, 5324–5327.

(73) Brown, N.; Xie, B.; Markina, N.; VanderVelde, D.; Perchellet, J. P. H.; Perchellet, E.

M.; Crow, K. R.; Buszek, K. R. *Bioorganic Med. Chem. Lett.* **2008**, *18*, 4876–4879.

(74) Zuercher, W. J.; Hashimoto, M.; Grubbs, R. H. *J. Am. Chem. Soc.* **1996**, *118*, 6634–6640.

(75) Fürstner, A. *Top. Catal.* **1997**, *4*, 285–299.

(76) Monfette, S.; Fogg, D. E. *Chem. Rev.* **2009**, *109*, 3783–3816.

(77) Jacobson, H.; Stockmayer, W. H. *J. Chem. Phys.* **1950**, *18*, 1600–1606.

(78) Yamamoto, K.; Biswas, K.; Gaul, C.; Danishefsky, S. J. *Tetrahedron Lett.* **2003**, *44*, 3297–3299.

(79) Fürstner, A.; Thiel, O. R.; Lehmann, C. W. *Organometallics.* **2002**, *21*, 331–335.

(80) Ghosh, A. K.; Cappiello, J.; Shin, D. *Tetrahedron Lett.* **1998**, *39*, 4651–4654.

(81) Yang, Q.; Xiao, W. J.; Yu, Z. *Org. Lett.* **2005**, *7*, 871–874.

(82) Mitchell, L.; Parkinson, J. A.; Percy, J. M.; Singh, K. *J. Org. Chem.* **2008**, *73*, 2389–2395.

(83) Van, T. N.; Debenedetti, S.; Kimpe, N. De. *Tetrahedron Lett.* **2003**, *44*, 4199–4201.

(84) Hong, B. C.; Chin, S. F. *Synth. Commun.* **1997**, *27*, 1191–1197.

(85) Trost, B. M.; Shin, S.; Sclafani, J. A. *J. Am. Chem. Soc.* **2005**, *127*, 8602–8603.

(86) Trost, B. M.; Yang, H.; Brindle, C. S.; Dong, G. *Chem. A Eur. J.* **2011**, *17*, 9777–9788.

(87) Inani, H.; Jha, A. K.; Easwar, S. *ChemistrySelect*. **2017**, *2*, 11666–11672.

(88) Jiang, Y.; Guo, C.; Xia, H.; Mahmood, I.; Liu, H. *Ind. Eng. Chem. Res.* **2008**, *47*, 9628–9635.

(89) Maheswaran, H.; Joseph, P. J. A.; Prasanth, K. L.; Priyadarshini, S.; Satyanarayana, P.; Likhar, P. R.; Kantam, M. L. *Tetrahedron Asymmetry.* **2010**, *21*, 2158–2166.

(90) Boxer, M. B.; Yamamoto, H. *J. Am. Chem. Soc.* **2006**, *12*, 48–49.

(91) Saksena, A. K.; Mangiaracina, P. *Tetrahedron Lett.* **1983**, *24*, 273–276.

(92) Evans, D. A.; Chapman, K. T.; Carreira, E. M. *J. Am. Chem. Soc.* **1988**, *110*, 3560–3578.

(93) Masamune, S. *Pure Appl. Chem.* **1988**, *60*, 1587–1596.

(94) Nakagawa-Goto, K.; Crimmins, M. T. *Synlett.* **2011**, *11*, 1555–1558.

(95) Gribble, G. W.; Ferguson, D. C. *Chem. Commun.* **1975**, *13*, 535–536.

(96) Payack, J. F.; Hughes, D. L.; Cai, D.; Cottrell, I. F.; Verhoeven, T. R. *Org. Synth.* **2002**, *79*, 19.

(97) Petasis, N. A.; Lu, S. P. *J. Am. Chem. Soc.* **1995**, *117*, 6394–6395.

(98) Petasis, N. A.; Lu, S. P. *Tetrahedron Lett.* **1995**, *36*, 2393–2396.

(99) Petasis, N. A.; Bzowej, E. I. *J. Am. Chem. Soc.* **1990**, *112*, 6392–6394.

(100) DeShong, P.; Rybczynski, P. J. *J. Org. Chem.* **1991**, *56*, 3207–3210.

(101) Petasis, N. A.; Patane, M. A. *Tetrahedron Letters*. **1990**, 31, 6799–6802.

(102) Curtis, N. R.; Holmes, A. B.; Looney, M. G. *Tetrahedron.* **1991**, *47*, 7171–7178.

(103) Fuhry, M. A. M.; Holmes, A. B.; Marshall, D. R. *J. Chem. Soc. Perkin Trans. 1.* **1993**, *0*, 2743–2746.

(104) Harrison, J. R.; Holmes, A. B.; Collins, I. *Synlett.* **1999**, *S1*, 972–974.

(105) Anderson, E. A.; Davidson, J. E. P.; Harrison, J. R.; O'Sullivan, P. T.; Collins, I.; Holmes, A. B.; Buhr, W. *Chem. Commun.* **2000**, 629–630.

(106) Burton, J. W.; O'Sullivan, P. T.; Anderson, E. A.; Collins, I.; Holmes, A. B. *Chem. Commun.* **2000**, *0*, 631–632.

(107) Chiang, G. C. H.; Bond, A. D.; Ayscough, A.; Pain, G.; Ducki, S.; Holmes, A. B. *Chem. Commun.* **2005**, *0*, 1860–1862.

(108) Burton, J. W.; Anderson, E. A.; O'Sullivan, P. T.; Collins, I.; Davies, J. E.; Bond, A. D.; Feeder, N.; Holmes, A. B. *Org. Biomol. Chem.* **2008**, *6*, 693–702.

(109) Wong, L. S.-M.; Turner, K. A.; White, J. M.; Holmes, A. B.; Ryan, J. H. *Aust. J. Chem.* **2010**, *63*, 529–532.

(110) O'Sullivan, P. T.; Buhr, W.; Fuhry, M. A. M.; Harrison, J. R.; Davies, J. E.; Feeder, N.; Marshall, D. R.; Burton, J. W.; Holmes, A. B. *J. Am. Chem. Soc.* **2004**, *126*, 2194–2207.

(111) Kinney, W. A.; Coghlan, M. J.; Paquette, L. A. *J. Am. Chem. Soc.* **1985**, *107*, 7352–7360.

(112) Sharpless, K. B.; Young, M. W.; Lauer, R. F. *Tetrahedron Lett.* **1973**, *14*, 1979–1982.

(113) Wipf, P.; Jahn, H. *Tetrahedron.* **1996**, *52*, 12853–12910.

(114) Hart, D. W.; Blackburn, T. F.; Schwartz, J. *J. Am. Chem. Soc.* **1975**, *97*, 679–680.

(115) Hart, D. W.; Schwartz, J. *J. Am. Chem. Soc.* **1974**, *96*, 8115–8116.

(116) Wailes, P. C.; Weigold, H.; Bell, A. P. *J. Organomet. Chem.* **1971**, *27*, 373–378.

(117) Wailes, P. C.; Weigold, H.; Bell, A. P. *J. Organomet. Chem.* **1970**, *24*, 405–411.

(118) Zhao, Y.; Snieckus, V. *Org. Lett.* **2014**, *16*, 390–393.

(119) Huang, Z.; Negishi, E. I. *Org. Lett.* **2006**, *8*, 3675–3678.

(120) White, J. M.; Tunoori, A. R.; Georg, G. I. *J. Am. Chem. Soc.* **2000**, *122*, 11995–11996.

(121) Swanson, D. R.; Nguyen, T.; Noda, Y.; Negishi, E. I. *J. Org. Chem.* **1991**, *56*, 2590–2591.

(122) Liu, X.; Ready, J. M. *Tetrahedron.* **2008**, *64*, 6955–6960.

(123) Byrne, P. A.; Gilheany, D. G. *Chem. Soc. Rev.* **2013**, *42*, 6670–6696.

(124) Bergelson, L. D.; Shemyakin, M. M. *Tetrahedron.* **1963**, *19*, 149–159.

(125) Vedejs, E.; Snoble, K. A. J. *J. Am. Chem. Soc.* **2005**, *95*, 5778–5780.

(126) Schlosser, M.; Schaub, B. *J. Am. Chem. Soc.* **1982**, *104*, 5821–5823.

(127) Olah, G. A.; Krishnamurthy, V. V. *J. Am. Chem. Soc.* **1982**, *104*, 3987–3990.

(128) Clayden, J.; Greeves, N.; Warren, S. *Organic Chemistry*, 2nd ed.; Oxford University Press: New York, 2012.

(129) Harris, R. K.; Howes, B. R. *J. Mol. Spectrosc.* **1968**, *28*, 191–203.

(130) Asano, K.; Matsubara, S. *Org. Lett.* **2009**, *11*, 1757–1759.

(131) Xu, K.; Zhao, S.; Xu, J.-K.; Shan, M.-W.; Yu, J.-L.; Wang, Y.-B.; Zhang, C.-F.; Chen, X. *Synth. Commun.* **2017**, *47*, 1848–1853.

(132) Jeffery, T.; Gueugnot, S.; Linstrumelle, G. *Tetrahedron Lett.* **1992**, *33*, 5757–5760.

(133) Pivnitsky, K. K.; Lapitskaya, M. A.; Vasiljeva, L. L. *Synthesis (Stuttg).* **1993**, *1993*, 65–66.

(134) Huang, L. F.; Xu, B. .; Shan, S. X.; Zhu, X. Y. *Chin. Chem. Lett.* **1993**, *4*, 13–16.

(135) Oger, C.; Balas, L.; Durand, T.; Galano, J.-M. *Chem. Rev.* **2013**, *113*, 1313–1350.

(136) Van Summeren, R. P.; Feringa, B. L.; Minnaard, A. J. *Org. Biomol. Chem.* **2005**, *3*, 2524–2533.

(137) Sonogashira, K.; Tohda, Y.; Hagihara, N. *Tetrahedron Lett.* **1975**, *50*, 4467–4470.

(138) Roughley, S. D.; Jordan, A. M. *J. Med. Chem.* **2011**, *54*, 3451–3479.

(139) Wang, X.; Song, Y.; Qu, J.; Luo, Y. *Organometallics.* **2017**, *36* (5), 1042–1048.

(140) Chinchilla, R.; Nájera, C. *Chem. Soc. Rev.* **2011**, *40*, 5084–5121.

(141) Batista-Pereira, L. G.; Dos Santos, M. G.; Corrêa, A. G.; Fernandes, J. B.; Dietrich, C. R. R. C.; Pereira, D. A.; Bueno, O. C.; Costa-Leonardo, A. M. *J. Braz. Chem. Soc.* **2004**, *15*, 372–377.

(142) Nicolaou, K. C.; Veale, C. A.; Webber, S. E.; Katerinopoulos, H. *J. Am. Chem. Soc.* **1985**, *107*, 7515–7518.

(143) Dobson, N. A.; Eglinton, G.; Krishnamurti, M.; Raphael, R. A.; Willis, R. G. *Tetrahedron.* **1961**, *16*, 16–24.

(144) Boland, W.; Schroer, N.; Sieler, C.; Bottmuhle, A. Der; Feigel, M. *Helv. Chem. Acta* **1987**, *70*, 1025–1040.

(145) Khrimian, A.; Klun, J. A.; Hijji, Y.; Baranchikov, Y. N.; Pet'Ko, V. M.; Mastro, V. C.; Kramer, M. H. *J. Agric. Food Chem.* **2002**, *50*, 6366–6370.

(146) Robles, O.; McDonald, F. E. *Org. Lett.* **2008**, *10*, 1811–1814.

(147) Baxter, A. D.; Binns, F.; Javed, T.; Roberts, S. M.; Sadler, P.; Scheinmann, F.; Wakefield, B. J.; Lynch, M.; Newton, R. F. *J. Chem. Soc. Perkin Trans. 1.* **1986**, 889–900.

(148) Golovanov, A. B.; Ivanov, I. V.; Groza, N. V.; Myagkova, G. I. *Chem. Nat. Compd.* **2015**, *51*, 1038–1041.

# Appendix: $^{1}H$ and $^{13}C$ NMR Spectra

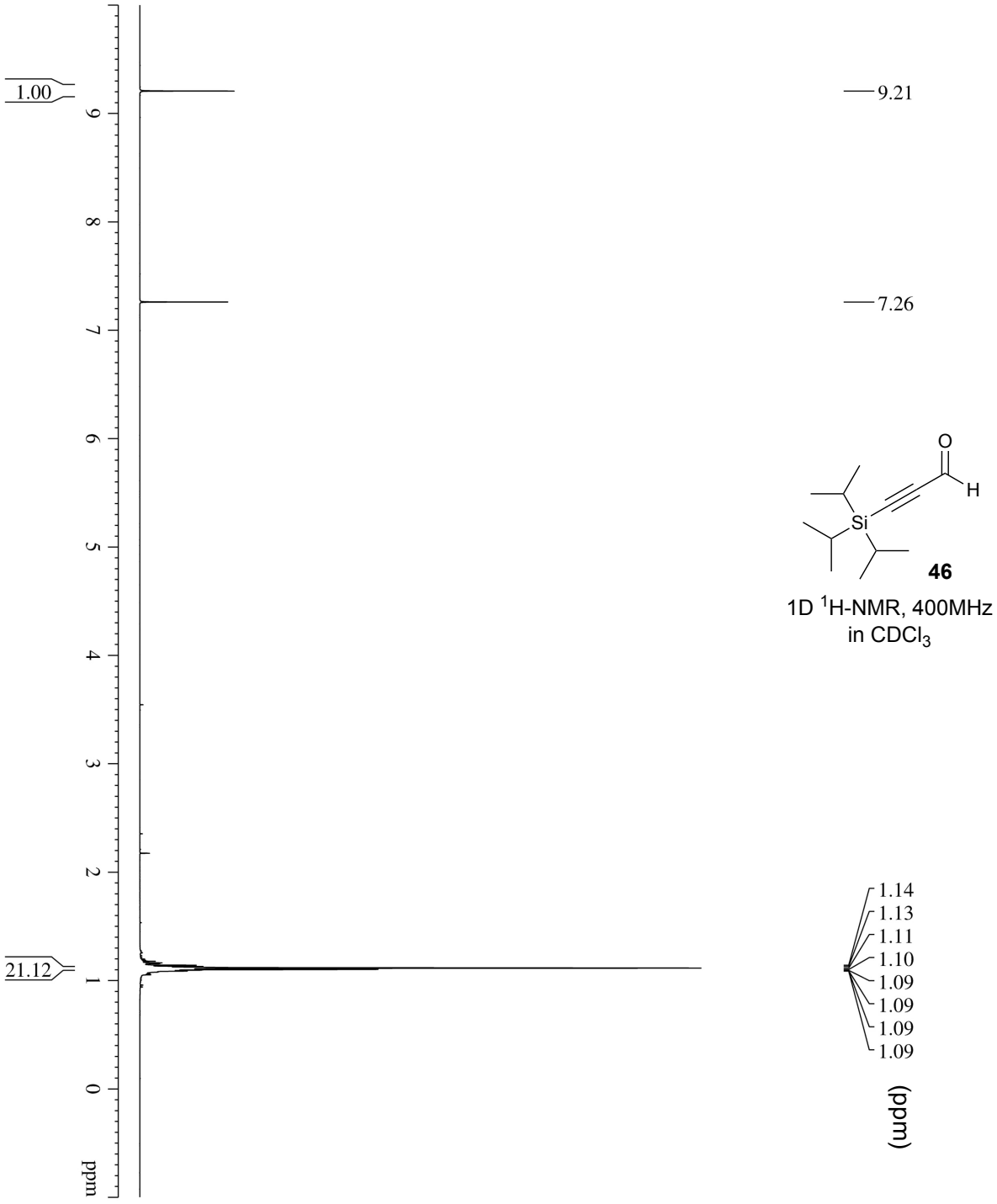


1D $^{1}H$-NMR, 400MHz
in $CDCl_3$

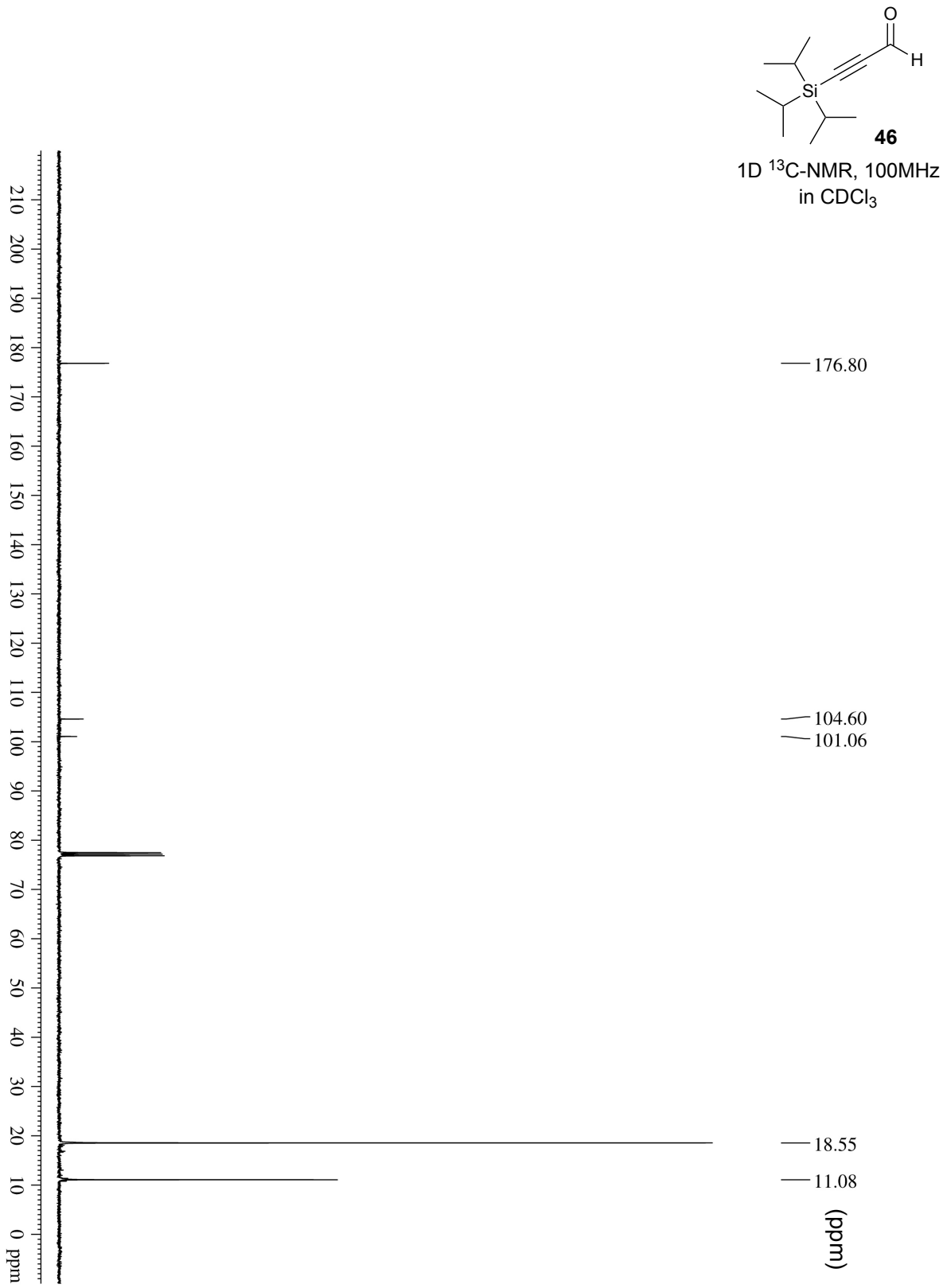
O
H
Si
46
1D 13C-NMR, 100MHz
in CDCl3
176.80
104.60
101.06
18.55
11.08
(ppm)
210 200 190 180 170 160 150 140 130 120 110 100 90 80 70 60 50 40 30 20 10 0 ppm

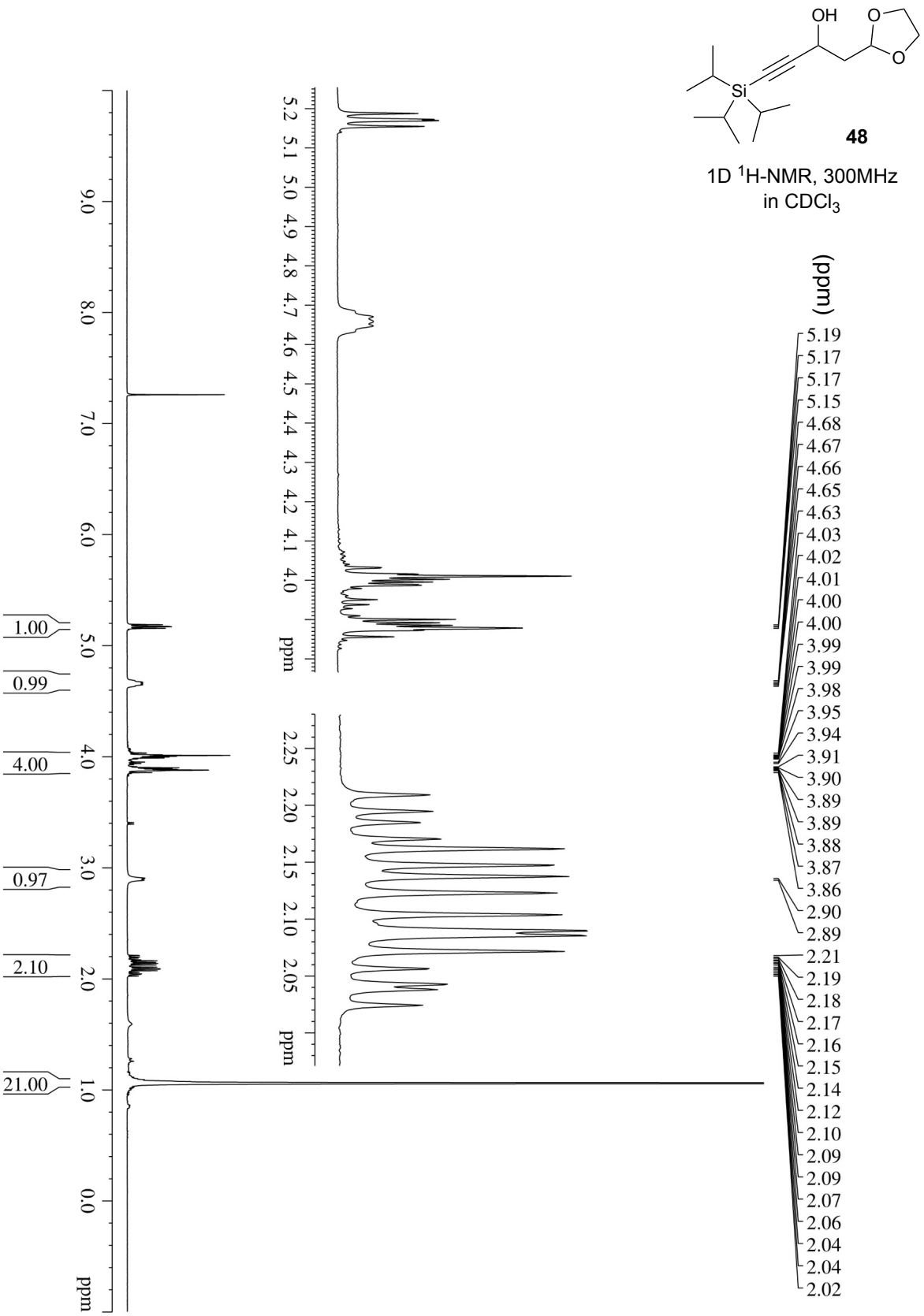
OH
O
O
Si
48
1D $^{1}$H-NMR, 300MHz
in $CDCl_3$
(ppm)
5.19
5.17
5.17
5.15
4.68
4.67
4.66
4.65
4.63
4.03
4.02
4.01
4.00
4.00
3.99
3.99
3.98
3.95
3.94
3.91
3.90
3.89
3.89
3.88
3.87
3.86
2.90
2.89
2.21
2.19
2.18
2.17
2.16
2.15
2.14
2.12
2.10
2.09
2.09
2.07
2.06
2.04
2.04
2.02
1.00
0.99
4.00
0.97
2.10
21.00
ppm

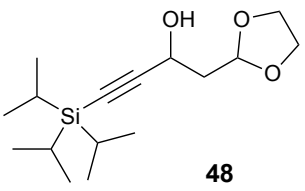


**48**

1D $^{13}$C-NMR, 75MHz
in $CDCl_3$

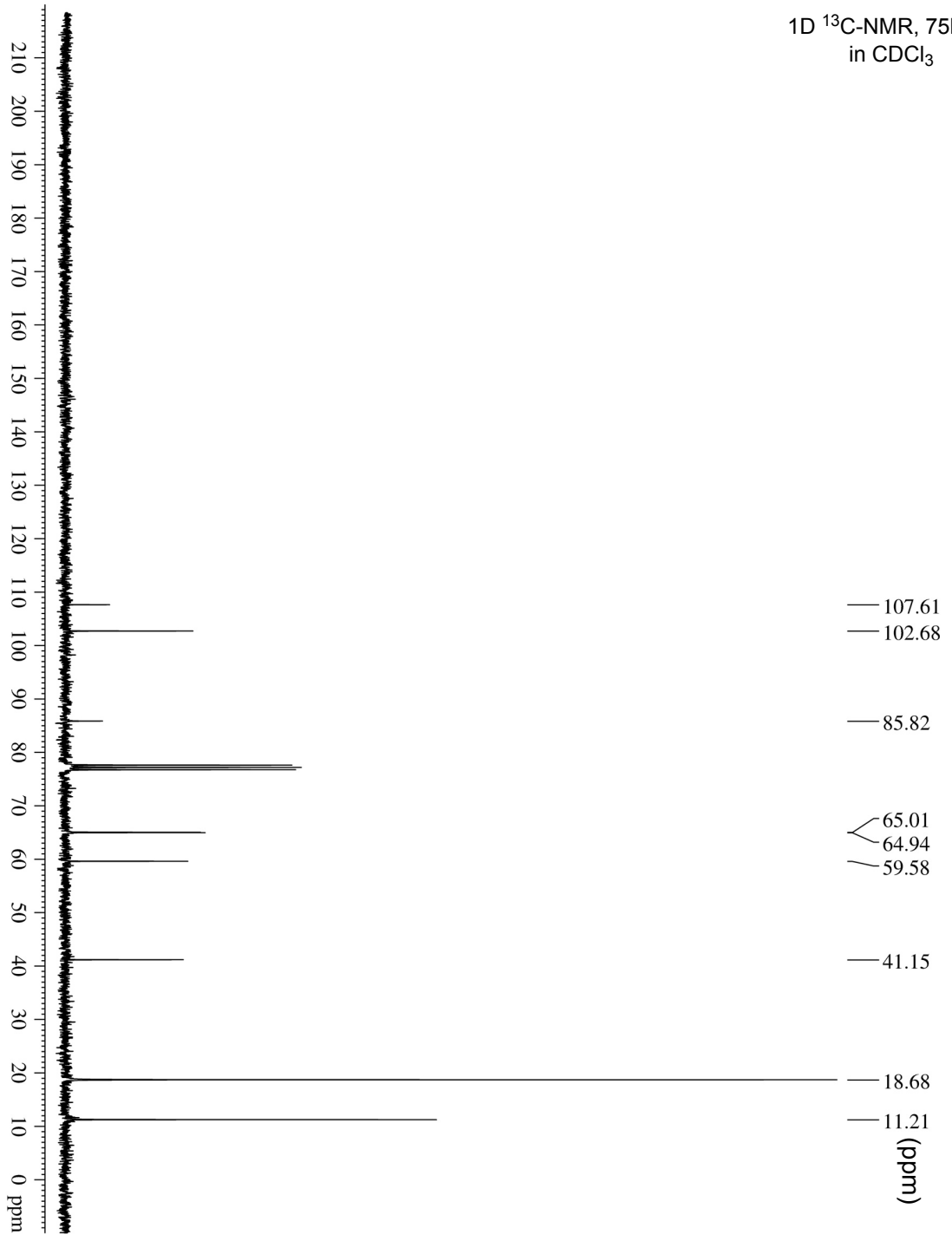

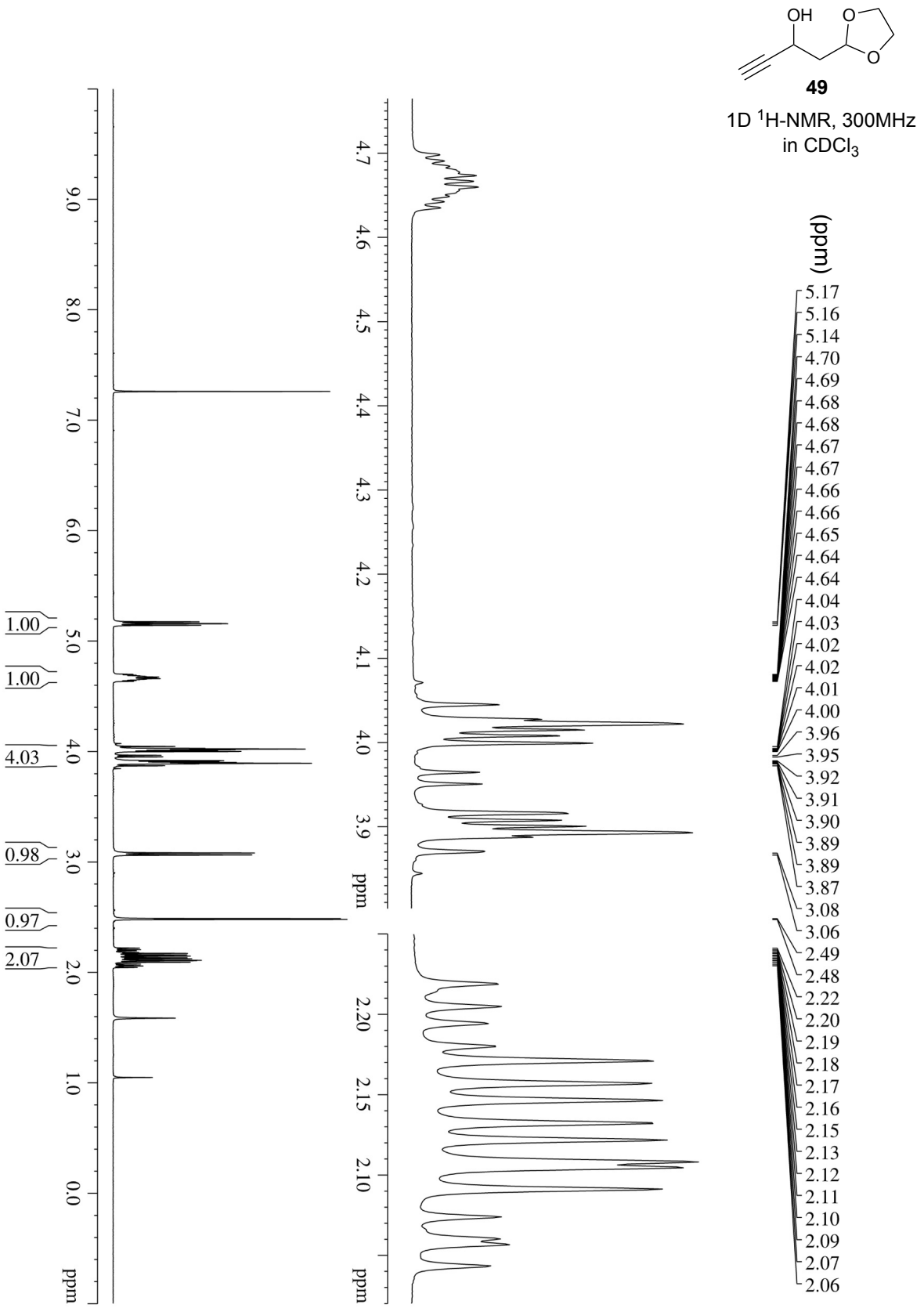
OH
O
O
49
1D $^1$H-NMR, 300MHz
in $CDCl_3$
(ppm)
5.17
5.16
5.14
4.70
4.69
4.68
4.68
4.67
4.67
4.66
4.66
4.65
4.64
4.64
4.04
4.03
4.02
4.02
4.01
4.00
3.96
3.95
3.92
3.91
3.90
3.89
3.89
3.87
3.08
3.06
2.49
2.48
2.22
2.20
2.19
2.18
2.17
2.16
2.15
2.13
2.12
2.11
2.10
2.09
2.07
2.06
1.00
1.00
4.03
0.98
0.97
2.07
ppm

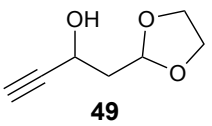


**49**

1D $^{13}$C-NMR, 75MHz
in $CDCl_3$

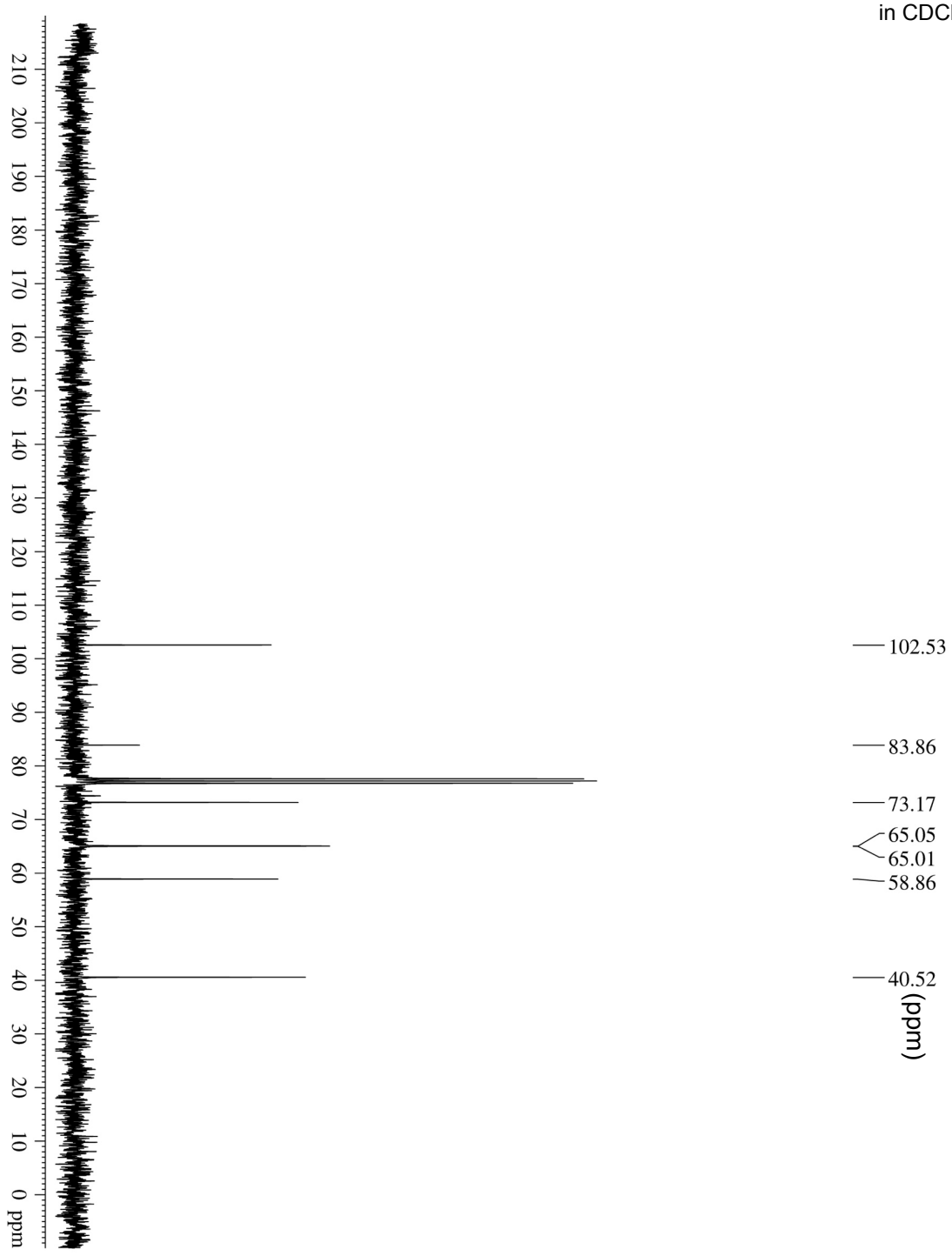

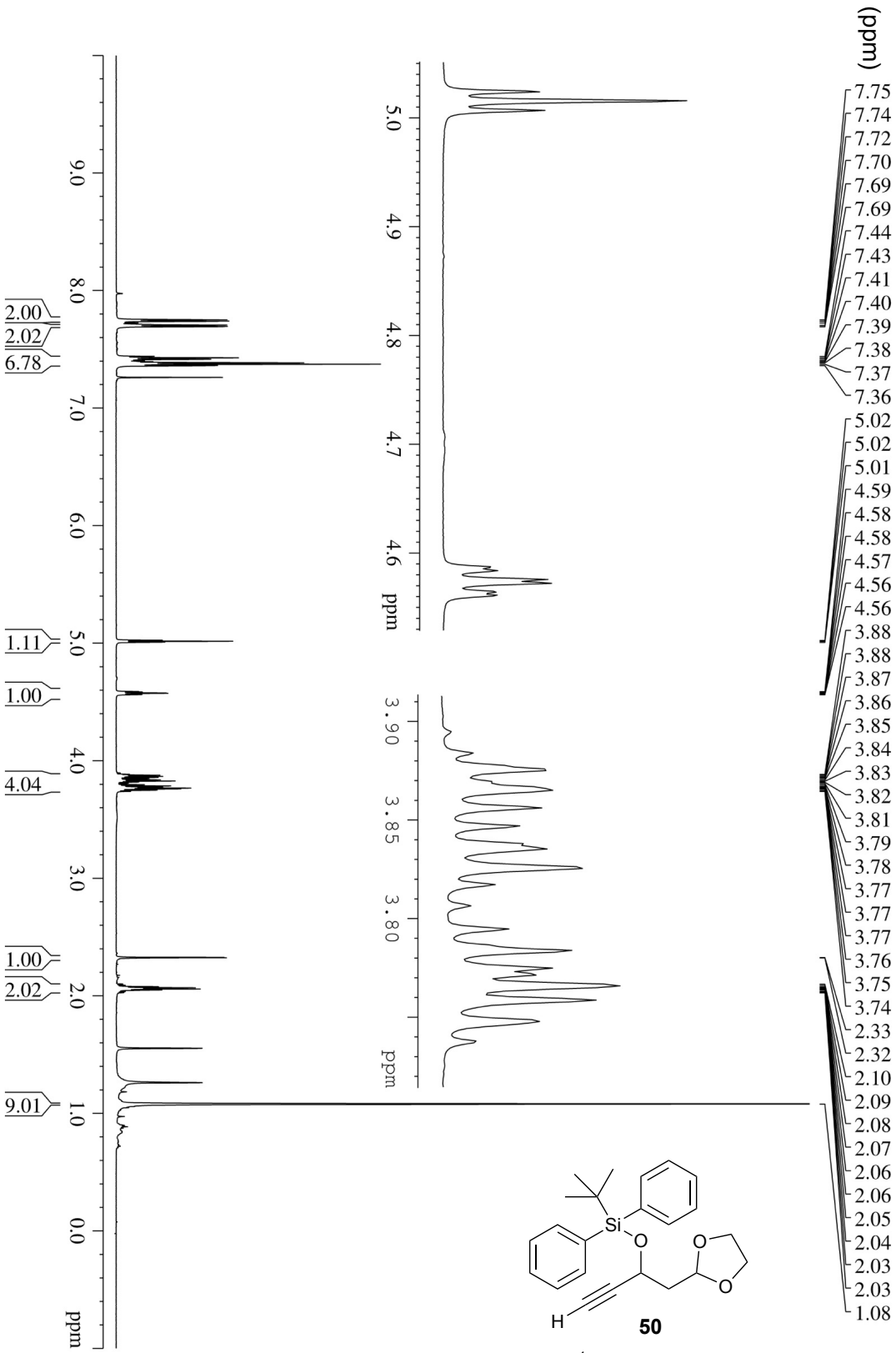


**50**

1D $^{1}$H-NMR, 600 MHz
in $CDCl_3$

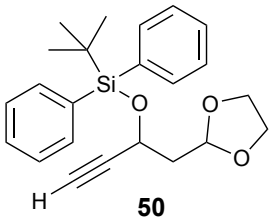


**50**

1D $^{13}$C-NMR, 150 MHz
in $CDCl_3$

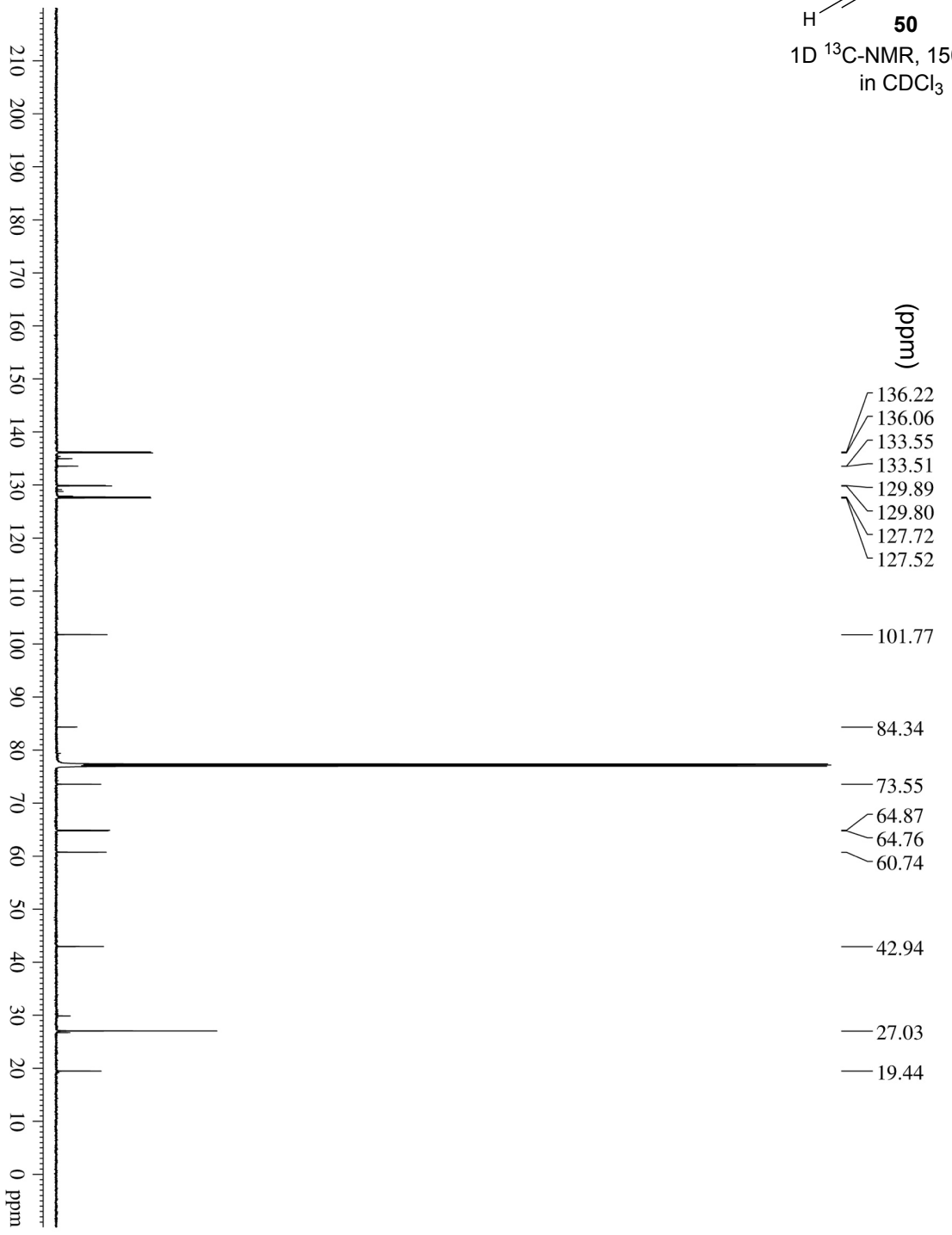

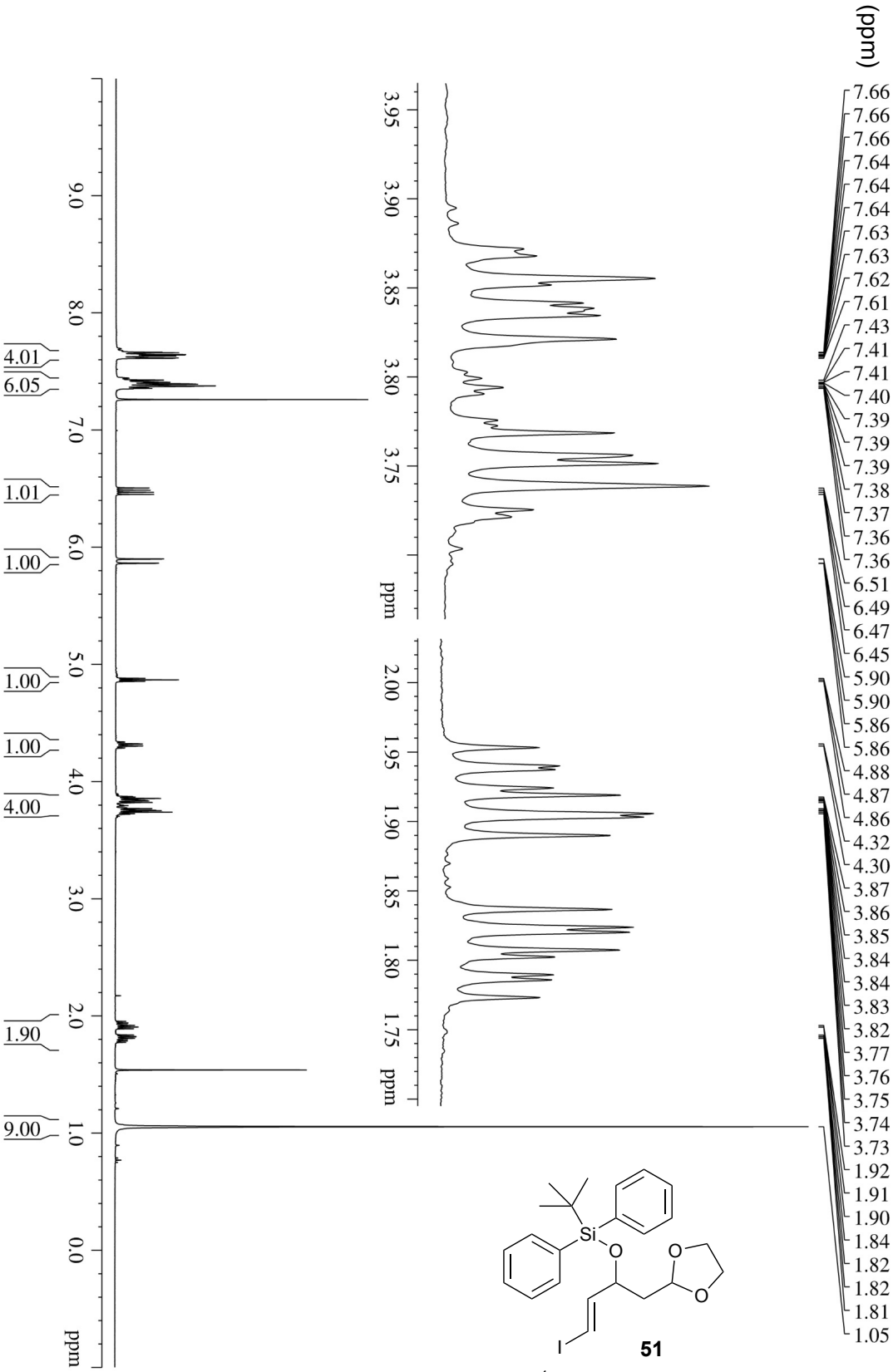


**51**

1D $^{1}$H-NMR, 400 MHz
in $CDCl_3$

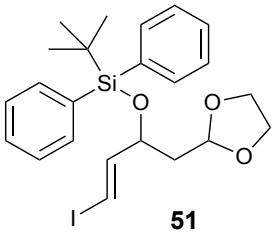


**51**

1D $^{13}$C-NMR, 100 MHz
in $CDCl_3$

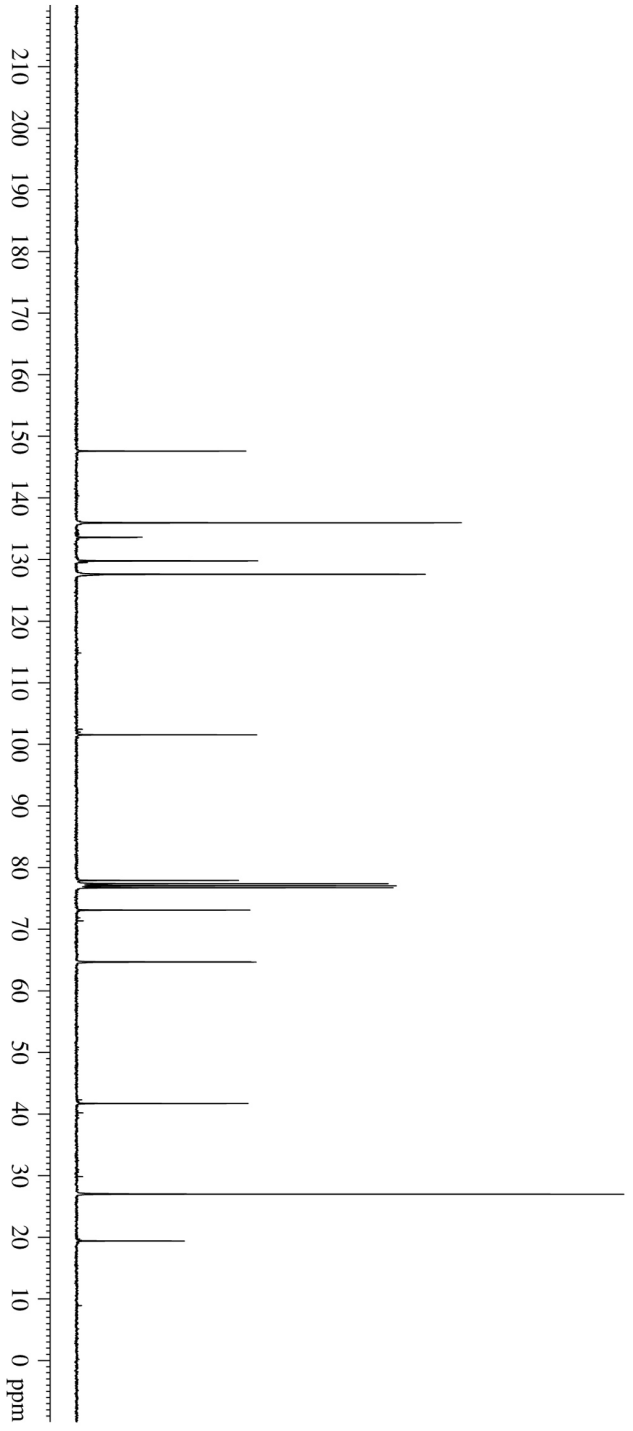


(ppm)

147.58
135.95
135.93
133.61
133.53
129.78
129.74
127.61
127.57
127.47
127.42
101.53
77.89
73.08
64.69
64.64
41.69
26.99
19.37

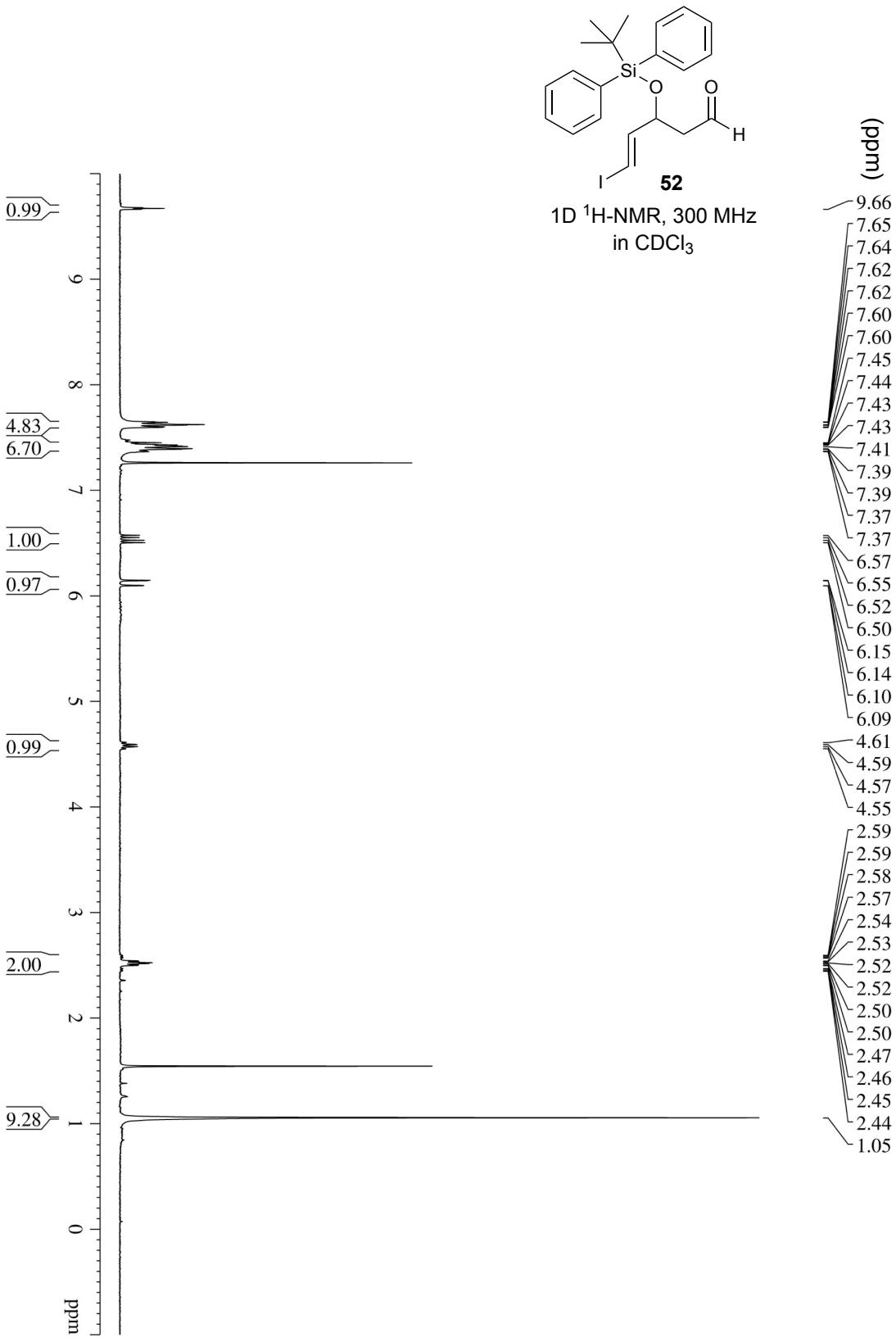
Si
O
O
H
I
52
1D $^{1}$H-NMR, 300 MHz
in $CDCl_3$
(ppm)
9.66
7.65
7.64
7.62
7.62
7.60
7.60
7.45
7.44
7.43
7.43
7.41
7.39
7.39
7.37
7.37
6.57
6.55
6.52
6.50
6.15
6.14
6.10
6.09
4.61
4.59
4.57
4.55
2.59
2.59
2.58
2.57
2.54
2.53
2.52
2.52
2.50
2.50
2.47
2.46
2.45
2.44
1.05
0.99
4.83
6.70
1.00
0.97
0.99
2.00
9.28
ppm

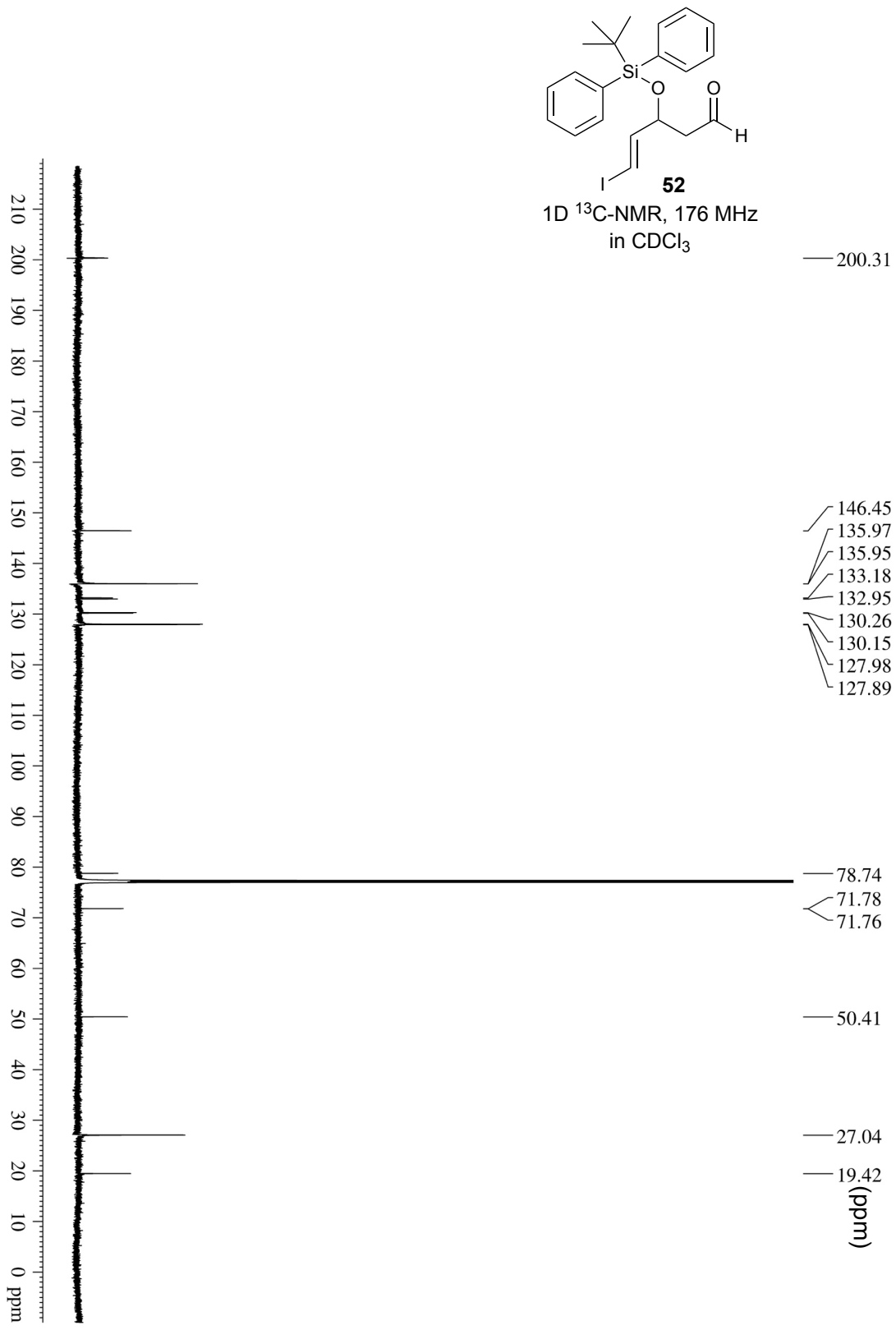
Si
O
O
H
I
52
1D 13C-NMR, 176 MHz
in CDCl3
200.31
146.45
135.97
135.95
133.18
132.95
130.26
130.15
127.98
127.89
78.74
71.78
71.76
50.41
27.04
19.42
(ppm)
210 200 190 180 170 160 150 140 130 120 110 100 90 80 70 60 50 40 30 20 10 0 ppm

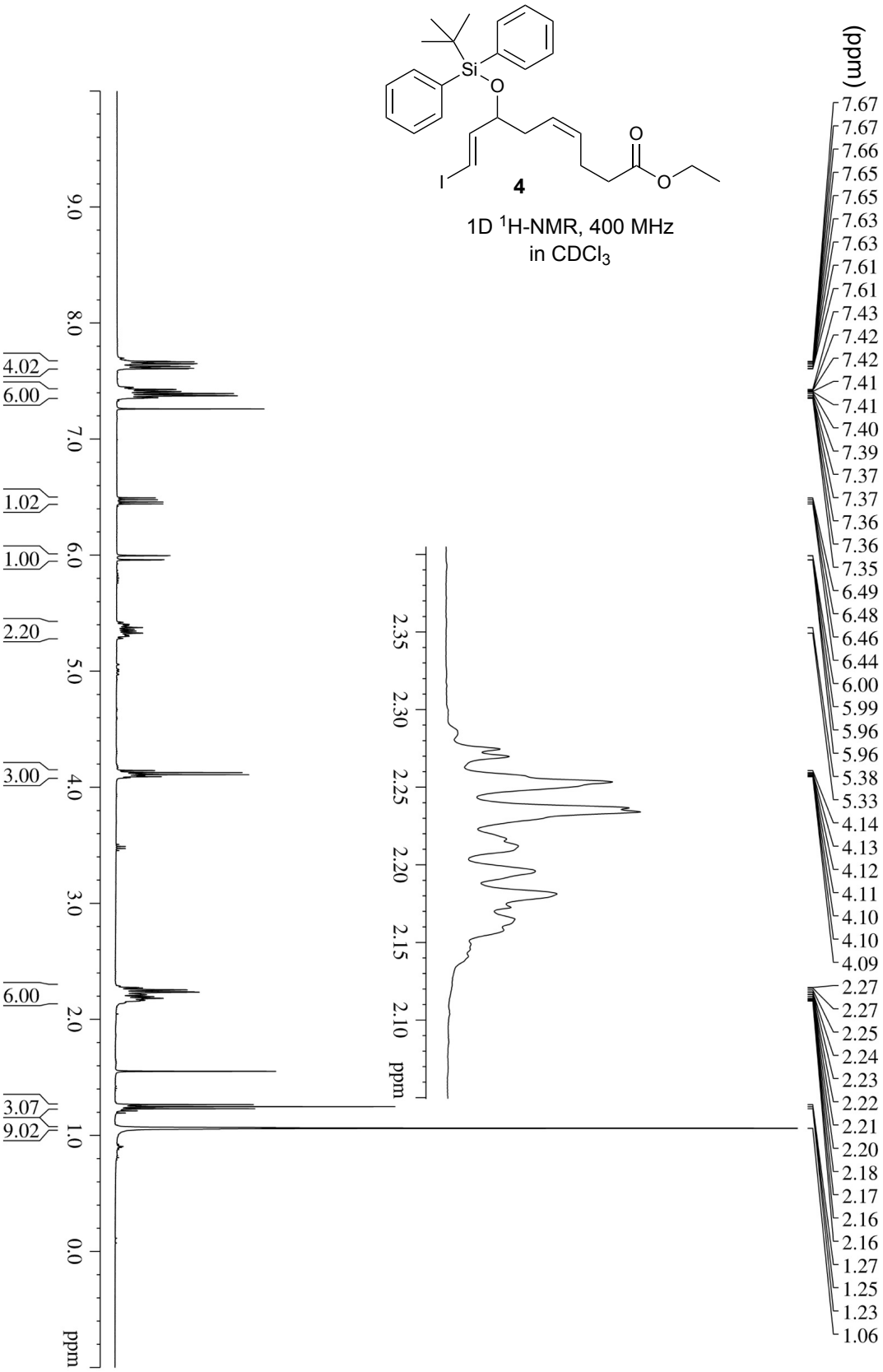
Si
O
O
O
I
4
1D $^1$H-NMR, 400 MHz
in $CDCl_3$
(ppm)
7.67
7.67
7.66
7.65
7.65
7.63
7.63
7.61
7.61
7.43
7.42
7.42
7.41
7.41
7.40
7.39
7.37
7.37
7.36
7.36
7.35
6.49
6.48
6.46
6.44
6.00
5.99
5.96
5.96
5.38
5.33
4.14
4.13
4.12
4.11
4.10
4.10
4.09
2.27
2.27
2.25
2.24
2.23
2.22
2.21
2.20
2.18
2.17
2.16
2.16
1.27
1.25
1.23
1.06
4.02
6.00
1.02
1.00
2.20
3.00
6.00
3.07
9.02
9.0
8.0
7.0
6.0
5.0
4.0
3.0
2.0
1.0
0.0
ppm
2.35
2.30
2.25
2.20
2.15
2.10
ppm

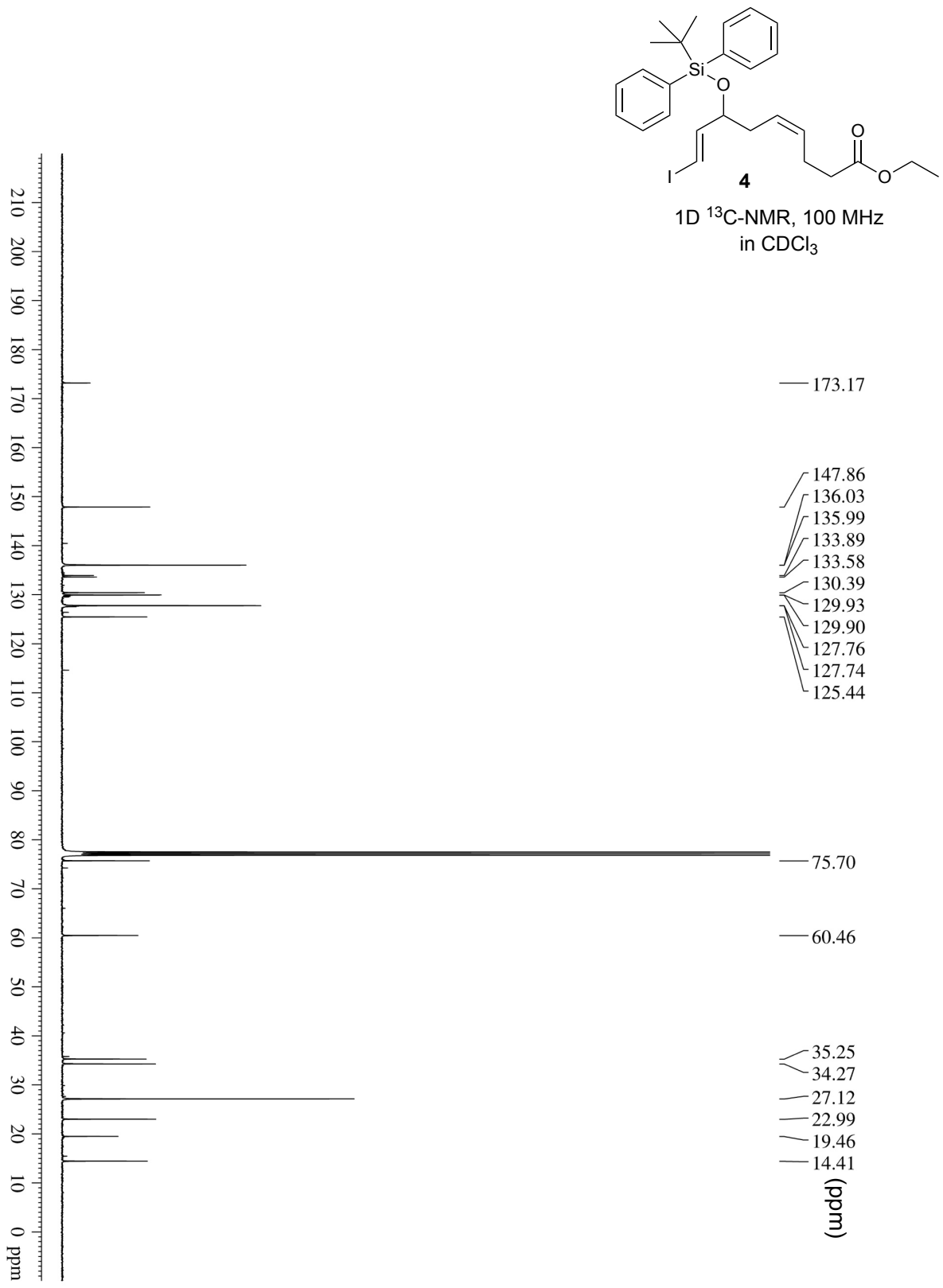
Si
O
O
O
I
4
1D $^{13}$C-NMR, 100 MHz
in $CDCl_3$
173.17
147.86
136.03
135.99
133.89
133.58
130.39
129.93
129.90
127.76
127.74
125.44
75.70
60.46
35.25
34.27
27.12
22.99
19.46
14.41
(ppm)
210 200 190 180 170 160 150 140 130 120 110 100 90 80 70 60 50 40 30 20 10 0 ppm

(ppm)
5.374
5.358
5.322
5.302
5.287
5.40 5.35 5.30 5.25 ppm
7.5 7.0 6.5 6.0 5.5 5.0 4.5 4.0 3.5 3.0 2.5 2.0 1.5 1.0 0.5 ppm
TBDPS
O
I
O
OEt
H H
H H
H H
1D homo-decoupled $^1$H-NMR,
700 MHz in $CDCl_3$
4
1D $^1$H-NMR, 700 MHz
in $CDCl_3$

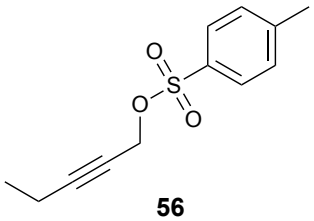

**56**

1D $^{1}$H-NMR, 400 MHz
in $CDCl_3$

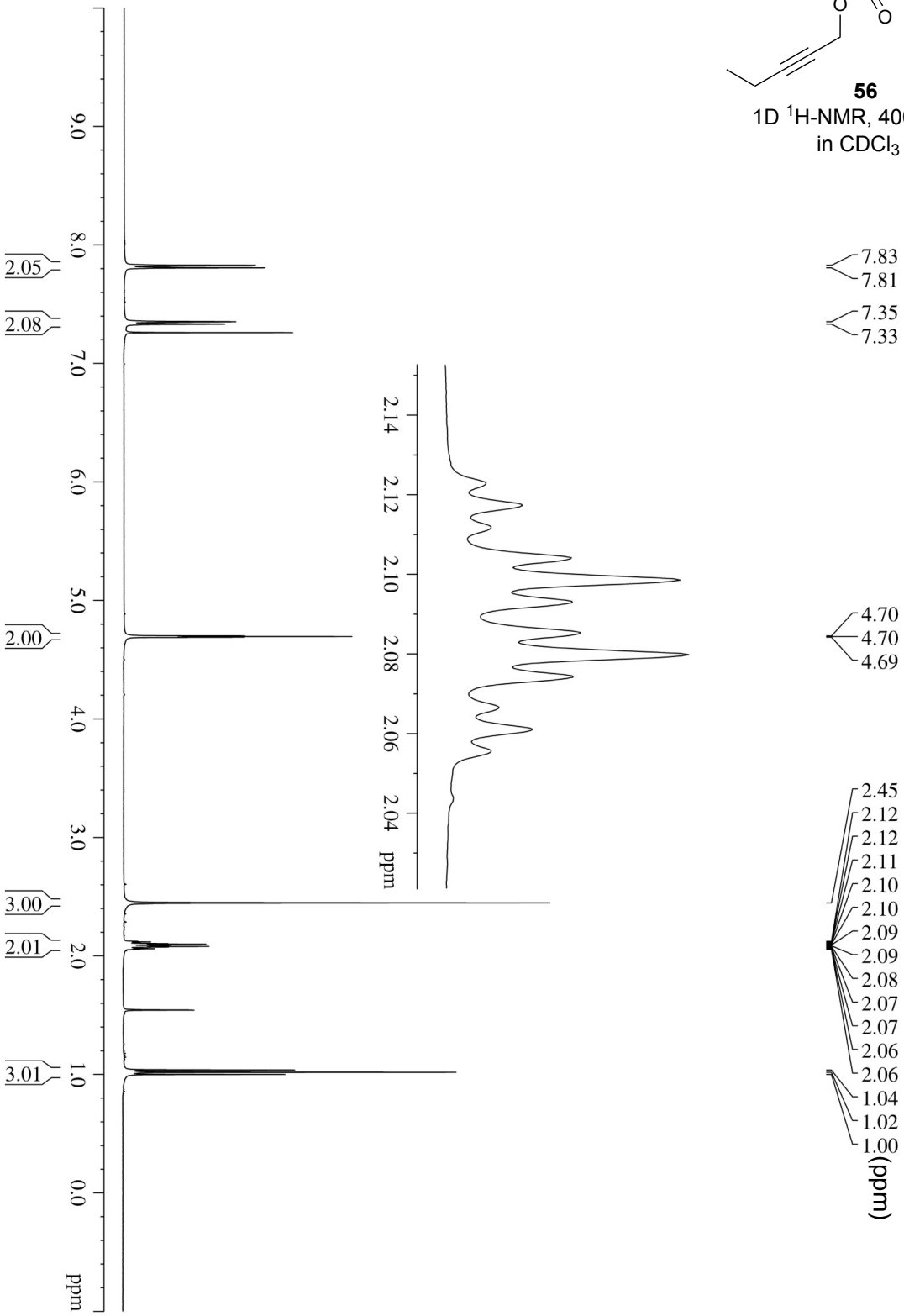

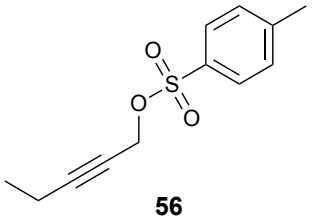


**56**
1D $^{13}$C-NMR, 100 MHz
in $CDCl_3$

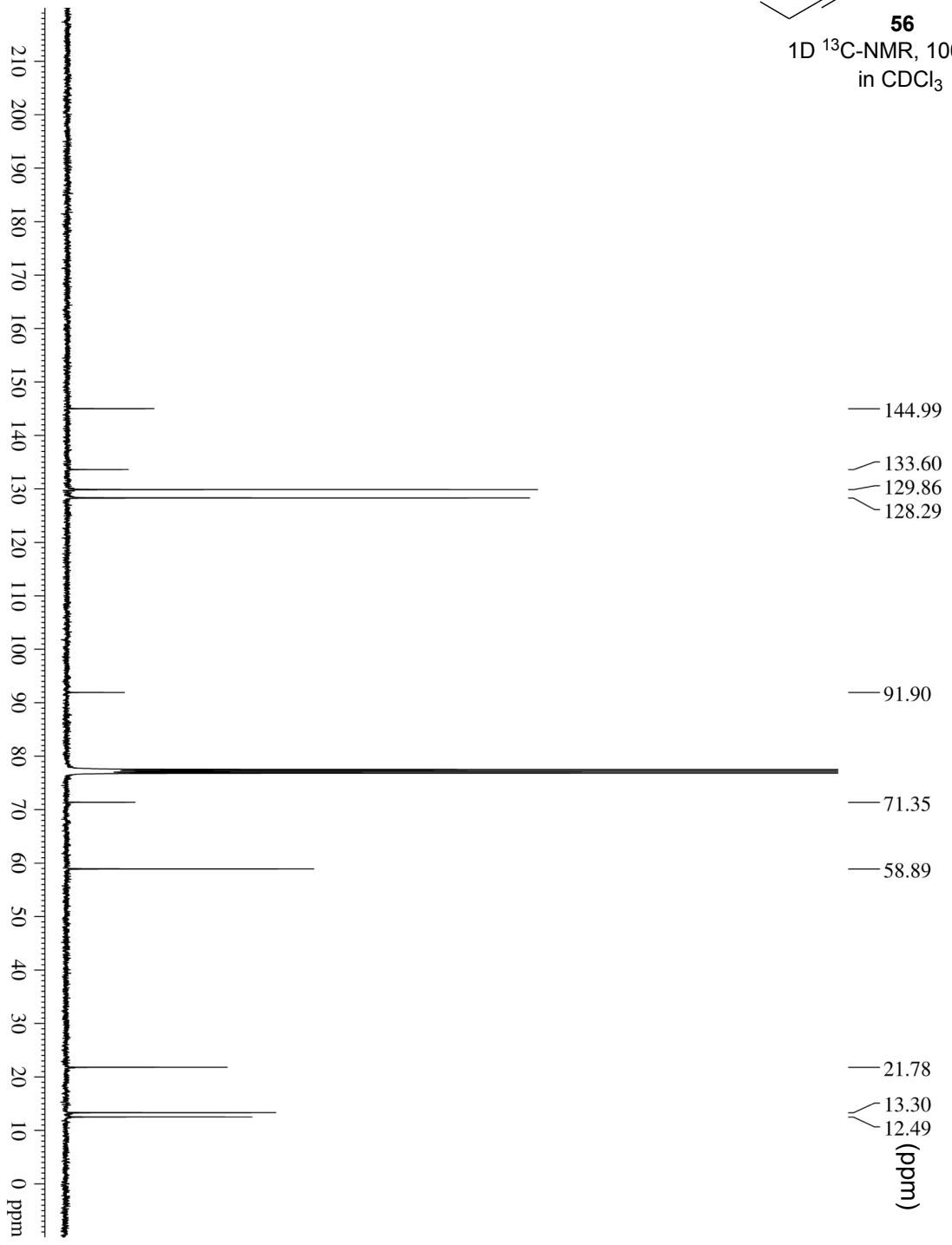

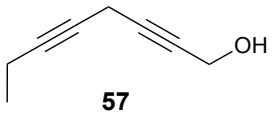


**57**

1D $^{1}$H-NMR, 400 MHz
in $CDCl_3$

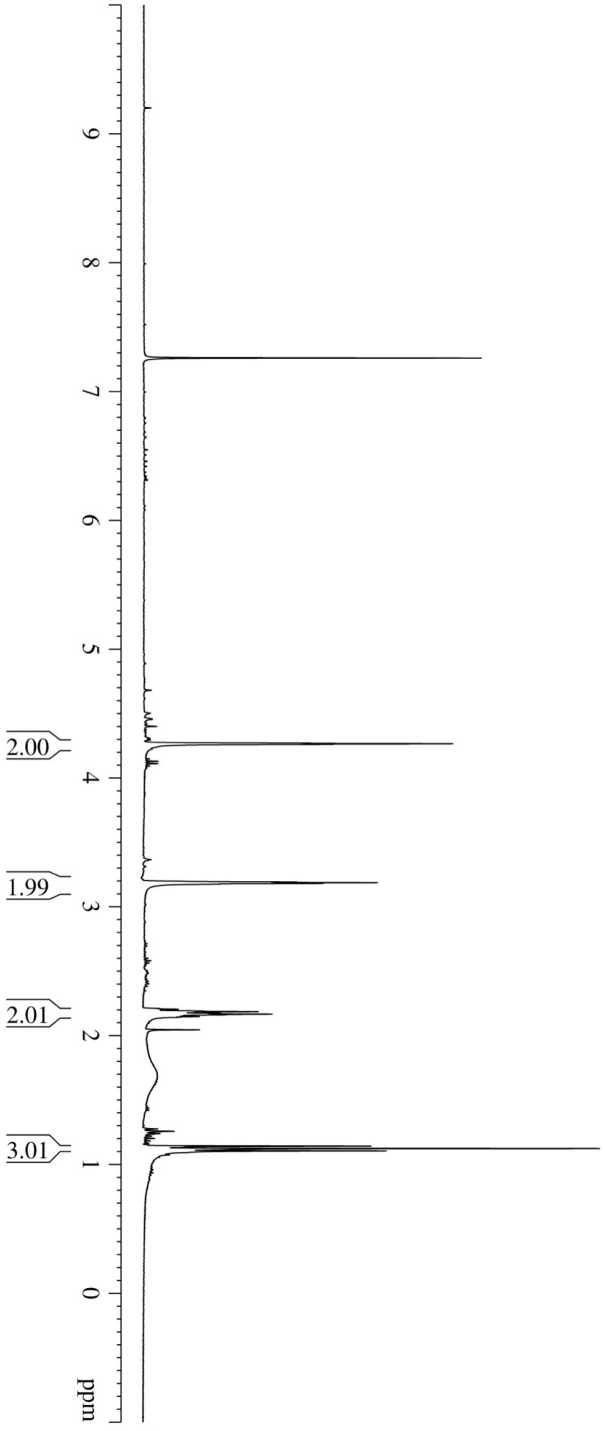


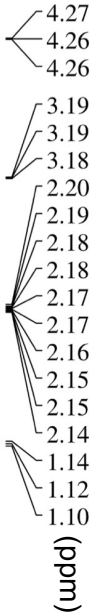

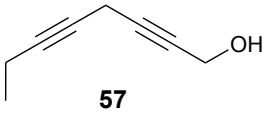


**57**

1D $^{13}$C-NMR, 100 MHz
in $CDCl_3$

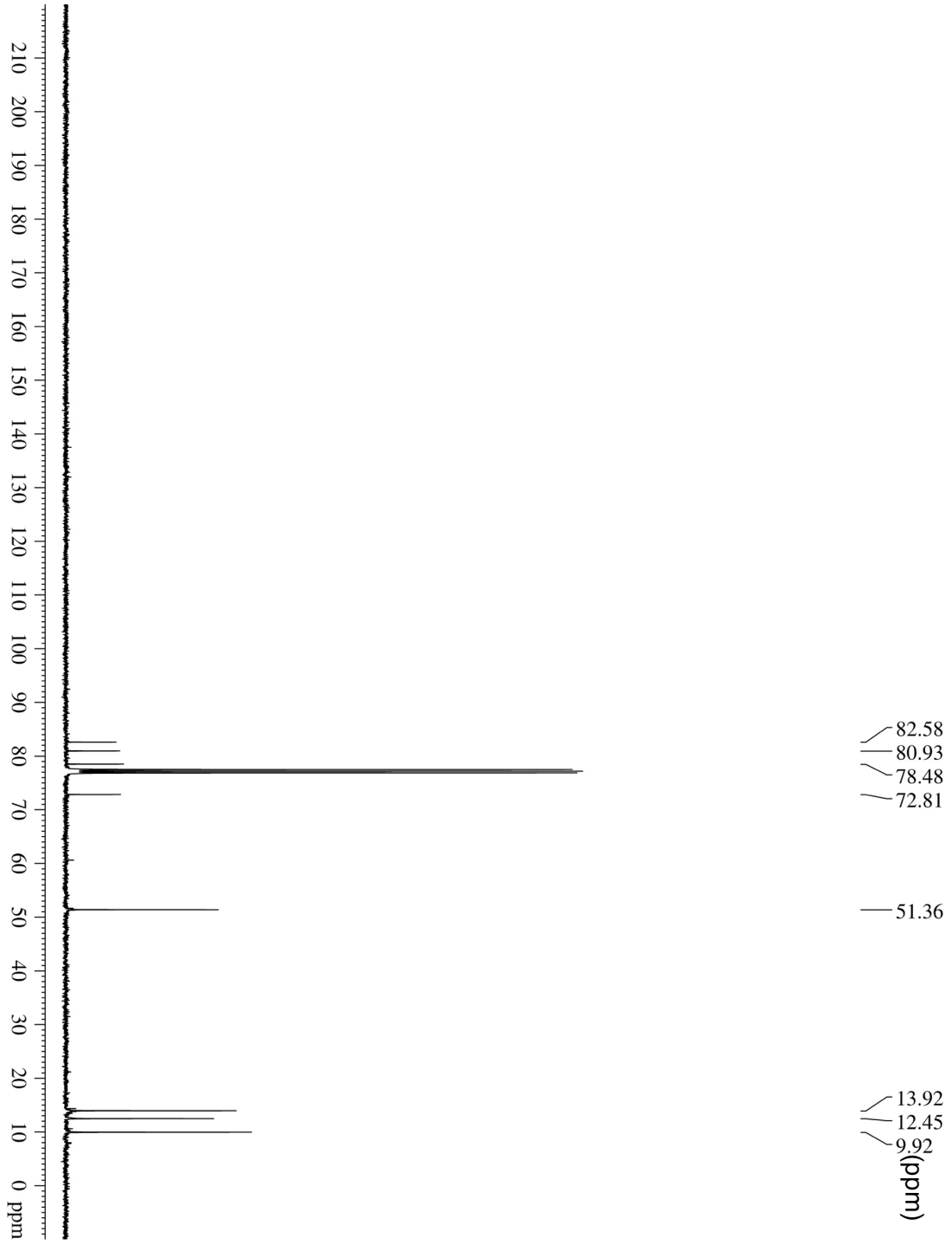

**58**

1D $^{1}$H-NMR, 600 MHz
in $CDCl_3$

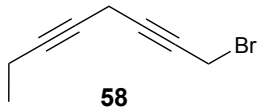


**58**

1D $^{13}$C-NMR, 150 MHz
in $CDCl_3$

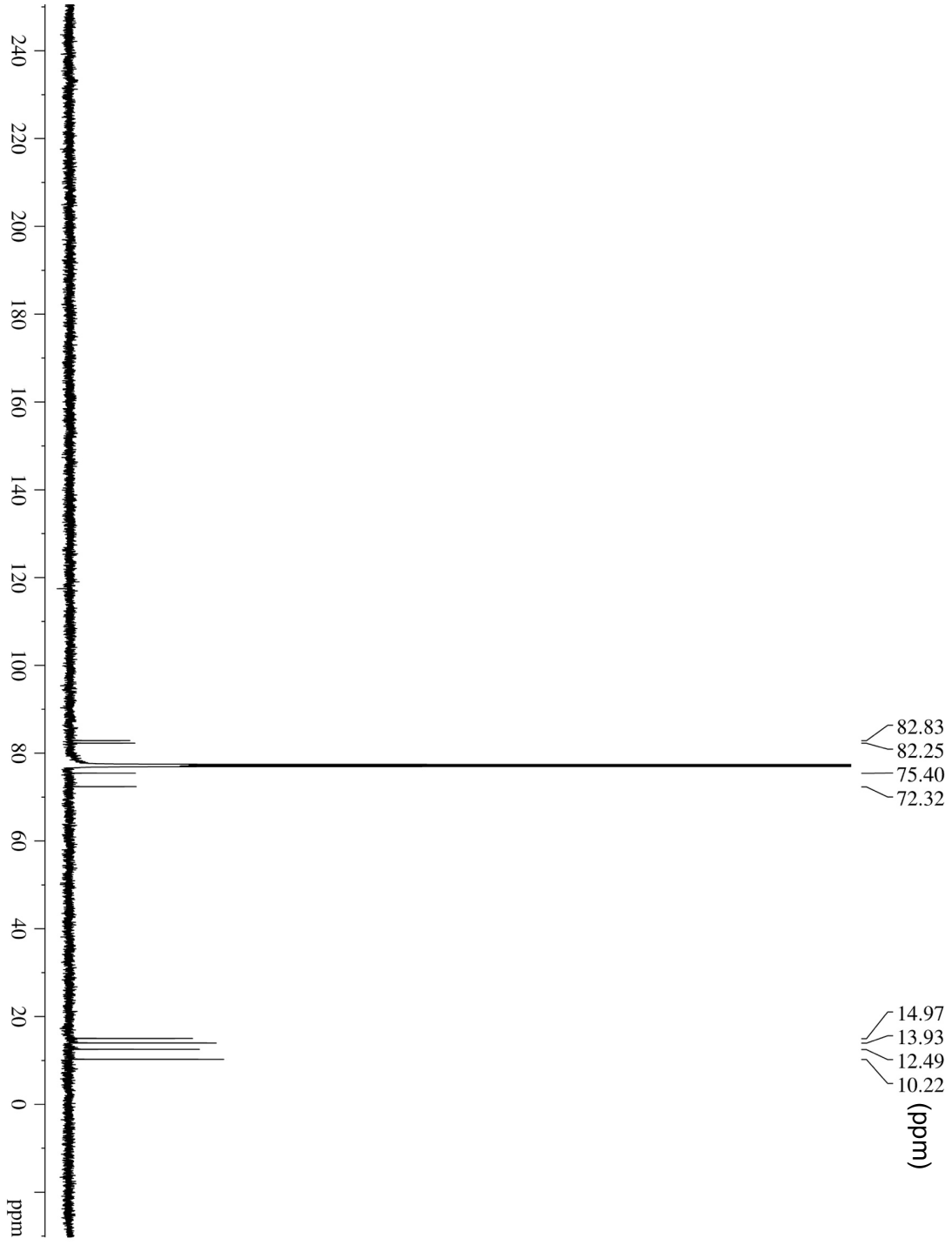

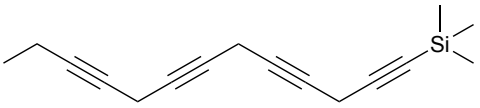


**60 (cude)**

1D $^{1}$H-NMR, 300 MHz
in $CDCl_3$

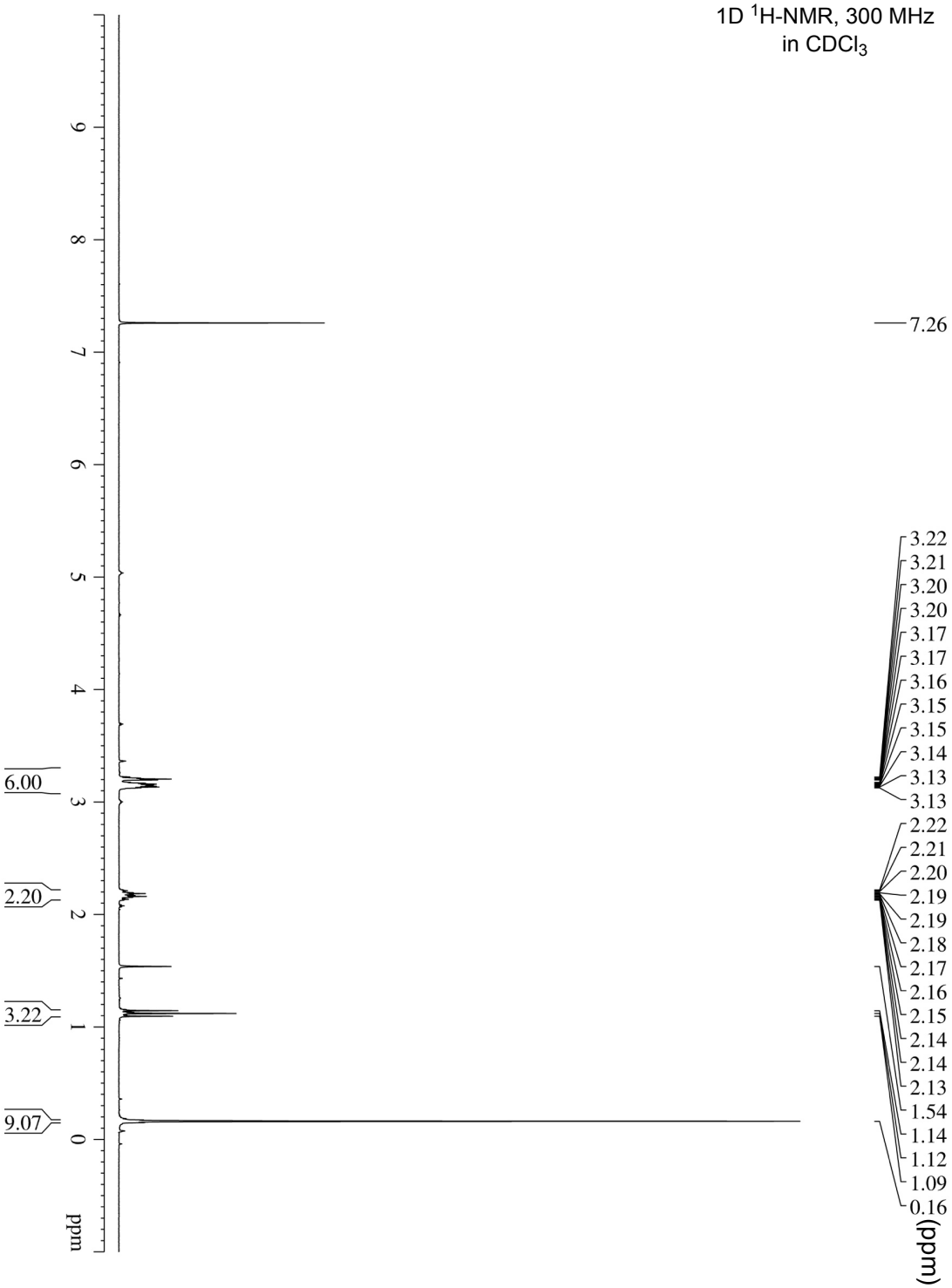

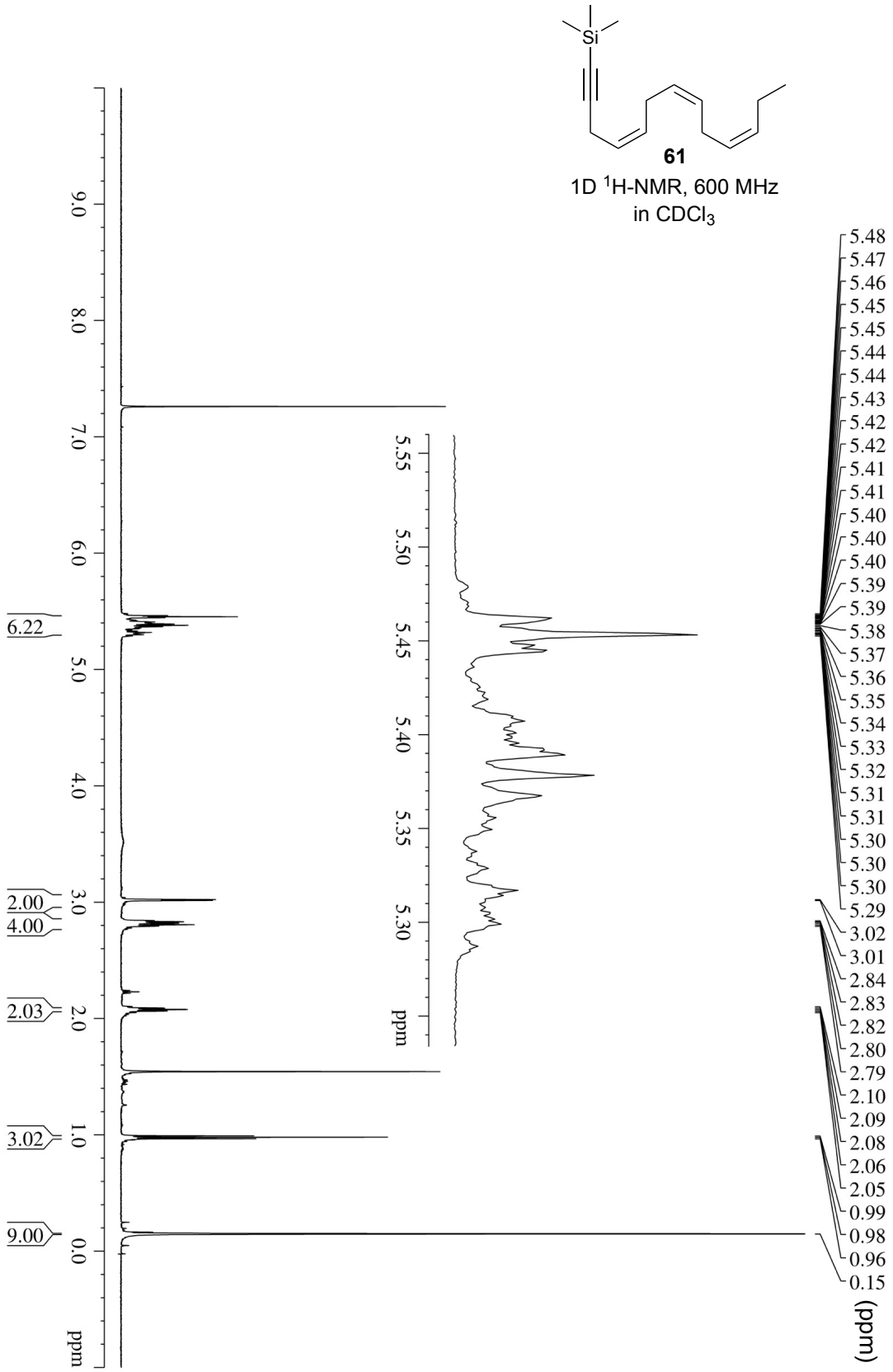
Si
61
1D $^{1}$H-NMR, 600 MHz
in $CDCl_3$
9.0
8.0
7.0
6.0
5.0
4.0
3.0
2.0
1.0
0.0
ppm
6.22
2.00
4.00
2.03
3.02
9.00
5.55
5.50
5.45
5.40
5.35
5.30
ppm
5.48
5.47
5.46
5.45
5.45
5.44
5.44
5.43
5.42
5.42
5.41
5.41
5.40
5.40
5.40
5.39
5.39
5.38
5.37
5.36
5.35
5.34
5.33
5.32
5.31
5.31
5.30
5.30
5.30
5.29
3.02
3.01
2.84
2.83
2.82
2.80
2.79
2.10
2.09
2.08
2.06
2.05
0.99
0.98
0.96
0.15
(ppm)

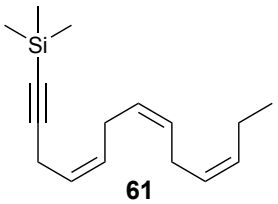


**61**

1D $^{13}$C-NMR, 150 MHz
in $CDCl_3$

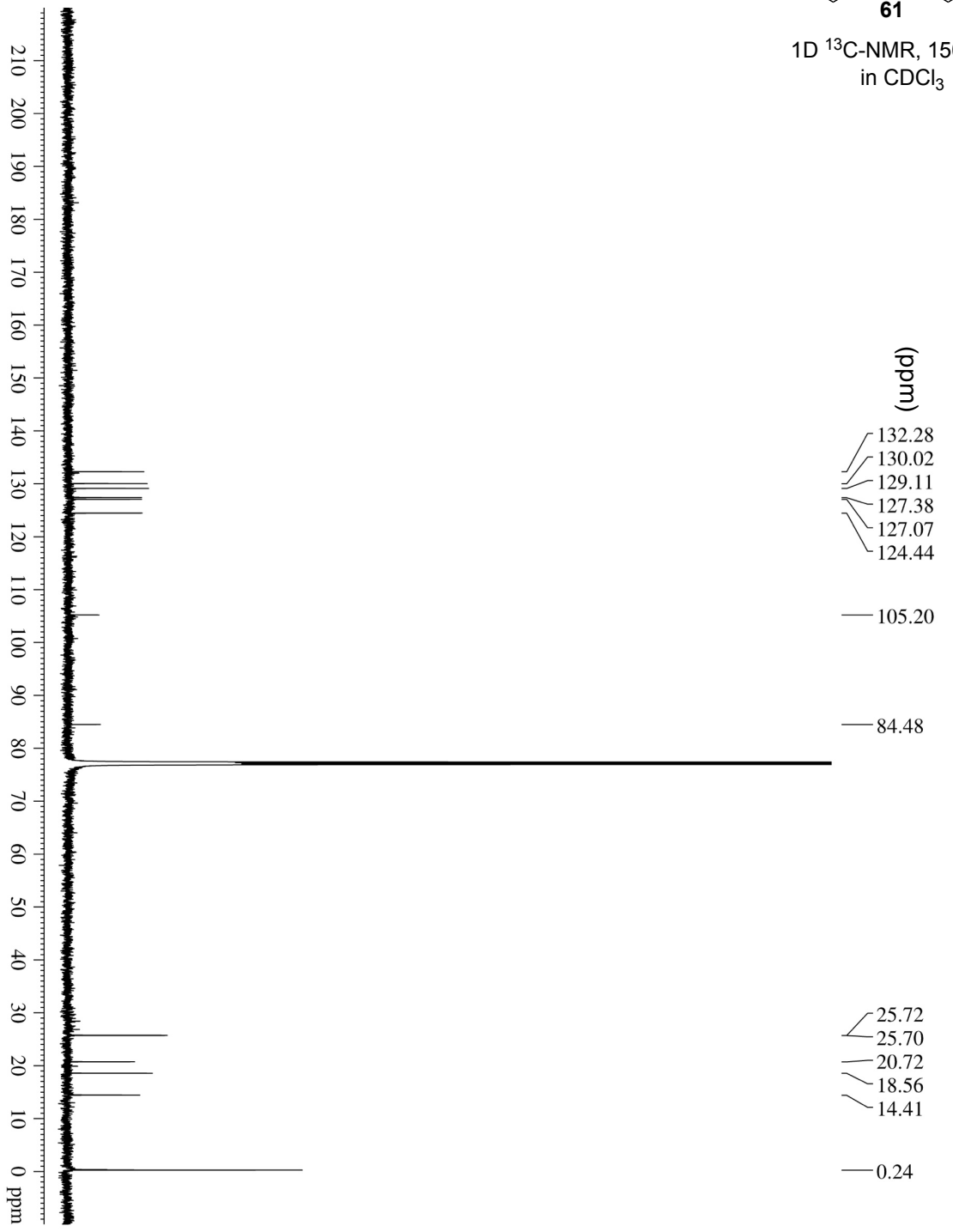

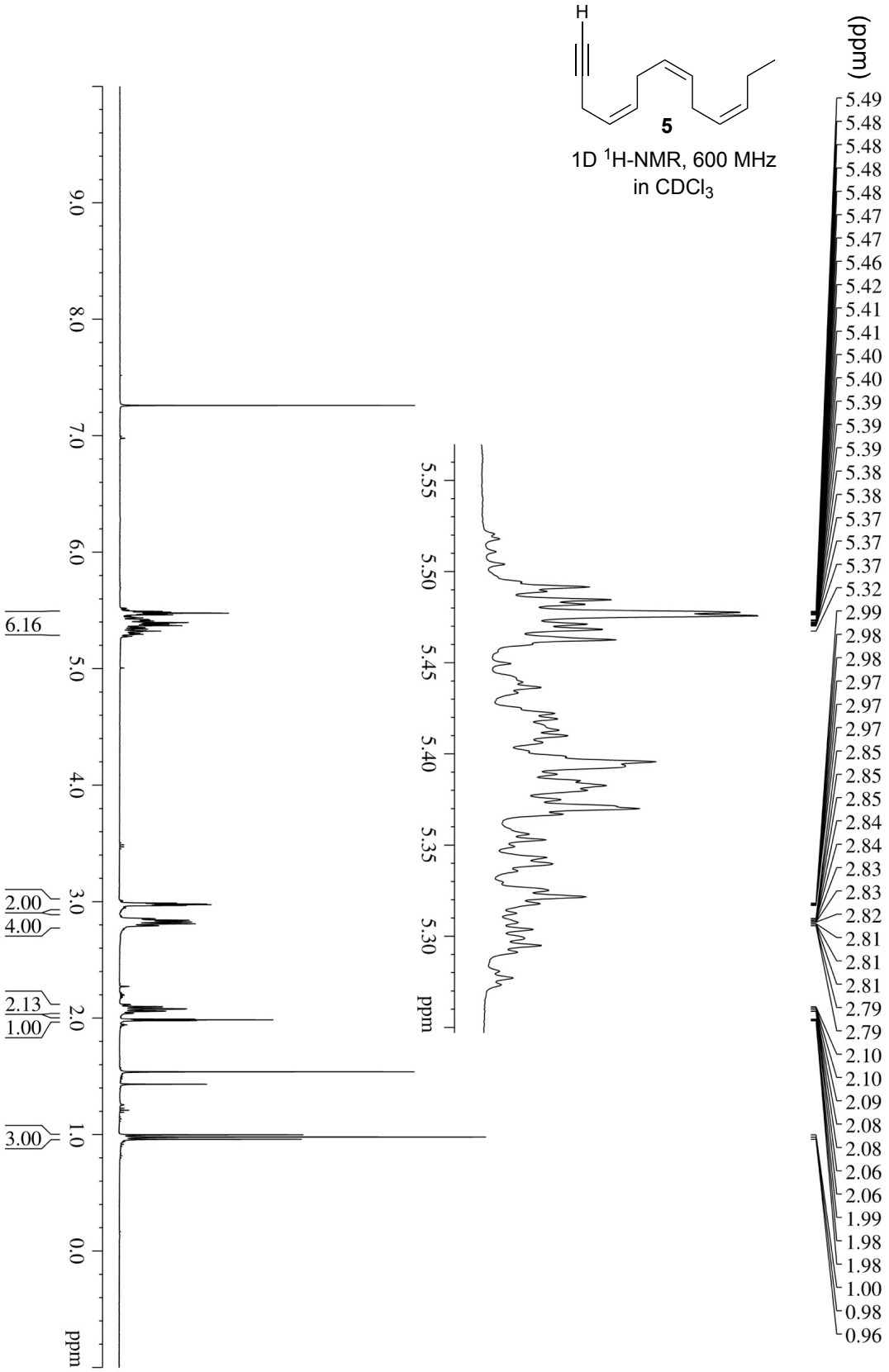
H
5
1D $^{1}$H-NMR, 600 MHz
in $CDCl_3$
(ppm)
5.49
5.48
5.48
5.48
5.48
5.47
5.47
5.46
5.42
5.41
5.41
5.40
5.40
5.39
5.39
5.39
5.38
5.38
5.37
5.37
5.37
5.32
2.99
2.98
2.98
2.97
2.97
2.97
2.85
2.85
2.85
2.84
2.84
2.83
2.83
2.82
2.81
2.81
2.81
2.79
2.79
2.10
2.10
2.09
2.08
2.08
2.06
2.06
1.99
1.98
1.98
1.00
0.98
0.96
9.0
8.0
7.0
6.0
5.0
4.0
3.0
2.0
1.0
0.0
ppm
6.16
2.00
4.00
2.13
1.00
3.00
5.55
5.50
5.45
5.40
5.35
5.30
ppm

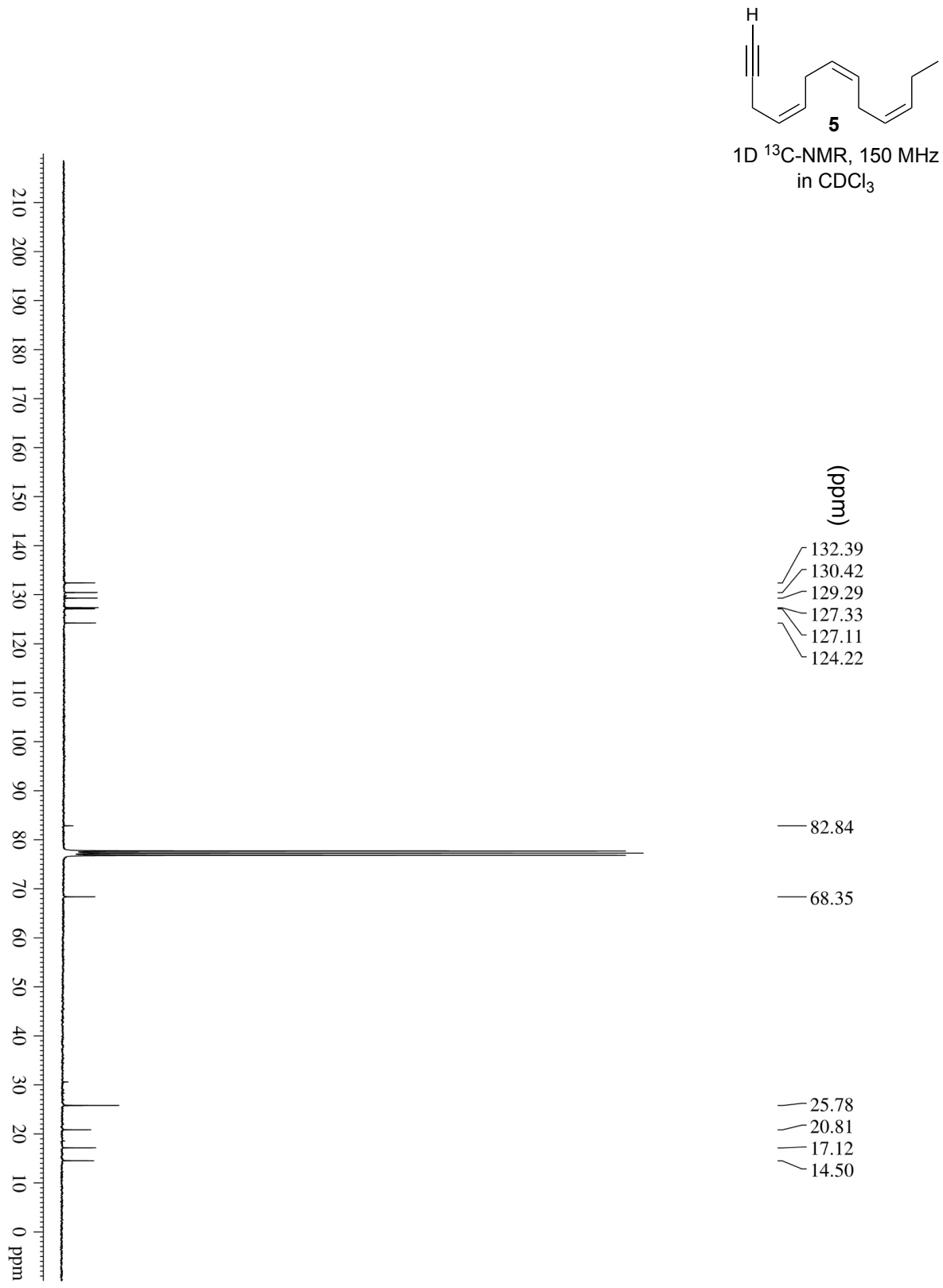
H
5
1D 13C-NMR, 150 MHz
in CDCl3
(ppm)
132.39
130.42
129.29
127.33
127.11
124.22
82.84
68.35
25.78
20.81
17.12
14.50
210 200 190 180 170 160 150 140 130 120 110 100 90 80 70 60 50 40 30 20 10 0 ppm

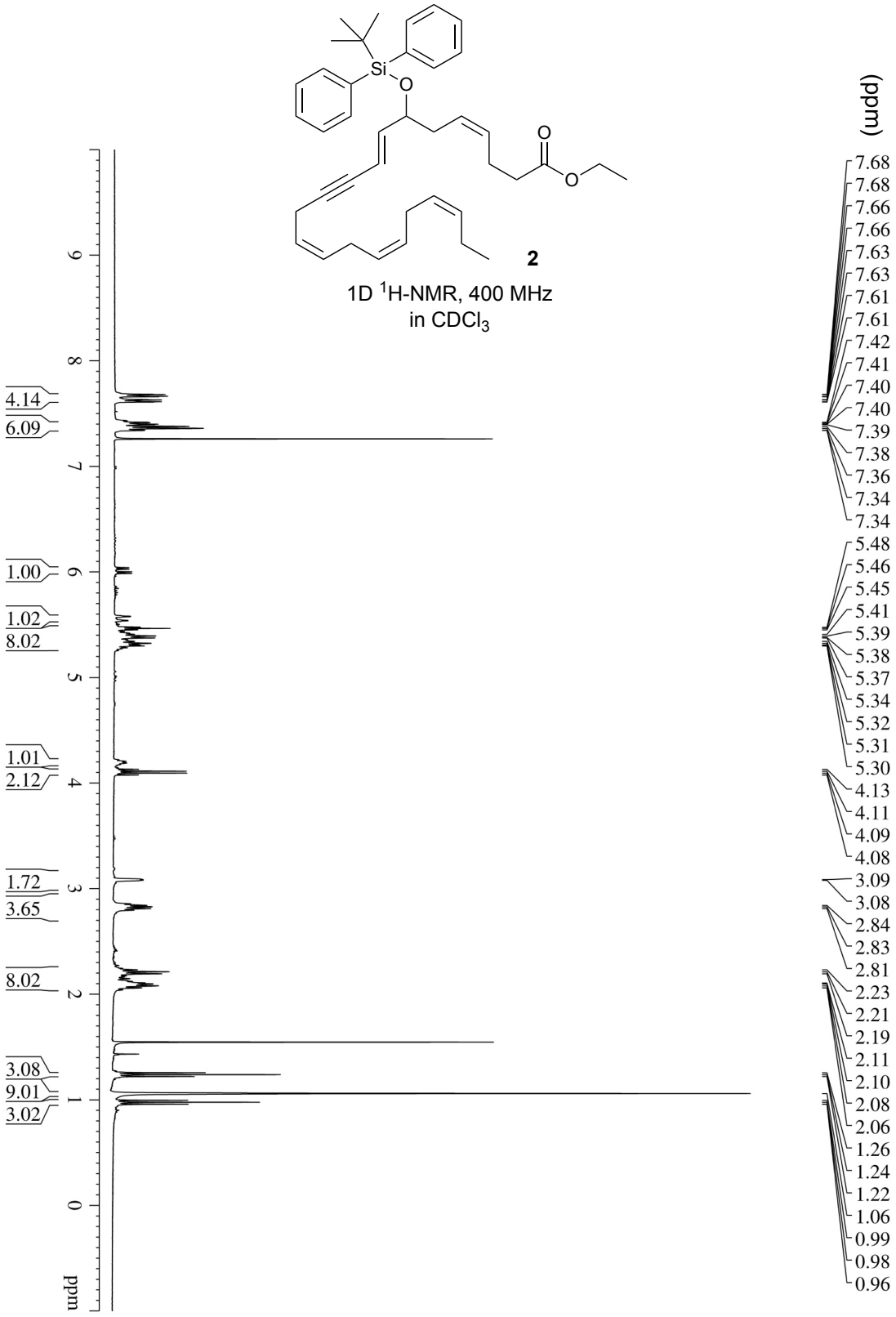
Si
O
O
O
2
1D $^{1}$H-NMR, 400 MHz
in $CDCl_3$
4.14
6.09
1.00
1.02
8.02
1.01
2.12
1.72
3.65
8.02
3.08
9.01
3.02
ppm
(ppm)
7.68
7.68
7.66
7.66
7.63
7.63
7.61
7.61
7.42
7.41
7.40
7.40
7.39
7.38
7.36
7.34
7.34
5.48
5.46
5.45
5.41
5.39
5.38
5.37
5.34
5.32
5.31
5.30
4.13
4.11
4.09
4.08
3.09
3.08
2.84
2.83
2.81
2.23
2.21
2.19
2.11
2.10
2.08
2.06
1.26
1.24
1.22
1.06
0.99
0.98
0.96

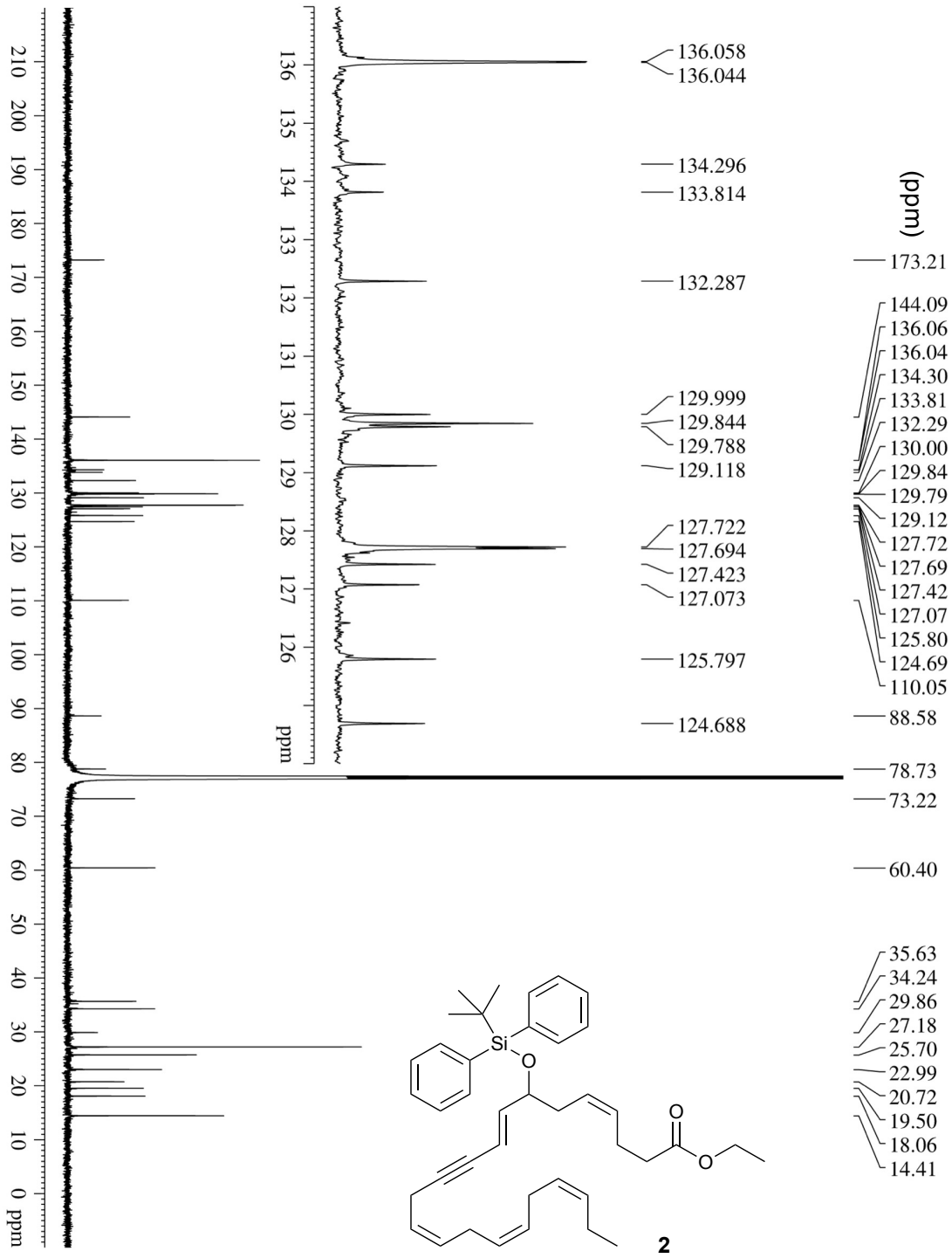


**2**

1D $^{13}$C-NMR, 150 MHz
in $CDCl_3$

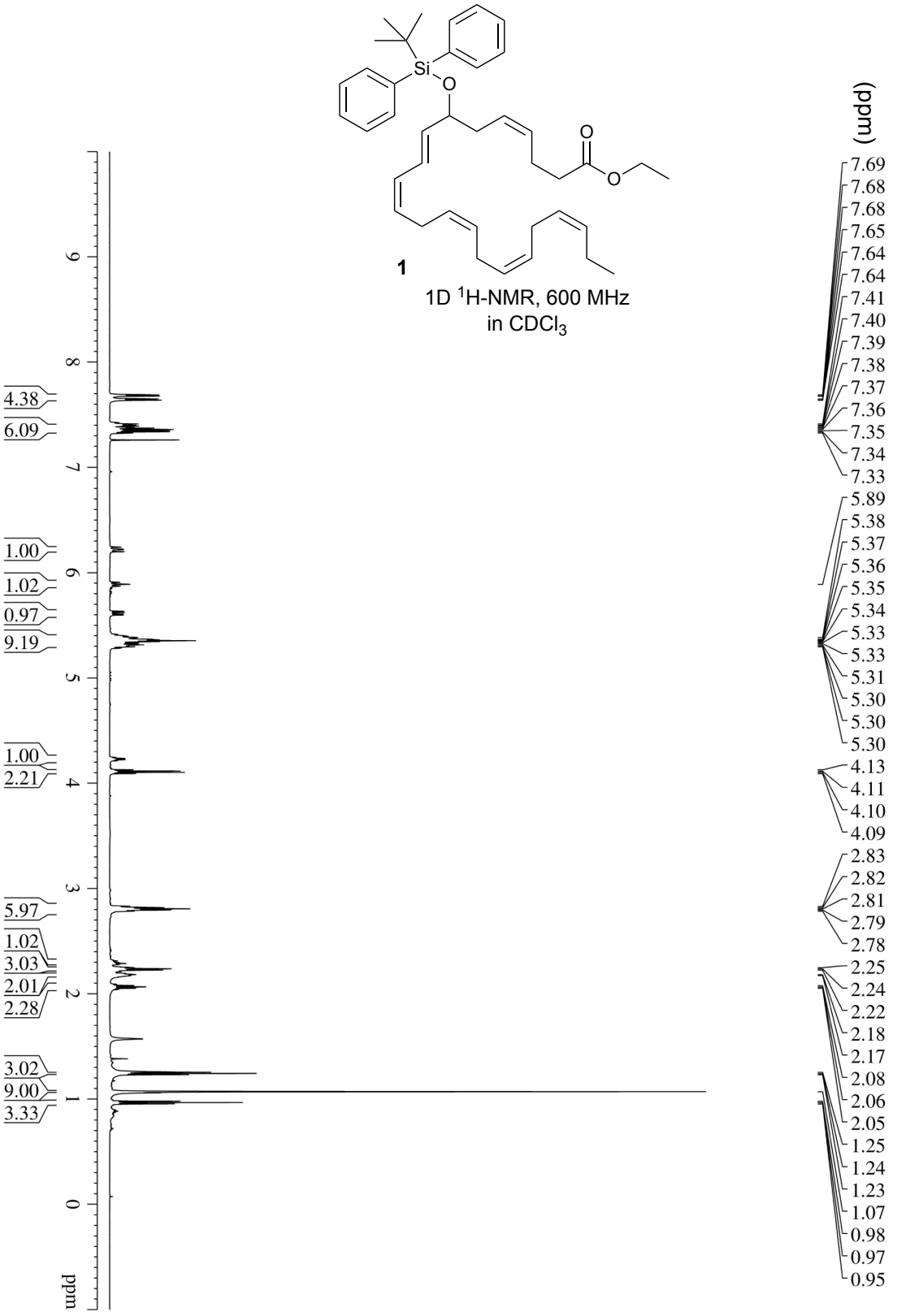
Si
O
O
O
1
1D $^{1}$H-NMR, 600 MHz
in $CDCl_3$
(ppm)
7.69
7.68
7.68
7.65
7.64
7.64
7.41
7.40
7.39
7.38
7.37
7.36
7.35
7.34
7.33
5.89
5.38
5.37
5.36
5.35
5.34
5.33
5.33
5.31
5.30
5.30
5.30
4.13
4.11
4.10
4.09
2.83
2.82
2.81
2.79
2.78
2.25
2.24
2.22
2.18
2.17
2.08
2.06
2.05
1.25
1.24
1.23
1.07
0.98
0.97
0.95
4.38
6.09
1.00
1.02
0.97
9.19
1.00
2.21
5.97
1.02
3.03
2.01
2.28
3.02
9.00
3.33
ppm

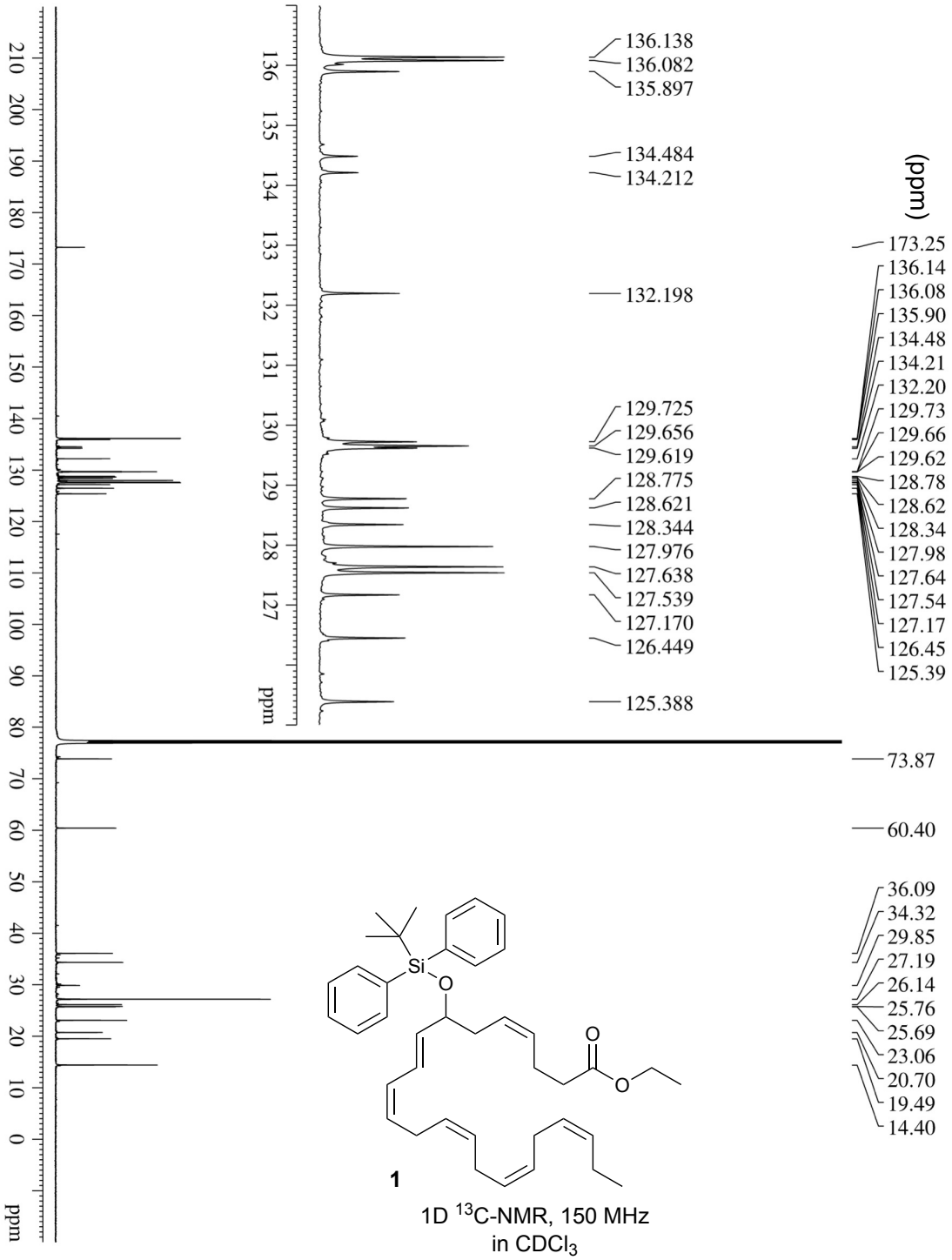


**1**

1D $^{13}$C-NMR, 150 MHz
in $CDCl_3$

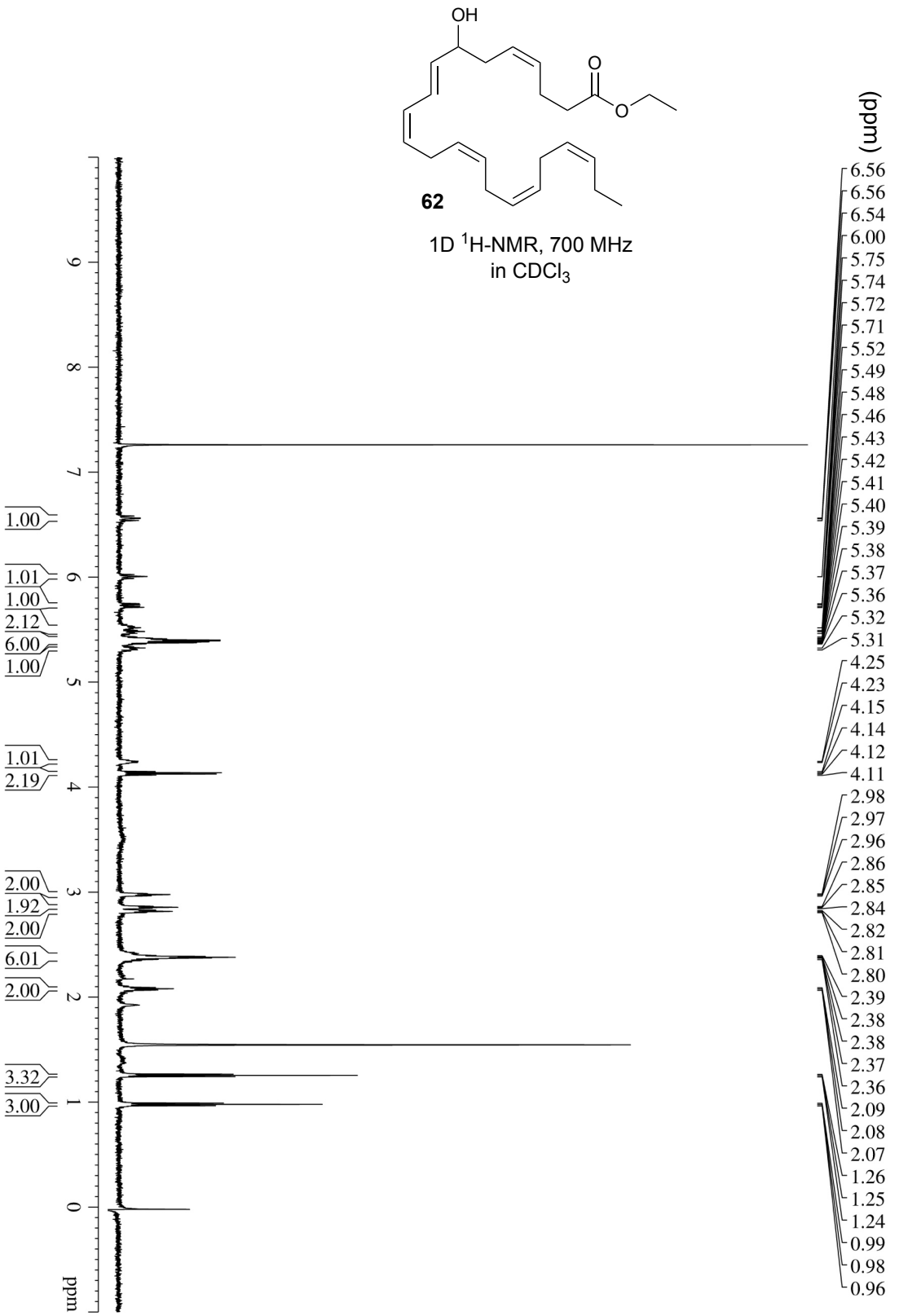
OH
O
O
62
1D $^{1}$H-NMR, 700 MHz
in $CDCl_3$
(ppm)
6.56
6.56
6.54
6.00
5.75
5.74
5.72
5.71
5.52
5.49
5.48
5.46
5.43
5.42
5.41
5.40
5.39
5.38
5.37
5.36
5.32
5.31
4.25
4.23
4.15
4.14
4.12
4.11
2.98
2.97
2.96
2.86
2.85
2.84
2.82
2.81
2.80
2.39
2.38
2.38
2.37
2.36
2.09
2.08
2.07
1.26
1.25
1.24
0.99
0.98
0.96
1.00
1.01
1.00
2.12
6.00
1.00
1.01
2.19
2.00
1.92
2.00
6.01
2.00
3.32
3.00
ppm

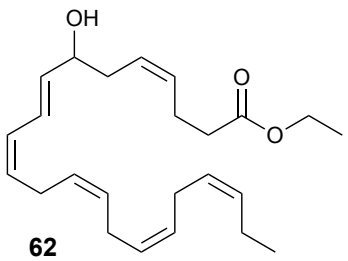


**62**

1D $^{13}$C-NMR, 150 MHz
in $CDCl_3$

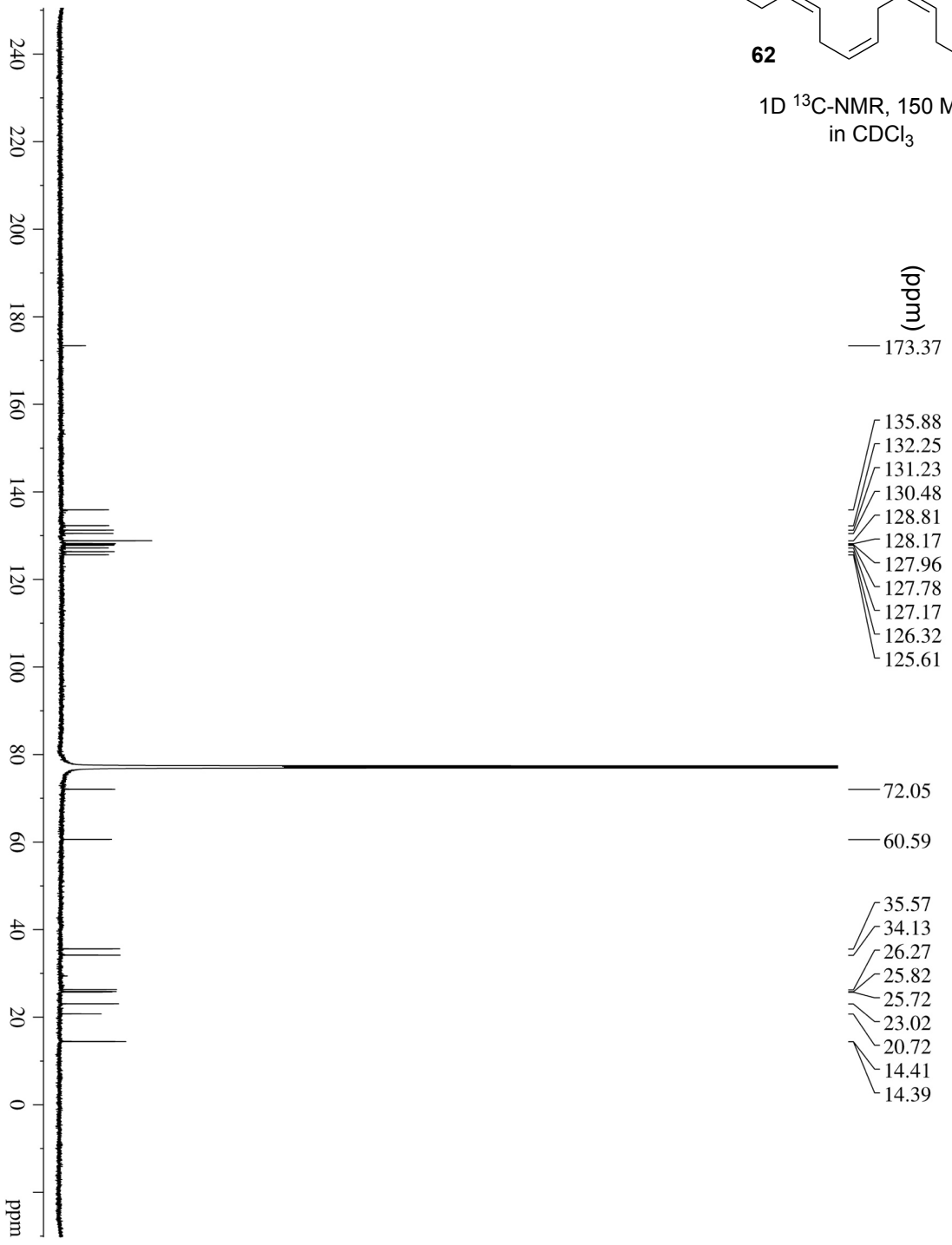

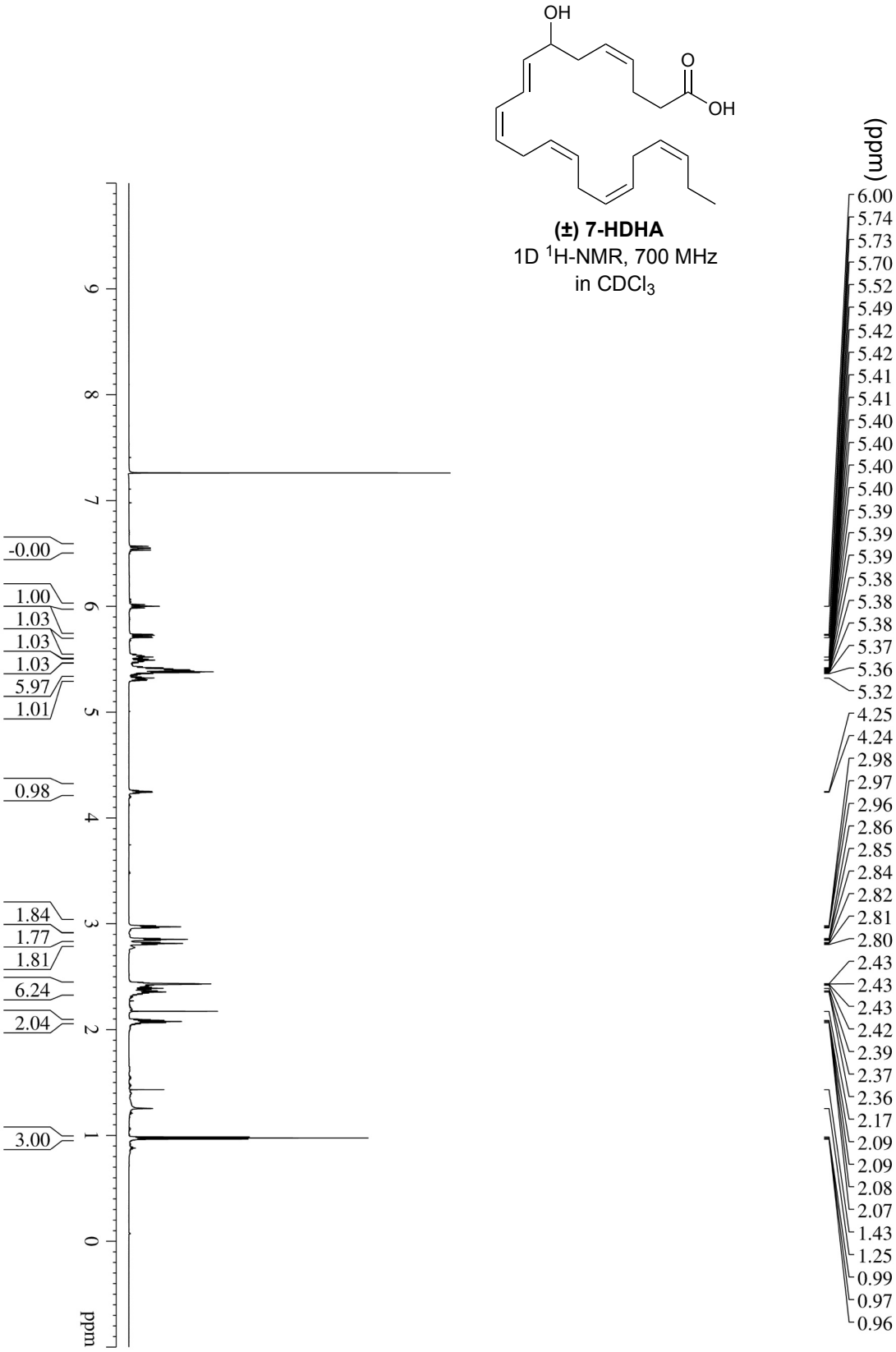
OH
O
OH
(±) 7-HDHA
1D $^{1}$H-NMR, 700 MHz
in $CDCl_3$
ppm
-0.00
1.00
1.03
1.03
1.03
5.97
1.01
0.98
1.84
1.77
1.81
6.24
2.04
3.00
6.00
5.74
5.73
5.70
5.52
5.49
5.42
5.42
5.41
5.41
5.40
5.40
5.40
5.40
5.39
5.39
5.39
5.38
5.38
5.38
5.37
5.36
5.32
4.25
4.24
2.98
2.97
2.96
2.86
2.85
2.84
2.82
2.81
2.80
2.43
2.43
2.43
2.42
2.39
2.37
2.36
2.17
2.09
2.09
2.08
2.07
1.43
1.25
0.99
0.97
0.96

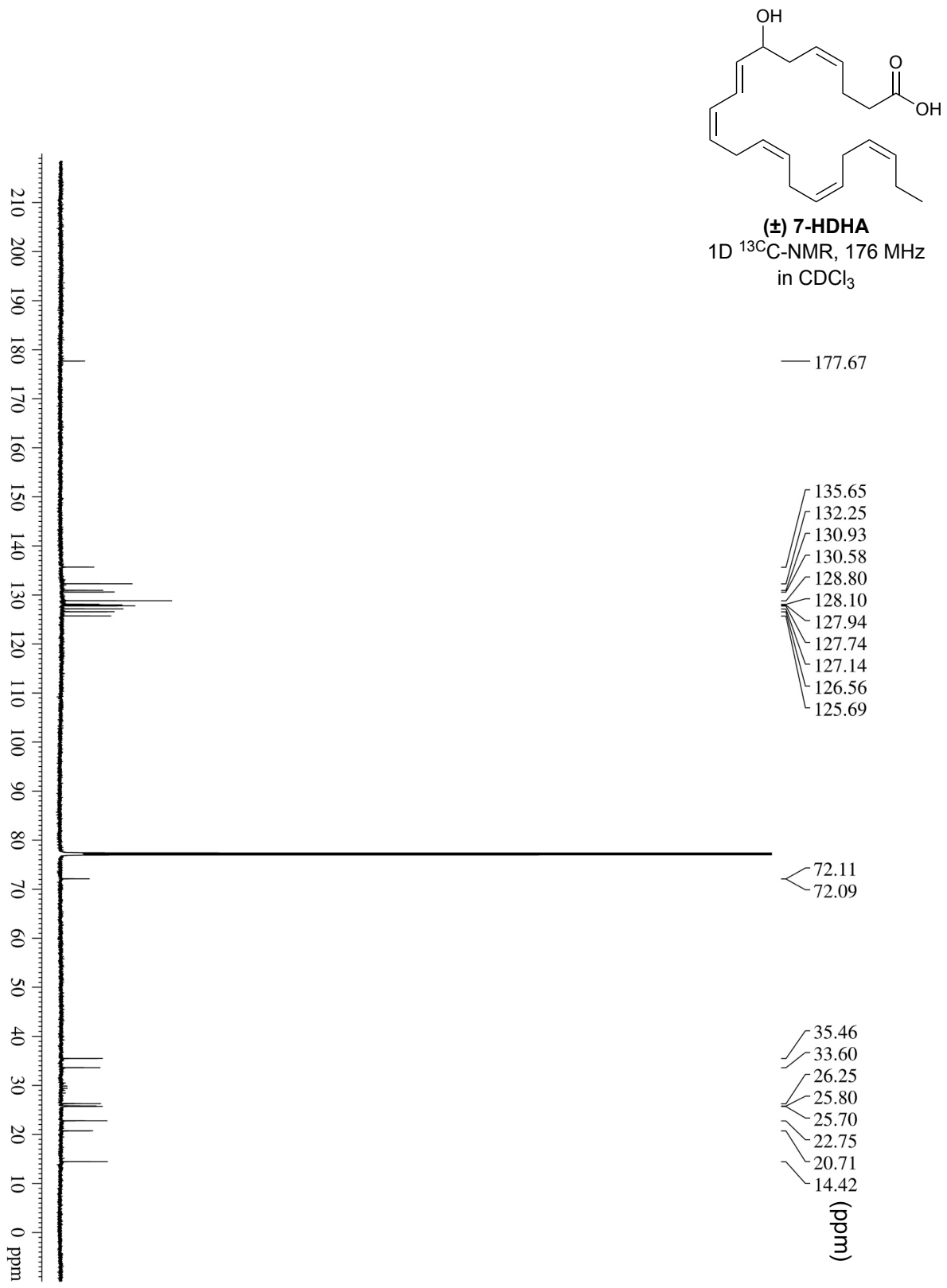
OH
O
OH
(±) 7-HDHA
1D 13C-NMR, 176 MHz
in CDCl3
177.67
135.65
132.25
130.93
130.58
128.80
128.10
127.94
127.74
127.14
126.56
125.69
72.11
72.09
35.46
33.60
26.25
25.80
25.70
22.75
20.71
14.42
210 200 190 180 170 160 150 140 130 120 110 100 90 80 70 60 50 40 30 20 10 0 ppm
(ppm)

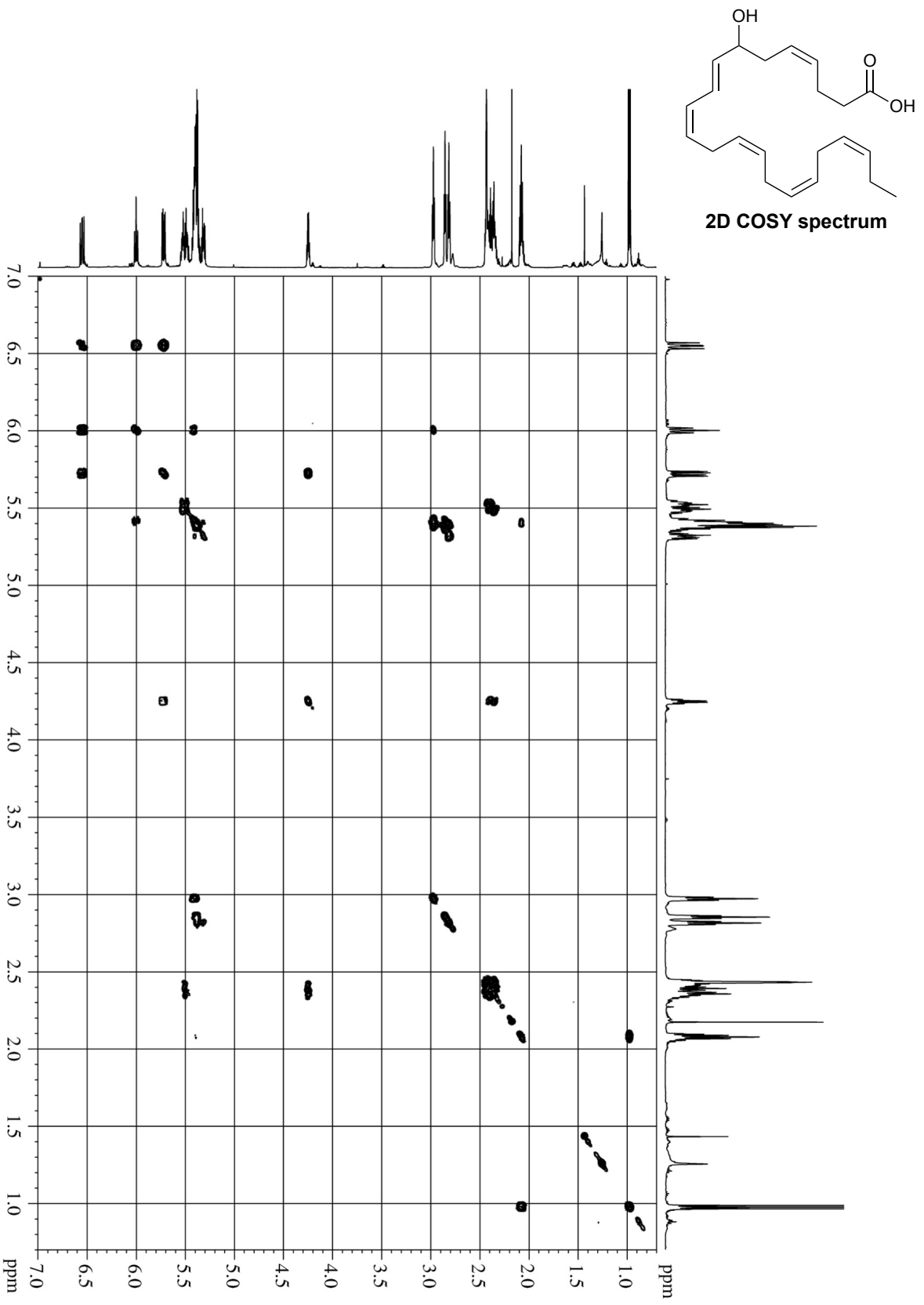
OH
O
OH
2D COSY spectrum
7.0
6.5
6.0
5.5
5.0
4.5
4.0
3.5
3.0
2.5
2.0
1.5
1.0
ppm

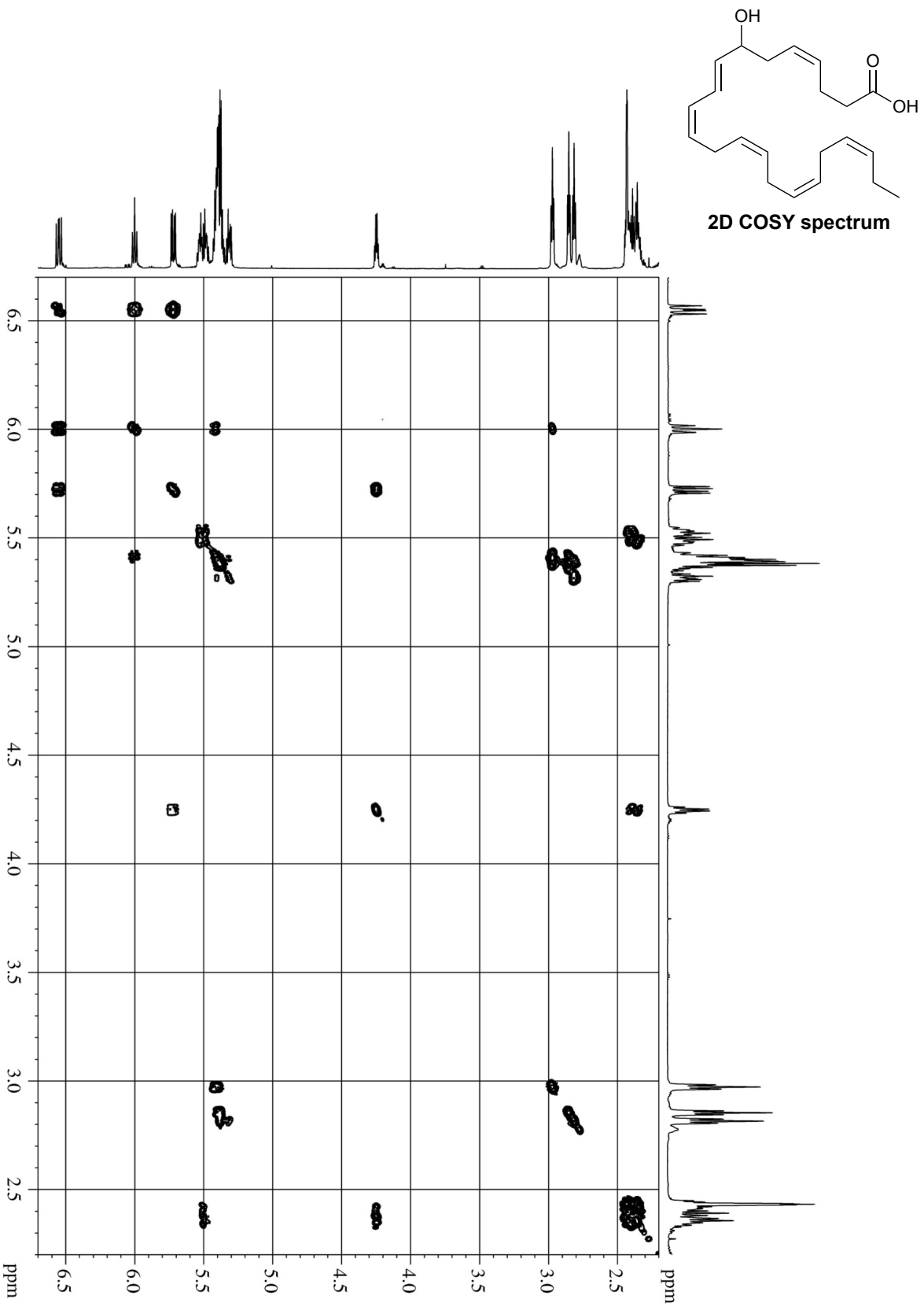
OH
O
OH
2D COSY spectrum
6.5
6.0
5.5
5.0
4.5
4.0
3.5
3.0
2.5
ppm

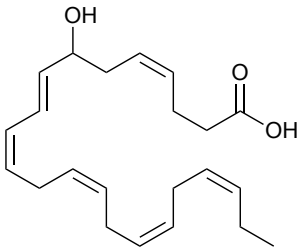


**2D TOCSY spectrum**

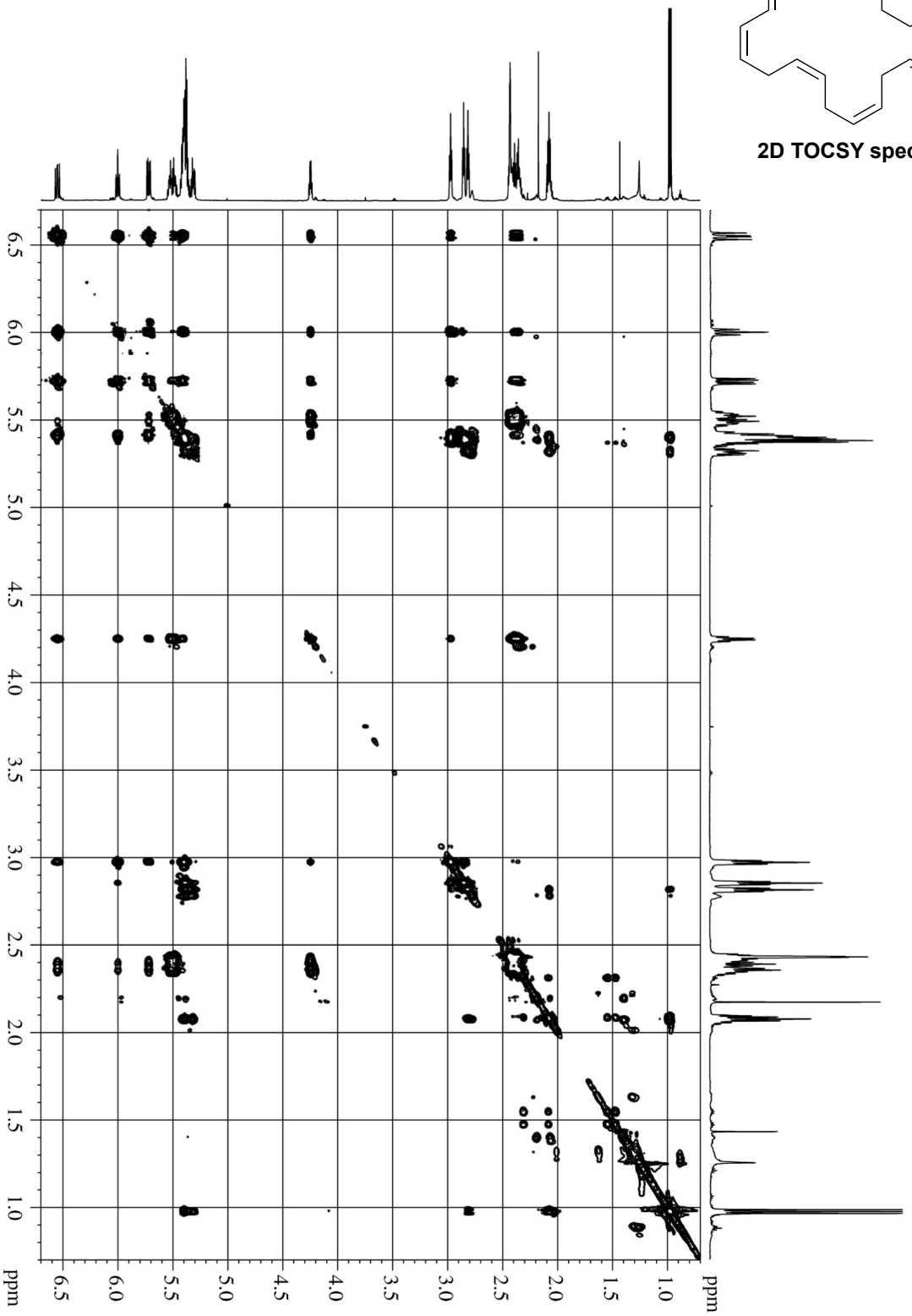

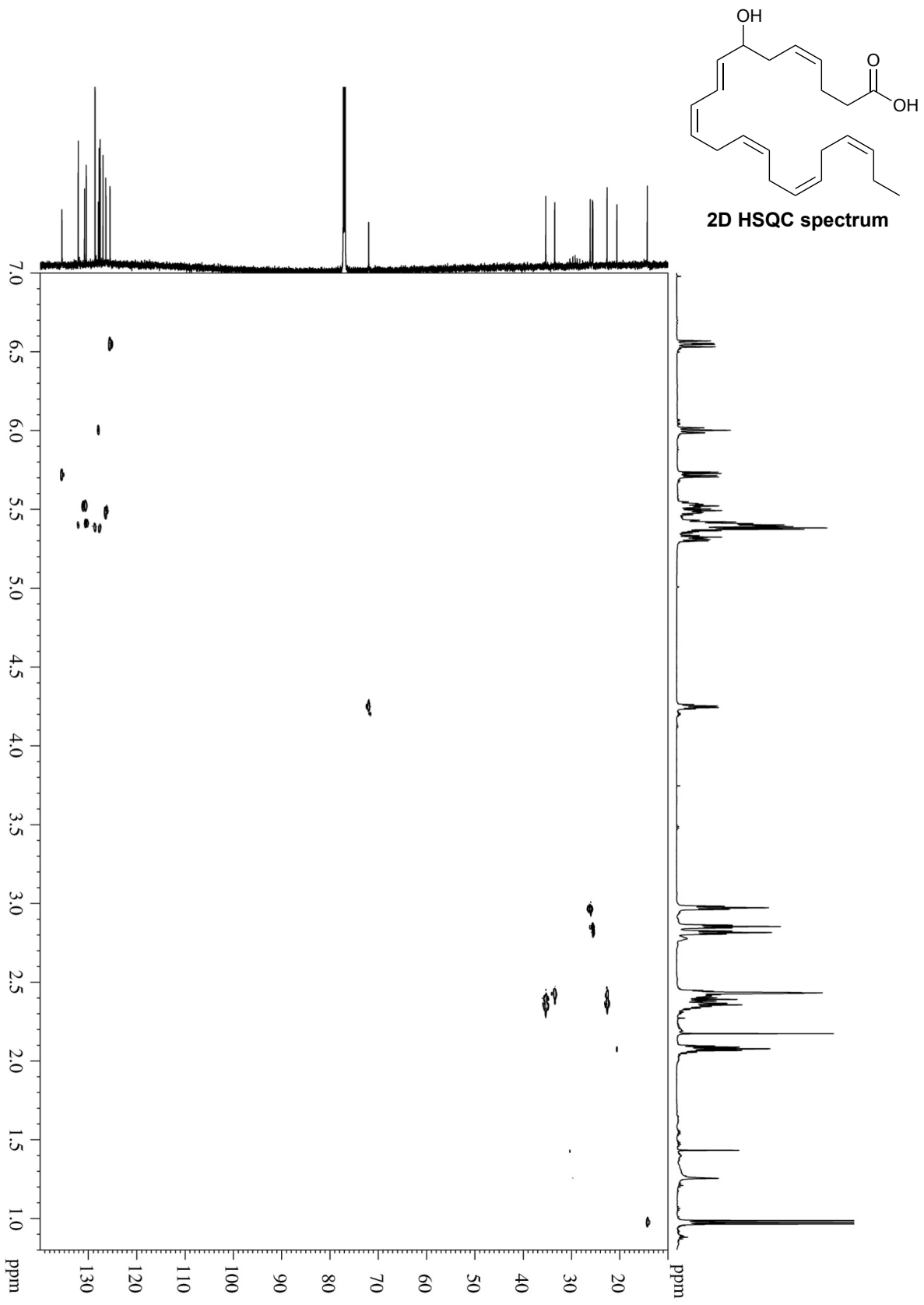
OH
O
OH
2D HSQC spectrum
7.0
6.5
6.0
5.5
5.0
4.5
4.0
3.5
3.0
2.5
2.0
1.5
1.0
ppm
130
120
110
100
90
80
70
60
50
40
30
20
ppm

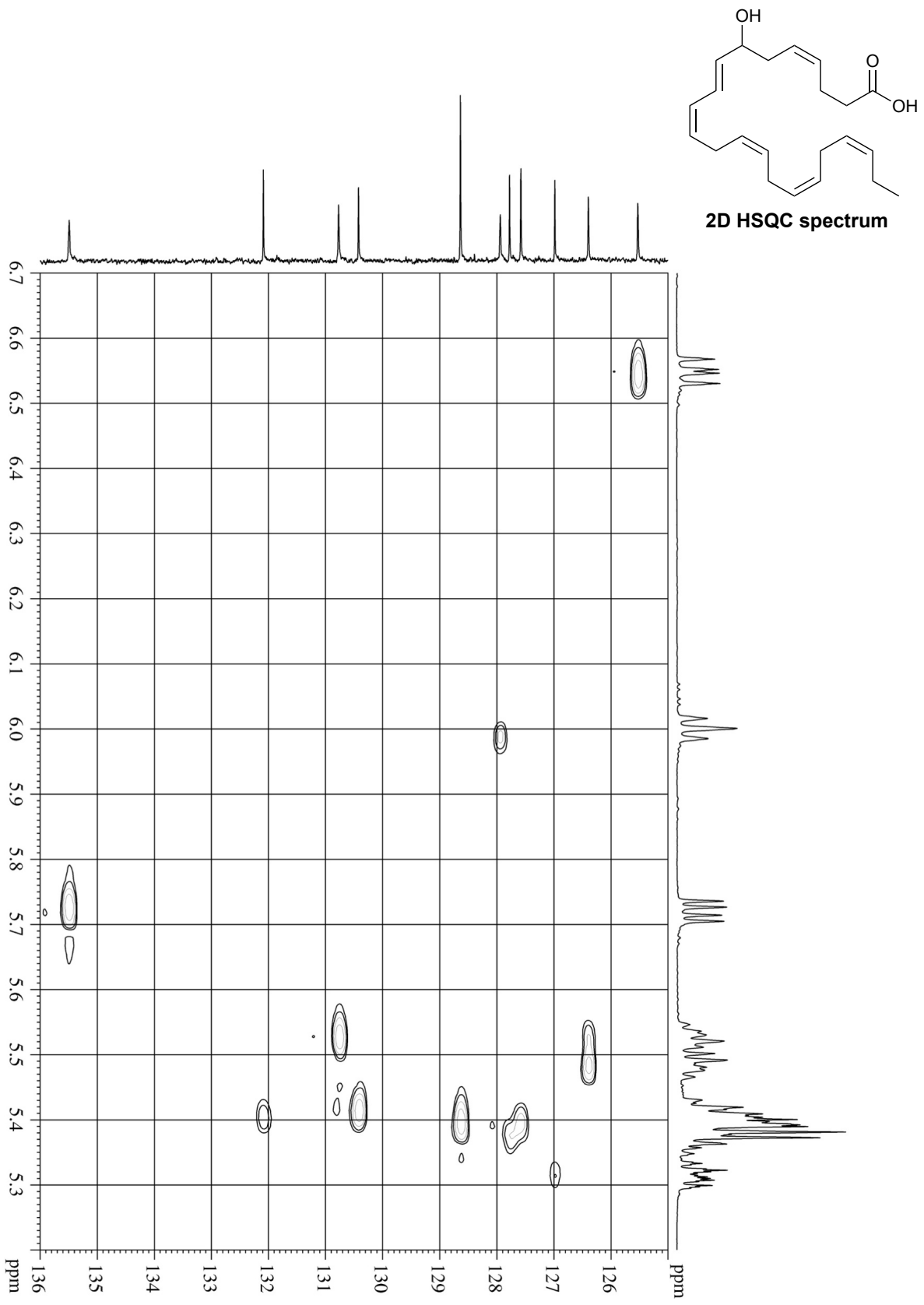
OH
O
OH
2D HSQC spectrum
6.7
6.6
6.5
6.4
6.3
6.2
6.1
6.0
5.9
5.8
5.7
5.6
5.5
5.4
5.3
ppm
136
135
134
133
132
131
130
129
128
127
126
ppm

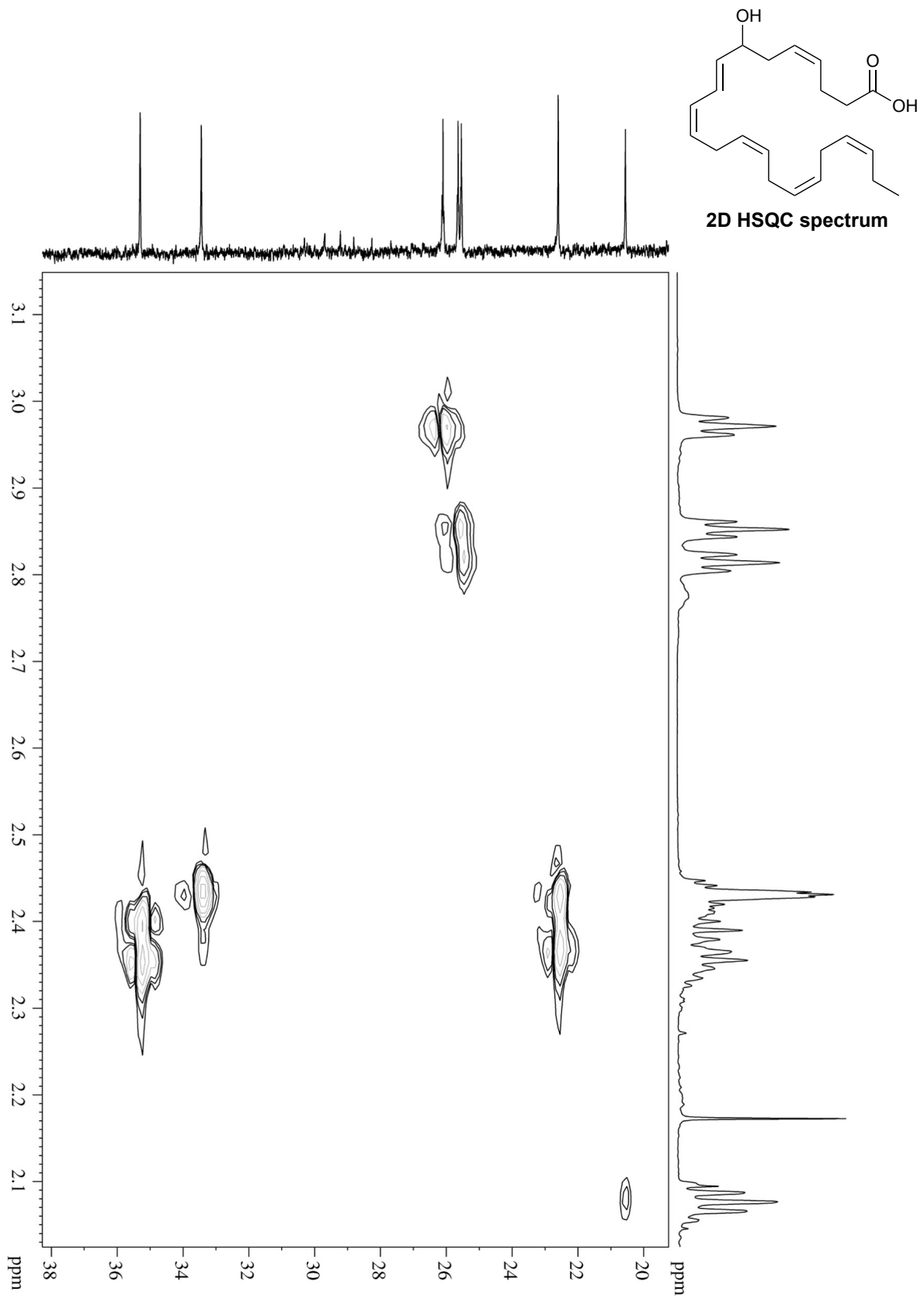
OH
O
OH
2D HSQC spectrum
3.1
3.0
2.9
2.8
2.7
2.6
2.5
2.4
2.3
2.2
2.1
ppm
38
36
34
32
30
28
26
24
22
20
ppm

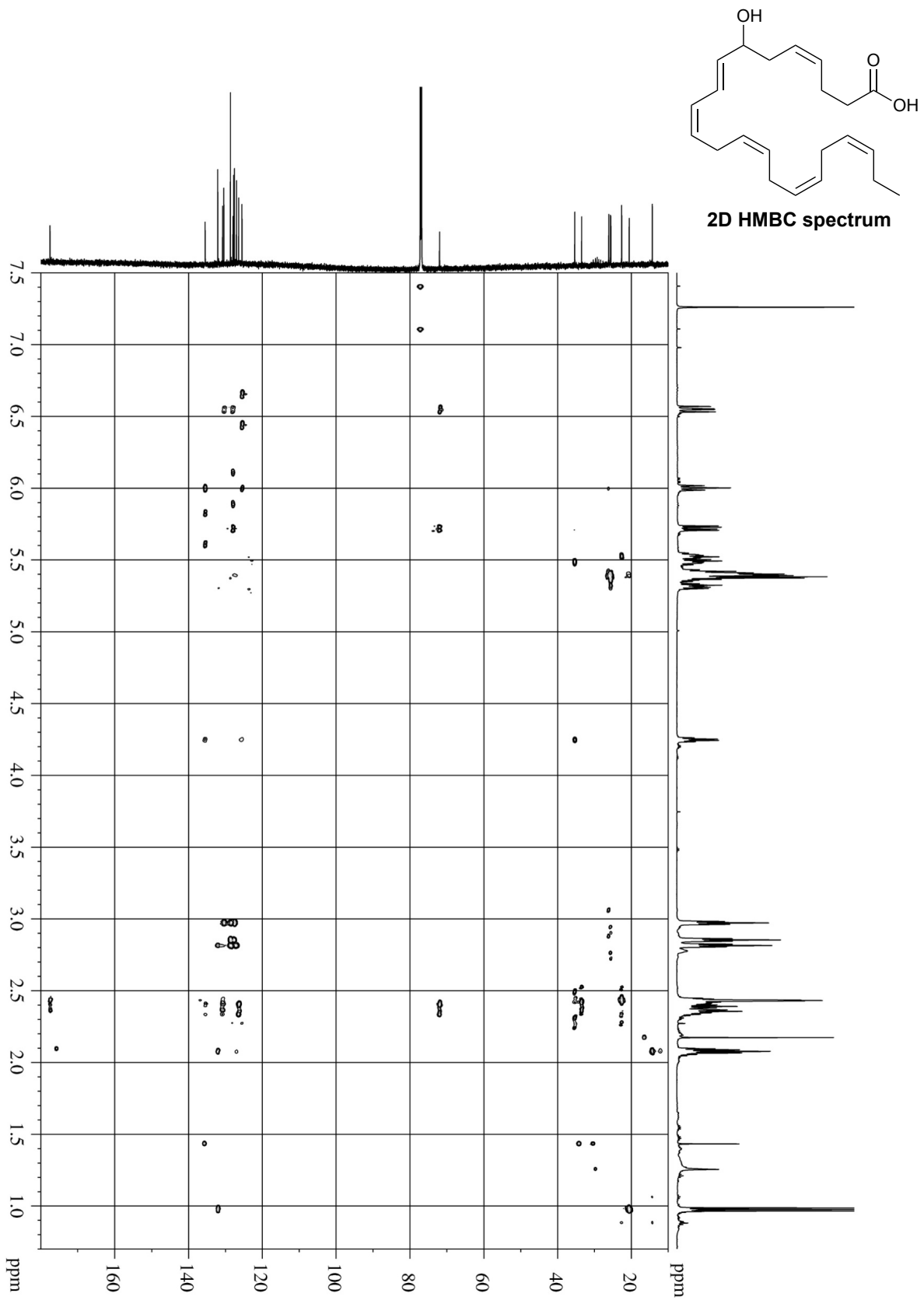
OH
O
OH
2D HMBC spectrum
7.5
7.0
6.5
6.0
5.5
5.0
4.5
4.0
3.5
3.0
2.5
2.0
1.5
1.0
ppm
160
140
120
100
80
60
40
20
ppm

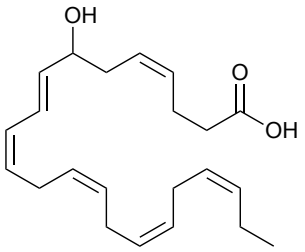


**2D HMBC spectrum**

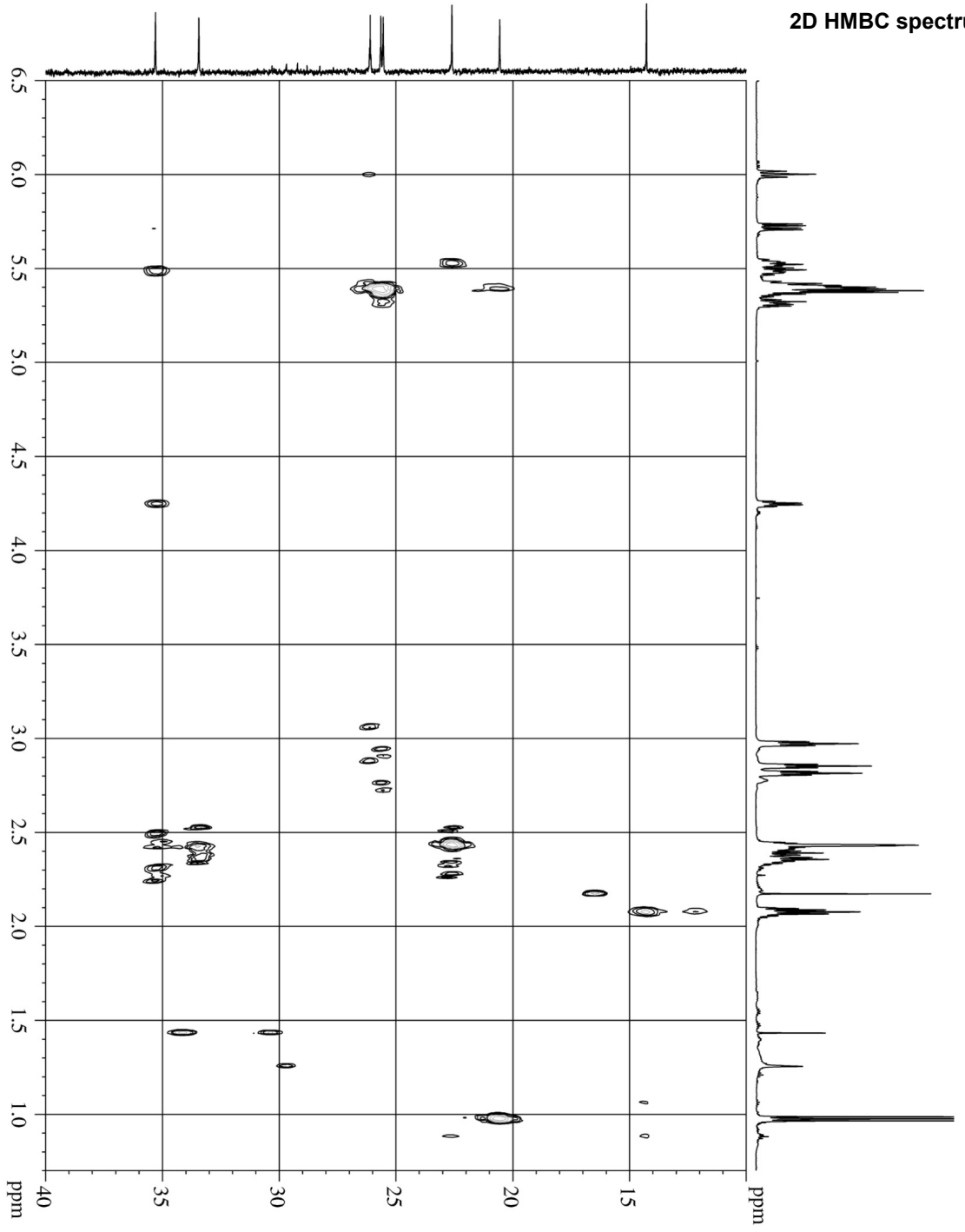

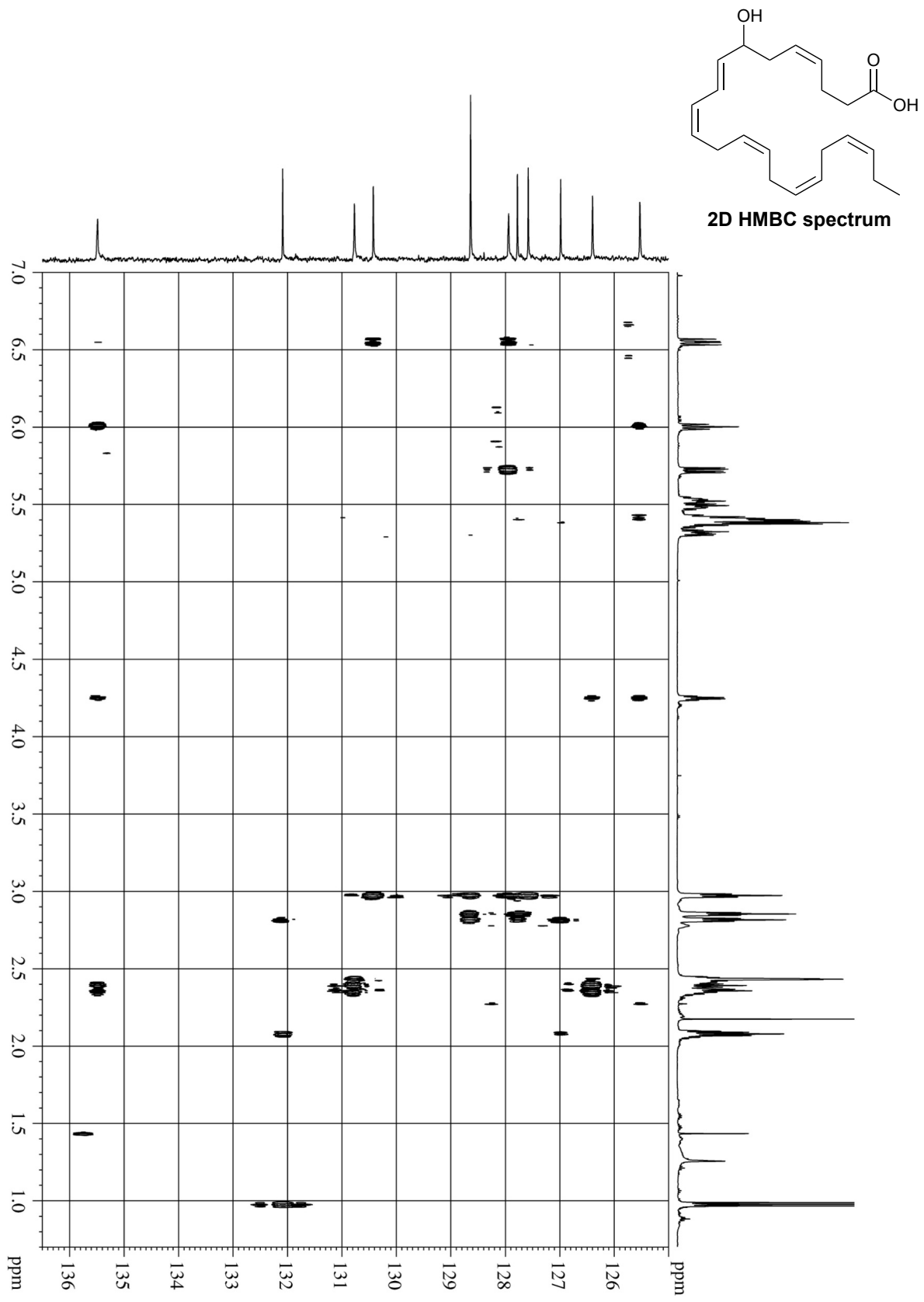
OH
O
OH
2D HMBC spectrum
7.0
6.5
6.0
5.5
5.0
4.5
4.0
3.5
3.0
2.5
2.0
1.5
1.0
ppm
136
135
134
133
132
131
130
129
128
127
126
ppm

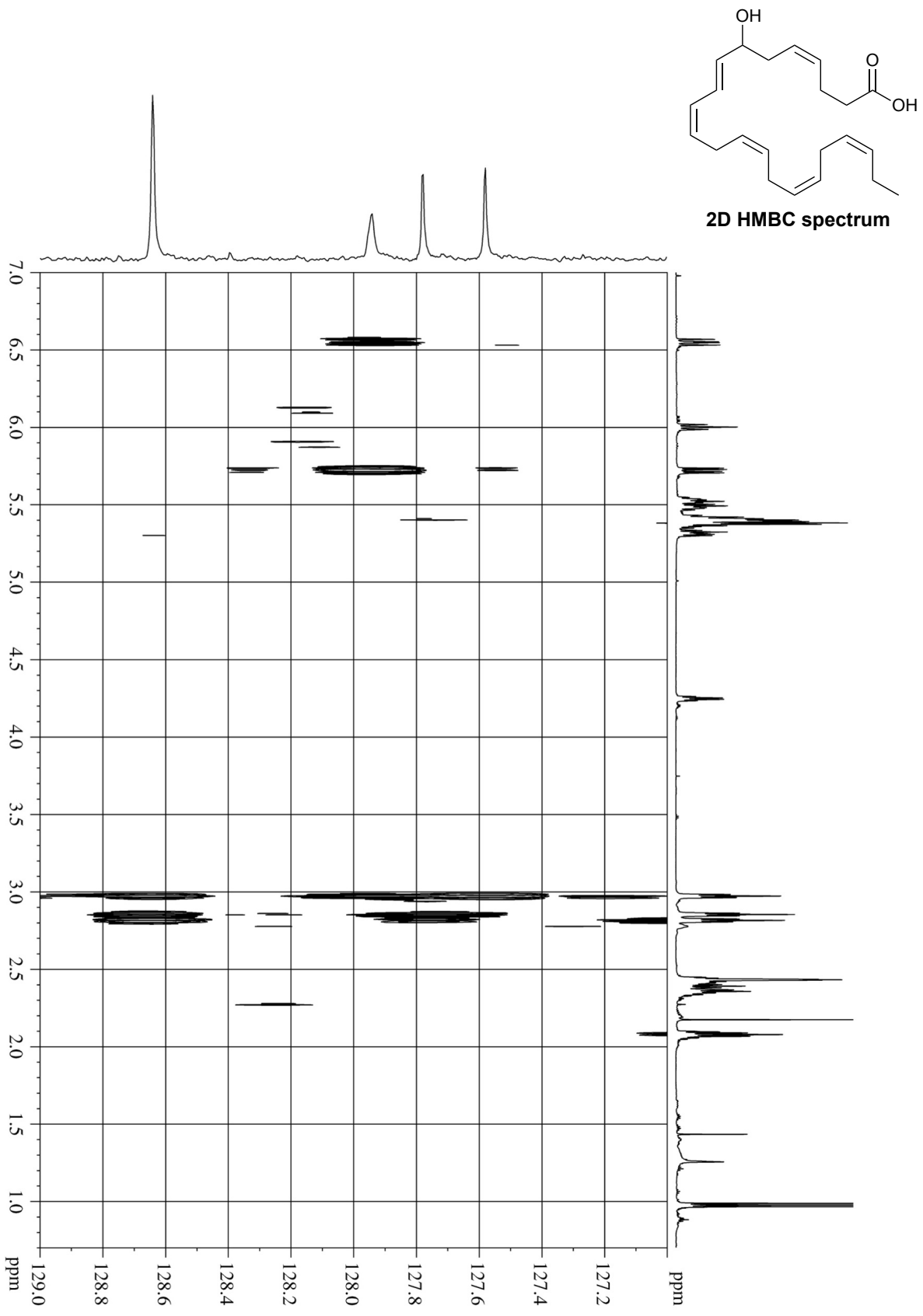
OH
O
OH
2D HMBC spectrum
7.0
6.5
6.0
5.5
5.0
4.5
4.0
3.5
3.0
2.5
2.0
1.5
1.0
ppm
129.0
128.8
128.6
128.4
128.2
128.0
127.8
127.6
127.4
127.2
ppm

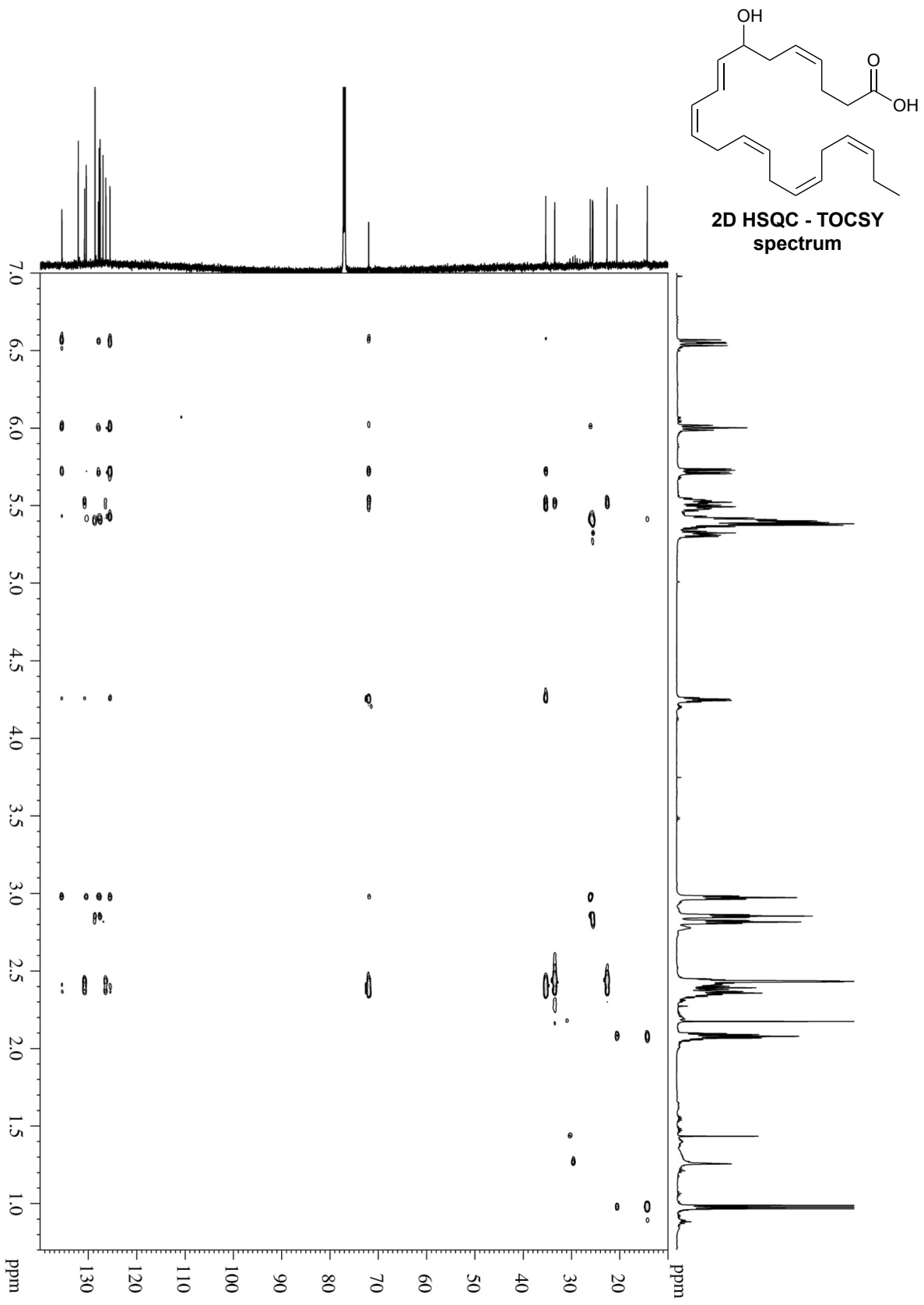


**2D HSQC - TOCSY spectrum**

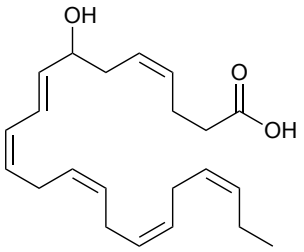


**2D HSQC - TOCSY spectrum**

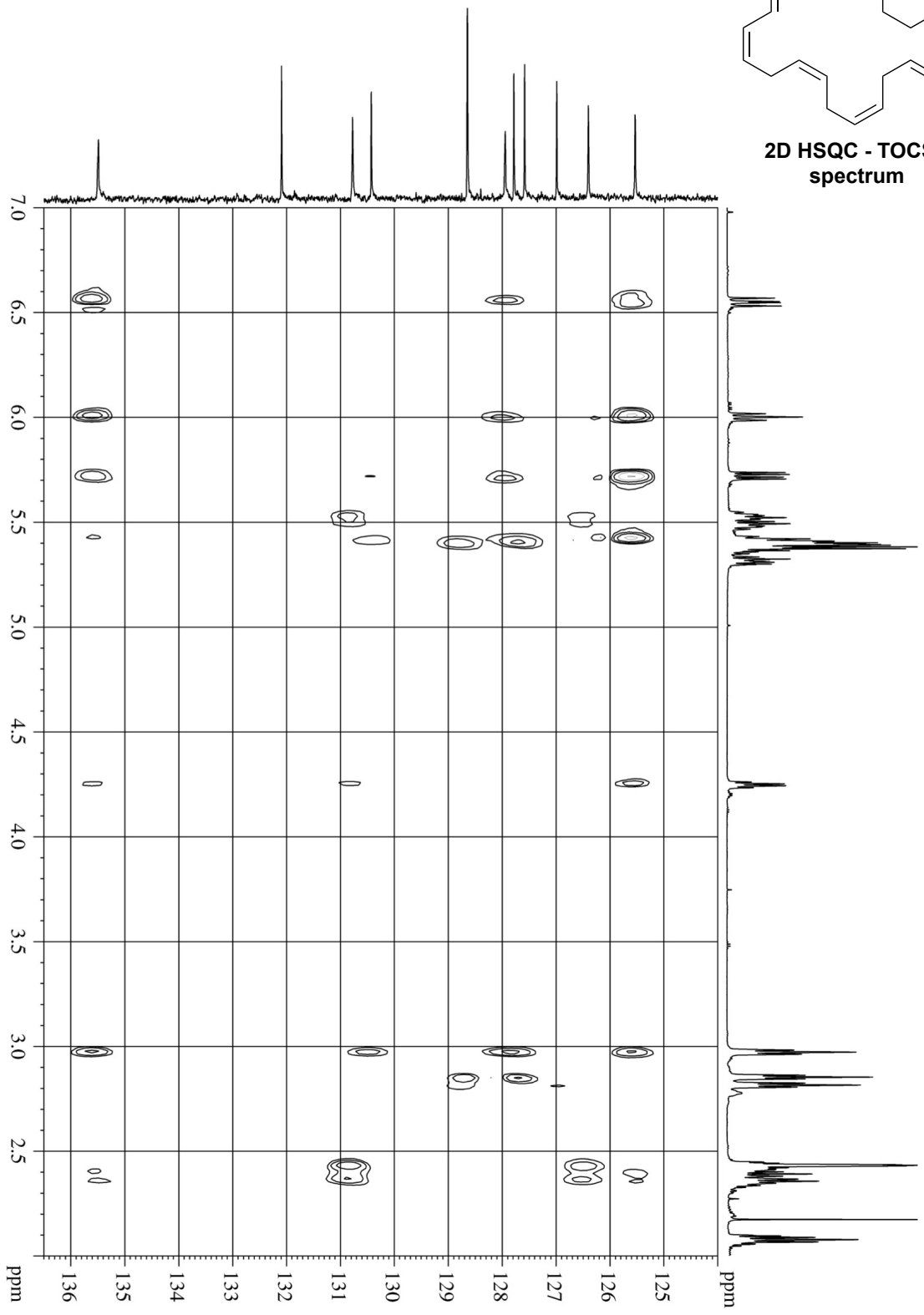

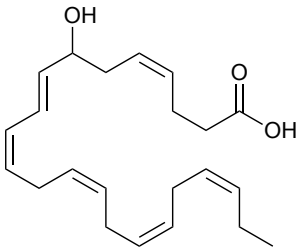


**2D HSQC - TOCSY spectrum**

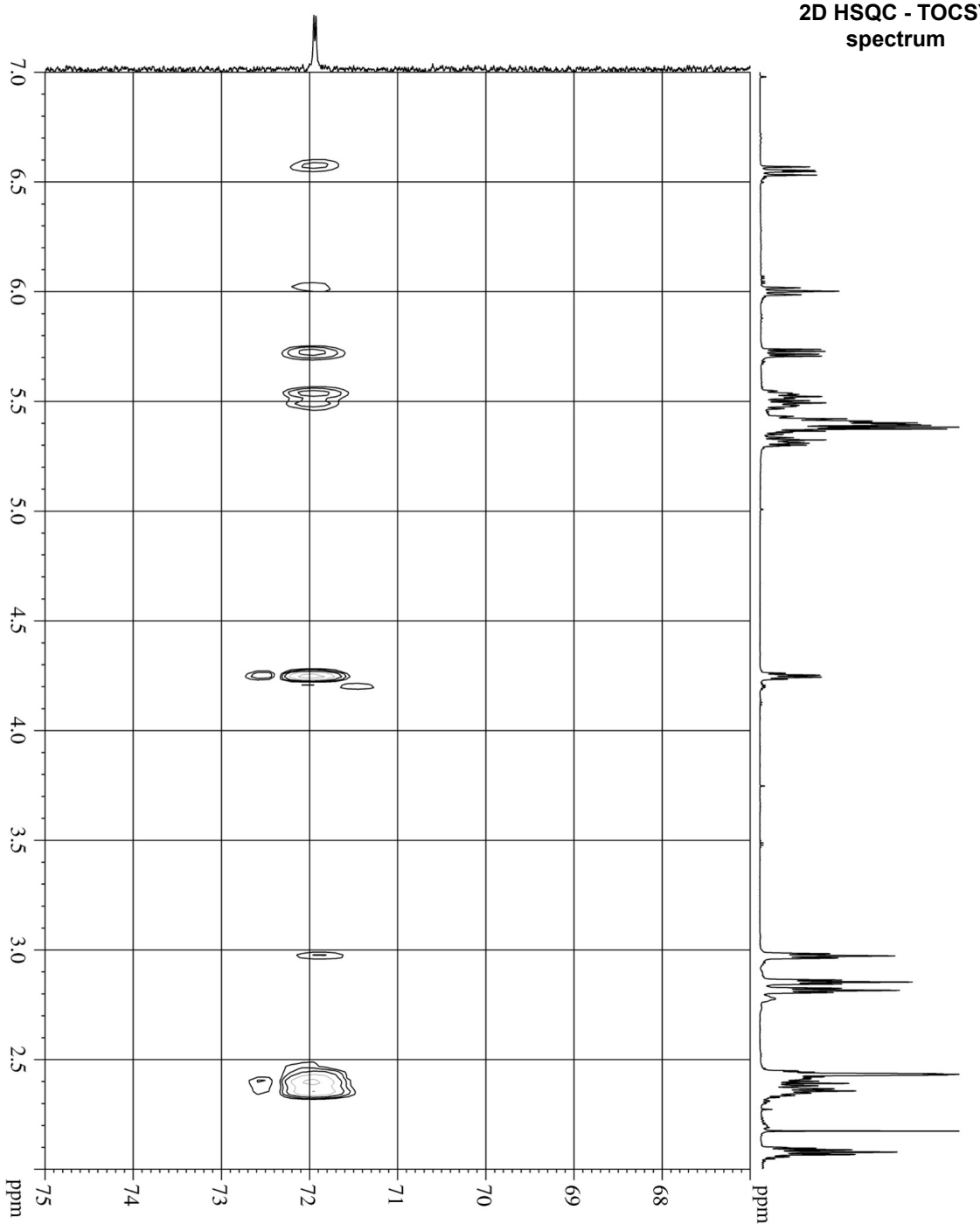

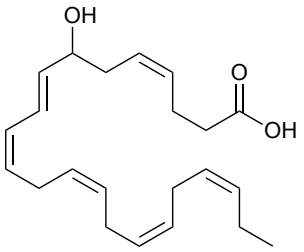


**2D HSQC - TOCSY spectrum**

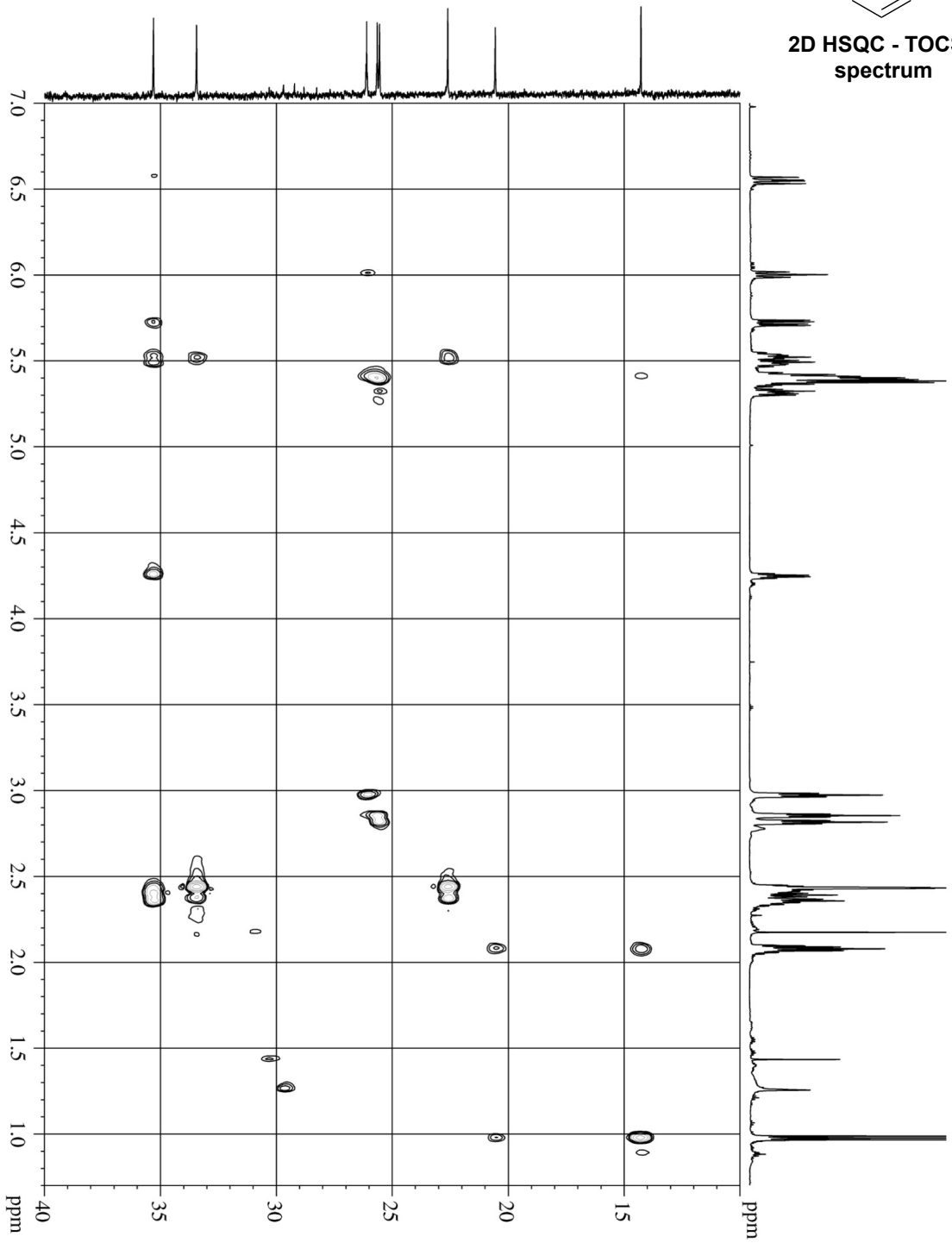

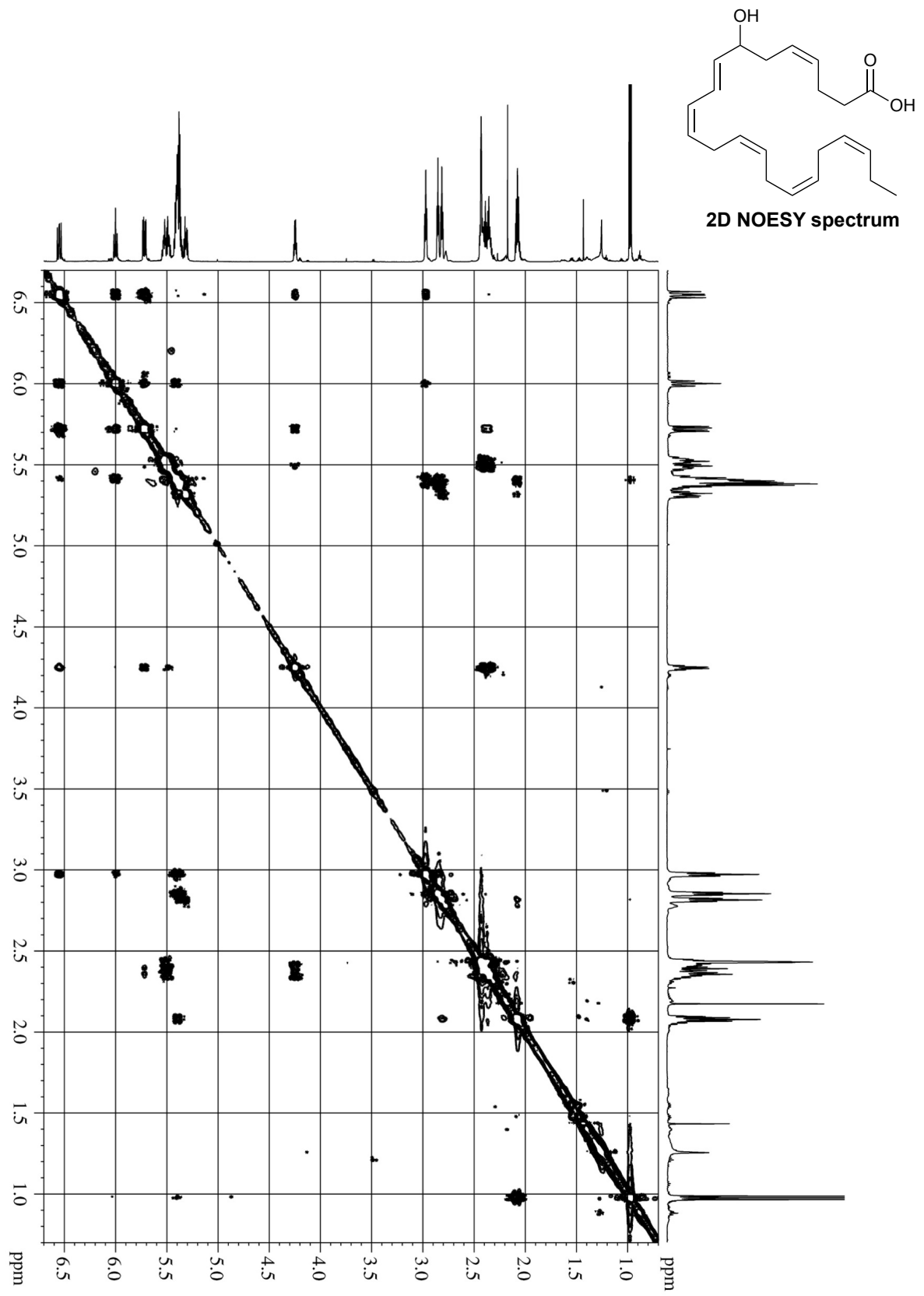
OH
O
OH
2D NOESY spectrum
6.5
6.0
5.5
5.0
4.5
4.0
3.5
3.0
2.5
2.0
1.5
1.0
ppm

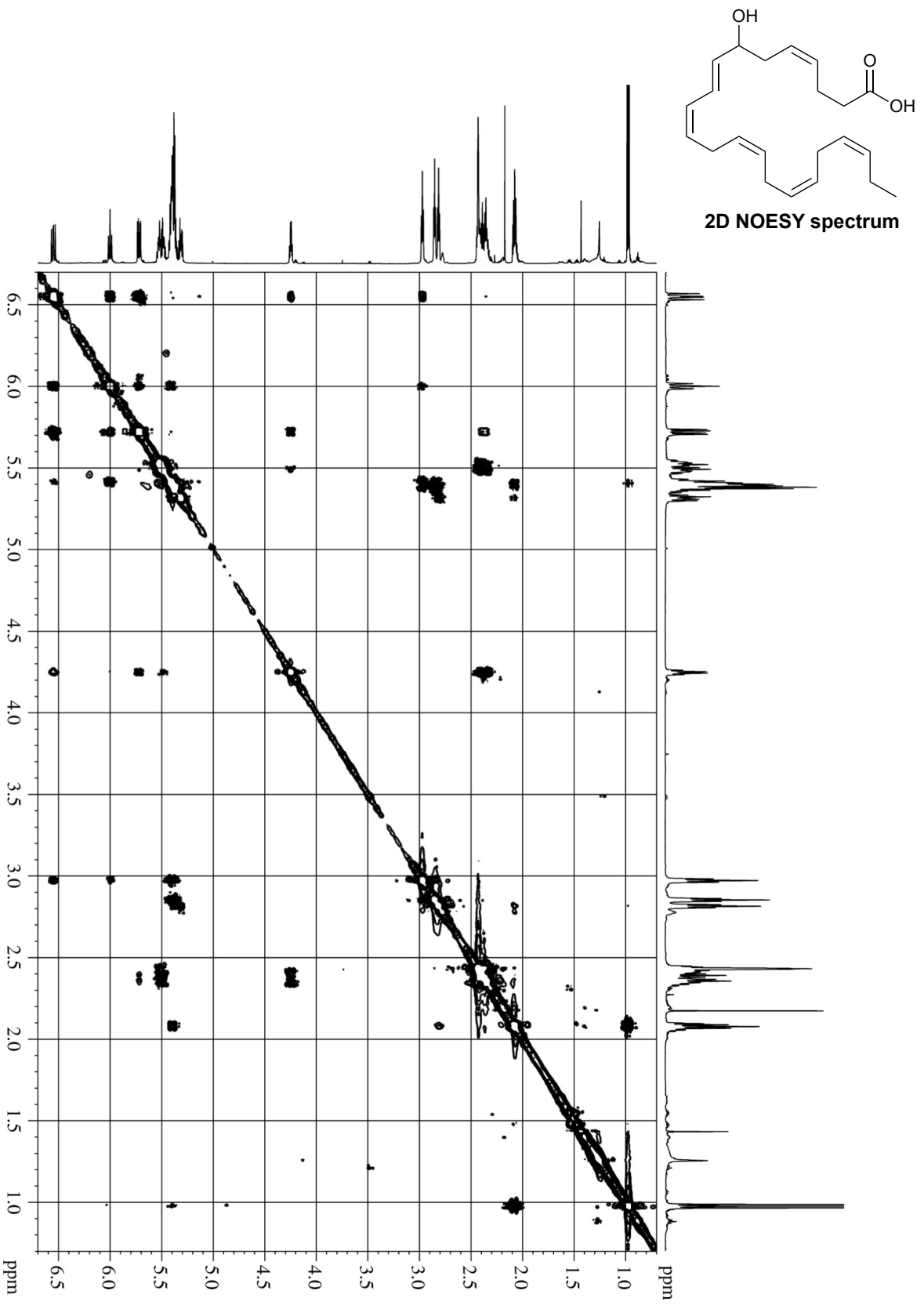
OH
O
OH
2D NOESY spectrum
6.5
6.0
5.5
5.0
4.5
4.0
3.5
3.0
2.5
2.0
1.5
1.0
ppm